1-12-2007

Mechanistic Insight into Subunit Stoichiometry for KIR Channel Gating: Ligand Binding, Gating, Binding-Gating Coupling, Coordination, and Cooperativity

Runping Wang

MECHANISTIC INSIGHT INTO SUBUNIT STOICHIOMETRY FOR KIR CHANNEL GATING: LIGAND BINDING, GATING, BINDING-GATING COUPLING, COORDINATION, AND COOPERATIVITY

by

RUNPING WANG

Under the Direction of Chun Jiang

ABSTRACT

Ligand-gated ion channels couple intra- and extracellular chemical signals to cellular excitability. In response to a specific ligand, these channels change their permeability to certain ions by opening or closing their ion conductive pathway, a controlling mechanism known as channel gating. Although recent studies with X-ray crystallography and site-directed mutagenesis have revealed several structures potentially important for channel gating, the gating mechanism is still elusive. Ligand-dependent channel gating involves a series of transient events and asymmetric movements of individual subunits. Understanding of these events appears to be a challenge to current approaches in gating studies by using the homomeric wild-type or mutant channels. I therefore took an alternative approach by constructing heteromeric channels. Subunit stoichiometric studies of the Kir1.1 channel showed that a minimum of one functional subunit was required for the pH-dependent gating of the channel. Four subunits in this channel were coordinated as dynamic functional dimers. In Kir6.2 channel, stoichiometry for proton-binding was almost identical to that for channel gating in the M2 helix,

suggesting a one-to-one direct coupling of proton binding in C-terminus to channel gating in M2 helix. Positive cooperativity was suggested among subunits in both the proton binding and channel gating. Ligand binding can be differentiated from channel gating by studying the ATP-dependent gating of Kir6.2 channel. Disruptions in ATP binding were found to change both the potency and efficacy of the concentration-dependent curves, while the baseline activity instead of maximum inhibition was affected by disruptions of channel gating. Four subunits in the Kir6.2 channel undergo negative cooperativity in ATP binding and positive cooperativity in channel gating. The ligand binding was coupled to the gating mechanism in the same subunit and neighboring subunits, although the intrasubunit coupling was more effective. These results are well described with the operational model which we have applied to ion channel studies for the first time. By manipulating the relative distance and the interaction of two transmembrane helices, the inner helix bundle of crossing was found to not only serve as a gate but also determine the consequence of ligand binding.

INDEX WORDS: ion channel, subunit Stoichiometry, ligand binding, channel gating, binding-gating coupling, subunit coordination, subunit cooperativity, Kir1.1, Kir6.2, pH dependent gating, ATP dependent gating.

MECHANISTIC INSIGHT INTO SUBUNIT STOICHIOMETRY FOR KIR CHANNEL GATING: LIGAND BINDING, GATING, BINDING-GATING COUPLING, COORDINATION, AND COOPERATIVITY

by

RUNPING WANG

A Dissertation Submitted in Partial Fulfillment of the Requirements for the Degree of

Doctor of Philosophy

in the College of Arts and Sciences

Georgia State University

2005

MECHANISTIC INSIGHT INTO SUBUNIT STOICHIOMETRY FOR KIR CHANNEL GATING: LIGAND BINDING, GATING, BINDING-GATING COUPLING, COORDINATION, AND COOPERATIVITY

by

RUNPING WANG

Major Professor:	Chun Jiang
Committee:	Deborah Baro
	Charles Derby
	Phang C. Tai

Electronic Version Approved:

Office of Graduate Studies

College of Arts and Sciences

Georgia State University

December 2005

A. ACKNOWLEDGEMENTS

Pursuing a doctoral degree is one of the most important events in my life which requires not only my personal efforts but also support from my surroundings. I sincerely appreciate all people for instructing, advising, assisting, and encouraging me in the course toward my Ph.D. degree.

First of all, I would like to thank my advisor, Dr. Chun Jiang, for all his efforts in instruction, inspiration, and assistance in completing this dissertation. He has had a tremendous influence not only on my career, but also on my personality.

I am particularly grateful to Drs. Phang C. Tai, Charles Derby, and Deborah Baro for serving on my dissertation committee and invaluable advice in my thesis design and accomplishment.

I would like to express my appreciation to the members in Dr. Jiang's laboratory for inspiration in discussions of my research projects and numerous technical assistance. Special thanks to Drs. Junda Su, Asheebo Rojas, Ningren Cui, Xueren Wang, and Yun Shi for their help with whole cell recordings, Drs. Jianping Wu, and Ningren Cui for the help with patch clamping, and Dr. Haoxing Xu, Hailan Piao, Xiaoli Zhang, Vivian A. Onyebuchi, Carmen Y. Adams, and Ying Wang for their assistance in DNA reconstruction and purification.

I also want to thank Drs. Phang C. Tai, Charles Derby, and Andrew Clancy for their guidance in the qualifying examination. Thanks to Ms. Ping Liang-Jiang for her help in the DNA sequencing and making primers. My appreciation is also extended to the

faculty and staff of the Department of Biology for their advice and assistance during my Ph. D. program.

Finally, my most heartfelt thanks go to my family, my husband Ge and my son Gary for their love, encouragement, and support. I want to thank my parents for giving me my early scientific education and encouraging me to pursue this Ph.D. degree. I am extremely grateful to my parents and my parents-in-law for taking care of my son during my graduate study.

B. TABLE OF CONTENTS

D. LIST OF FIGURES AND TABLES

E. LIST OF ABBREVIATIONS

AA	amino acid;
Ach	acetylcholine;
BK	large conductance Ca^{2+}-activated K^+ channel;
C	closed state;
cAMP	cyclic adenosine monophosphate;
cGMP	cyclic guanosine monophosphate;
CNB	cyclic nucleotide binding domain;
CNG	cyclic nucleotide-gated;
DAG	diacylglycerol;
DFD	dynamic functional dimers;
EC_{50}	concentration for 50% activation;
EGTA	ethylene glycol-bis(2-amino-ethylether)-N, N, N', N' –tetra-acetic acid;
ER	endoplasmic reticulum;
FRET	fluorescence resonance energy transfer;
GABA	gamma-aminobutyric acid;
GIRK	G-protein activated inward rectifier K^+ channel;
h	Hill coefficient;
HCN	cyclic nucleotide-gated channel;
HEPES	N-[2-Hydroxyethyl]piperazine-N'-[2-. ethanesulfonic acid];
HH	Hodgkin-Huxley model;
IC_{50}	concentration for 50% inhibition;
IK	intermediate conductance K_{Ca} channel;
IP_3	inositol 1, 4, 5-trisphosphate;
IRK	inward rectifier K+ channel;
K_{ATP}	ATP-sensitive K^+ channel;
K_{Ca}	Ca^{2+}-activated K^+ channels;
KcsA	K^+ channel from *Streptomyces lividans*;
Kir	inward rectification K^+ channel;

Kir6.2ΔC36	Kir6.2 channel with 36 amino acid truncated at the C terminal end;
KirBac1.1	bacterial inward rectifier potassium channel 1.1;
KNF	Koshland, Nemethy and Filmer model;
Kv	voltage-gated K^+ channel;
LTP	long-term potentiation;
LTD	long-term depression;
MscL	bacterial mechanosensitive channel;
MTS	methanethiosulfonate;
MWC	Monod, Wyman and Changeux model;
NMR	nuclear magnetic resonance;
O	open state;
P	pore-forming loop;
PCR	polymerase chain reaction;
PIP3	phosphatidylinositol 3,4,5 triphosphate;
PKA	protein kinase A;
pKa	pH value at 50% effect;
PKC	protein kinase C;
PKG	protein kinase G;
P_{open}	open-state probability;
ROMK	renal outer medullary potassium channel;
RyR	ryanodine receptors;
s.e.m.	standard error of the mean;
SK	small conductance K_{Ca} channel;
SR	sarcoplasmic reticulum;
SUR	sulfonylurea receptor;
TM1	first membrane-spanning helix;
TM2	second membrane-spanning helix;
wt	wild-type;

E. SPECIFIC AIMS AND HYPOTHESES

Membrane excitability is the foundation of a variety of cellular functions. Ligand-gated ion channels couple intra- and extracellular chemical signals to cellular excitability. They play a crucial role in cell-cell communication and cellular responses to changes in the internal and external environment. In response to a specific ligand, ion channels are open or closed allowing certain ionic species to pass through. The change in channel opening or closure states refers to *gating*. Although the gating mechanism is still incompletely known, recent crystallographic studies have remarkably improved our understanding. A study on the bacterial MthK channel has shown that eight Ca^{2+}-binding domains form a four-fold symmetric gating ring in the cytosol. Ligand binding to which causes conformational changes in the channel protein, producing a lateral extension force which expands the gating ring and removes the physical barrier of the ion conduction pore (Kuo et al., 2003). Studies on the mechanosensitive (MscL) channel have indicated that the transmembrane helices tilt in response to mechanical stretch of the plasma membrane producing an iris like movement, expanding the channel pore and opening the ion permeable pathway (Betanzos et al., 2002). The pentameric nicotinic acetylcholine receptor has two rings of hydrophobic side chains projecting to the pore. The pore-lining helices undergo a clockwise rotation after ligand binding, widening these rings, and opening the pore (Unwin, 1995). Despite of the progress in understanding of channel gating, a number of **questions** remain open. For instance, gating is a dynamic process while the crystallographic studies allow a resolution of only the open or closed state. How can all transient events from ligand binding to channel gating be illustrated? The time course is not the only problem, as channel gating also involves asymmetric

movements of individual subunits in a multimeric channel. It is a challenge to have a large number of asymmetric channels crystallized and studied with today's technology. In addition, there are many other open questions as to what the minimum requirement of functional subunits is for the channel gating; how subunits are coordinated for ligand binding and channel gating; whether there is cooperativity among subunits; and what determines the opening or closure of a channel following binding to a given ligand. Since none of these questions can be addressed with homomeric channels, I proposed studies based on a rather cost-efficient approach, which were **specifically aimed** at answering the above questions. The following **hypotheses** were tested:

E-I. Disruption of a given number of subunits in a tetrameric channel can reveal events in proton-dependent Kir1.1 channel gating, such as the minimum number of subunits required, dominant-negative effects, subunit coordination, substate conductance, and other single channel biophysical properties.

E-II. Kir6.2 channel gating by intracellular protons involves one-to-one coupling of ligand binding to channel gating.

E-III. There are specific subunit stoichiometries for ATP binding, channel gating, and binding gating couplings in the Kir6.2 channel:

E-IV. ATP binding and channel gating behave differently in the Kir6.2 channel.

E-V. Ligand binding is coupled to channel gating in the same and adjacent subunits.

E-VI. There are special subunit coordination and cooperativity among subunits.

E-VII. The interaction and relative positions of the inner helices determine the consequence of ligand binding.

F. BACKGROUND

Ion channels are protein pores in plasma membranes that are permeable to specific ions. They are the molecular basis for the electrical signals in nerve, muscle, and a wide range of other cells and tissues. Channels located in these cells and tissues detect changes in the external and internal environment. By opening and closing the channel pores according to environmental changes, many types of channels work together to generate and modify the electrical signals and responses of excitable cells.

Ion channels are encoded by at least 429 genes (Li, www.molecularinteraction.org). The number of channels will be much greater than the number of genes because of alternative splicing, protein modification, and numerous combinations of heteromeric channels. These channels belong to different subfamilies. Each subfamily can be named according to their selectivity to ions, such as K^+ channel, Na^+ channel, Ca^{2+} channel, Cl^- channel, non-selective cation channel, and anion channel. Subfamilies can also be differentiated depending on their gating mechanisms, for instance ligand-gated, voltage-gated, and stretch-activated channels. Ligand-gated ion channels couple the intra- and extracelluar signals to cellular excitability. Extracellular ligand-gated channels are mainly composed of ionotropic receptors. Intracellular ligand gated channels include cyclic nucleotide-gated (CNG) channels, Ca^{2+}-activated channels, G-protein gated channels, ATP-sensitive K^+ channels, and inward rectification K^+ channels.

Ion channels play important roles in cell and tissue functions. Dysfunctions of ion channels therefore are some of the major causes of diseases. The structural-functional

relationship studies provide important information for the understanding of mechanisms underlying certain diseases and contribute to the therapeutical approach to these diseases.

F-I. Function and regulatory mechanisms of ligand-gated ion channels

F-I-1. Historical review Studies of channels can be traced back to late 18th century. In 1791, Luigi Galvani firstly found that electrical stimulation of frog sciatic nerve caused contraction of the gastronomic muscle. By the 1880s, physiologists had already known that ions were critical for the excitability of nerves and muscles. Sidney Ringer pointed out that the heart needed perfusate containing precise proportion of Na^+ and K^+ to beat. Hermann von Helmholtz pioneered shows action potential propagation. He measured the speed of frog nerve impulses in 1872 and was the first one to observe changes and propagation of electrical impulse in nerves (Hille, 2001). Walther Nernst (1888) noticed that a membrane potential changed during diffusion of electrolytes, and described the phenomenon with mathematics later known as the Nernst equation for membrane potential (Hille, 2001). His work inspired numerous speculations about the origin and mechanism of membrane and excitation potentials. In 1902 and 1912, Julius Bernstein correctly proposed that membranes of excitable cells were permeable to K^+ at rest and their permeability to other ions increased during excitation (Hille, 2001). Without knowing the nature of the molecules involved, pioneer studies tried to explain the dynamic and equilibrium properties of action potentials with equations and models of classic biophysics. The first observation of the involvement of ions in action potentials was done by Cole and Crutis using the voltage-clamp technique invented by themselves (1939). A major breakthrough in ion channel studies occurred in early 1950s when Alan

Lloyd Hodgkin and Andrew Fielding Huxley performed their famous voltage clamp studies and described for the first time that resting membrane potential was produced by K^+ currents and action potentials result from a sequential activation of Na^+ and K^+ currents (Hodgkin and Huxley, 1952). They proposed that since these currents were produced by their selective permeability of plasma membranes, they were probably conducted through membrane ion channels.

The understanding of ion channels was rather phenomenal and conceptual until the mid-1970s when Erwin Neher and Bert Sakmann developed the patch-clamp technique (Hamill, et al., 1981). With patch clamp, they showed for the first time what ion channels are and how they work in conducting ionic currents. Subsequently, they developed a new way to describe channel kinetics with their colleagues, establishing a remarkable technique that remains today as the most sensitive bioassay for functional studies of channels molecules. The resolution of patch clamp brought attention of scientists to single molecules. Meanwhile, developments in protein chemistry and molecular biology made it possible to understand ion channels at molecular levels. In 1982, Numa and his colleagues successfully cloned the nicotinic acetylcholine receptor from the electric marine ray Torpedo (Noda et al., 1982). They first purified the channel protein and determined part of its amino acid (AA) sequence. This sequence was then used to design a series of probes to screen the cDNA library to obtain the correct clone (Noda et al., 1982). Using the same approach, his group later cloned the voltage-gated Na^+ channel from the electric eel (Noda et al., 1984) and L-type Ca^{2+} channel (Mikami et al, 1989). A number of ion channels were cloned by other groups in the same way

(Papazian et al., 1987; Kubo et al., 1993; Kohler et al., 1996). Molecular cloning has greatly improved our understanding of ion channels. The studies on ion channels became interdisciplinary involving biophysics, pharmacology, protein chemistry, molecular and medical genetics, and cell biology. More than 429 genes encoding different subunits of ion channel proteins have been revealed in the Human Genome Projects. It is now known that these genes are translated and combined to form a large number of ion channels belong to a number of subfamilies. The AA sequences of these ion channels have been known and their critical domains have been identified. Many three dimensional structures were resolved by X-ray crystallography. The first description of channel structure by Mackinnon's group in 1998 opened a new chapter for studies of ion channel (Doyle et al., 1998). Studies on structure-function relationships further extended the understanding of and therapeutical approach to diseases.

F-I-2. Role of ligand gated channels in cellular function Ligand-gated channels couple intra- and extracellular chemical signals to cellular excitability. They are found in plasma membranes of all eukaryotic and prokaryotic cells, and play important roles in nerve and muscle excitation, hormonal secretion, learning and memory, cell proliferation, sensory transduction, control of salt and water balances, regulation of blood pressure (Ashcroft, 2000). The extracellular-ligand gated channels mostly refer to ionotropic receptors for neurotransmitters and hydrophilic hormones such as nicotinic receptors, 5-HT_3 receptors, glycine receptors, $GABA_A$ and $GABA_C$ receptors, glutamate receptors. These receptors are responsible for communication between neurons and effector cells and between neurons themselves. Dysfunction of these channels causes a

wide range of neuronal, muscular, and developmental diseases (Lester, 2004; Connolly, 2004).

Intracellular-ligand gated channels are those that can be regulated by intracellular messengers or chemical signals. For example, CNG channels play a central role in olfaction, taste, and visual transduction. These CNG channels are permeable to cations after the ion pathway is opened. CNG channel activation following the increase of cyclic nucleotide levels after the detection of odorants leads to depolarization of olfactory sensory cells, activation of neuronal pathways, and central reception (Nakamura and Gold, 1987). CNG channel knock-out mice lose their response to odorants (Brunet et al., 1996).

Ca^{2+}-activated K^+ channels (K_{Ca}) are activated by an increase in intracellular Ca^{2+} concentration. They play a key role in shaping action potentials and regulating cellular excitability. They are also involved in K^+ secretion in some epithelium cells. Three types of K_{Ca} channels are identified according to their conductance. Large conductance K_{Ca} (100-250pS) channels (BK) are found in all kinds of cells except the heart. They contribute to action potential repolarization and play important roles in controlling neuronal excitability, transmitter release, and regulation of smooth muscle excitability. These channels are voltage-sensitive and can be opened by depolarization. Small conductance K_{Ca} (SK) channels (5-20pS) are found in the brain, heart, adrenal gland, and skeleton muscle. These channels are insensitive to voltage (Aschroft 2000). Defects in these channels have been correlated with myotonic muscular dystrophy (Renaud et al., 1986; Behrens et al, 1994). Intermediate conductance (20-80pS) K_{Ca} (IK) channels are

densely expressed in vascular smooth muscle but not in brain. They play a role in regulating the excitability of vascular smooth muscles (Neylon et al., 1999).

Intracellular ligand-gated Ca^{2+} channels include two major classes: ryanodine receptors (RyR) and inositol 1, 4, 5-triphosphate (IP_3) receptors. Both of these receptors are located in the membrane of many organelles including sarcoplasmic reticulum (SR) in striated muscles and endoplasmic reticulum (ER) in other cells. RyR1 and RyR2 are responsible for Ca^{2+} release from intracellular stores, and play an important role in muscle contraction and cell signaling. IP_3 receptors are activated by the second messenger IP_3 mediating the effect of hormones, neurotransmitters, and growth factors (Berridge, 1993). The channel is important in smooth muscle contraction, olfactory desensitization, synaptic transmission, and hormone secretion. They are also involved in the regulation of cell growth and division.

Inward rectification K^+ (Kir) channels form another large family of ion channels that are found in neurons, cardiac muscles, skeleton muscles, pancreatic β cells, and retina. All members of this family are characterized by their property of inward rectification. It is so called because the inward current evoked by hyperpolarization is bigger than the outward current produced by depolarization. These channels have two major functions. They stabilize resting membrane potentials near the K^+ equilibrium potential and mediate K^+ transportation (Nichols and Lopatin, 1997). Dysfunction or mis-regulation of Kir channels leads to neuronal degeneration, defects in renal salt reabsorption, and insulin secretion, etc. (Ashcroft, 2000). G-protein activated inward rectifier K^+ (GIRK) channels are crucial for coupling activation of metabotropic receptors

to electrical activity of cells, playing a role in neurotransmission and other cell-cell communications (Lei et al., 2003). ATP-sensitive K^+ (K_{ATP}) channels play important roles in insulin secretion and vascular smooth muscle contraction. K_{ATP} channel knockout mice develop diabetes-like phenotypes (Seino, 1999). A number of Kir channels are inhibited directly by protons, such as Kir1.1, Kir2.3, Kir4.1 and heteromeric Kir4.1 plus Kir5.1. These channels may protect the cells from injury during hypoxia (Jiang, 2002a).

F-I-3. Regulatory mechanisms of ligand-gated ion channels The activity of ligand-gated ion channels is regulated by specific ligands. For extracellular ligand-gated ion channels, ligands are often neurotransmitters released by presynaptic neurons or other signal molecules such as ATP and hormones. In the absence of an agonist, extracellular ligand-gated channels normally have a very low open probability. Following binding of a specific ligand, the likelihood of channel opening increases, allowing certain ions to pass through the channel. The responses of the extracellular ligand-gated channels also depend on other regulatory mechanisms such as protein phosphorylation and dephosphorylation. The activity of protein kinases and protein phosphotases is regulated by second messengers such as Ca^{2+}, cyclic adenosine monophosphate (cAMP), cyclic guanosine monophosphate (cGMP), diacylglycerol (DAG), inositol 1, 4, 5-triphosphate (IP3), PIP_2, and others. Phosphorylation and dephosphorylation of the channels therefore shape the electrical potential induced by those ligands depending on the cell's prio-experience, which is critical for the long-term potentiation and depression (LTP and LTD) underlying the learning and memory (Aschroft, 2000).

Intracellular ligand gated channels are mainly regulated by intracellular messengers and intermediary metabolites. Each channel has its specific ligand such as cyclic nucleotides for the CNG channel, ATP for the K_{ATP} channel, G-proteins for the GIK channel, protons for the ROMK channel, and Ca^{2+} for the MthK channel. They have regulatory mechanisms similar to those of extracellular ligand-gated channels. Phosphorylation by PKA, PKC, and protein kinase G (PKG) can augment or reduce channel activity. Protons have been found to play a role in the activity of a variety of channels. Phospholipids such as PIP_2, phosphatidylinositol 3,4,5 triphosphate (PIP_3), and long-chain acytyl–CoA are general regulators of intracellular ligand-gated ion channels (Hilgemann et al., 2001). These membrane lipid molecules have been found to play a key role in channel activation and prevention of channel rundown. They may work on the open gate to set a range for open probability. These molecules may control channel sensitivity to other messengers by allosteric regulation (Du et al., 2004,). In addition, most intracellular ligand-gated ion channels are regulated by multiple compounds besides their specific ligands.

F-II. Current understanding of ligand channel interaction and gating mechanisms

F-II-1. Protein structures Channels allow certain ions to pass through the plasma membrane along their electrochemical gradients. To fulfill this function, an ion channel must have a conductive pathway that is selective to certain ion species, and a mechanism to control the opening and closure of the ion-conduction pathway.

Protein structure of most extracellular ligand-gated channels is not resolved except the Cys-loop superfamily that includes nicotinic Ach receptors, 5-HT_3 receptors, $GABA_A$ and $GABA_C$ receptors, and glycine receptors. These receptors consist of four transmembrane domains with both N- and C-termini located on the extracellular side. The ligand binding domain is in the N-terminus. The hair-pin loop formed by a disulfide bond between two cysteine residues in the N-terminus is the signature structure of this superfamily which is important for ligand binding. Channels in this superfamily share similar secondary and tertiary structures in their extracellular domains, although their primary structures show limited homology (Deane and Lummis; 2001, Jin et al., 2004). Five TM2 transmembrane helices form the pentameric ion permeable pore in the membrane. The TM2 helices bend outward, so both anions and cations appear to be able to access the outer end of the pore (Akabas et al., 1992). The ion charge selectivity of the channel is determined by the intracellular end of the TM2 region extending to the TM1-TM2 cytoplasm loop (Wilson et al., 2001). A second barrier to ion flow is formed by the intracellular loop between the third and fourth transmembrane domains (TM3-TM4). Five loops form a cytoplasmic vestibule, and charged residues that line this tunnel determine which kinds of ions can be transported efficiently (Miyazawa et al., 1999). In the Cys-loop superfamily of ligand-gated ion channels, ligand binding to the interface of the extracellular ligand binding domains causes an asymmetric structural change within the extracellular domains and distal region. During channel opening, the five subunits, however, undergo a gating movement at the same time. How the asymmetrical binding is transferred to the symmetrical gating is not clear.

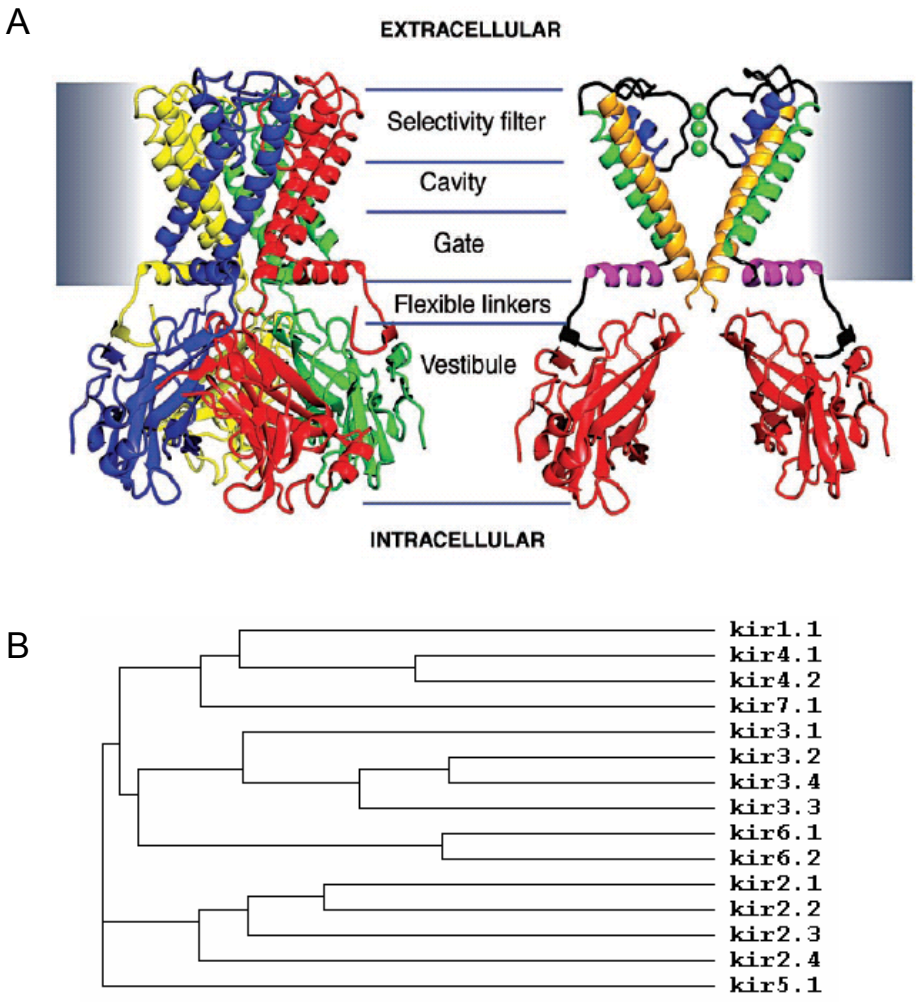

Fig. F-1. Crystal structure of the KirBac1.1 channel (***A***, Kuo et al., 2003) and the phylogenetic tree of mammalian Kir channel family (***B***). The KirBac1.1 channel is composed of four identical subunits with each of the subunit possessing intracellular N- and C- termini, transmembrane TM1 and TM2 helices and a pore loop. The ion permeable pathway formed by the interface of four subunits can be divided into five parts: the selectivity filter, central cavity, gate, flexible linker, and cytoplasmic vestibule. Sequence alignment of this channel with mammalian Kir channels shows high similarity.

The knowledge about intracellular ligand-gated channels is obtained mostly from bacterial K^+ channels. A view of the channel structure in different states can be obtained by comparing the K^+ channel from *Streptomyces lividans* (KcsA), bacterial inward rectifier potassium channel 1.1 (KirBac1.1), and MthK structures (Roux and Mackinnon, 1999; Jiang et al., 2002b; Kuo et al., 2003). These channels have two transmembrane domains linked by a pore loop. The short N-terminus and the long C-terminus located in the cytoplasm comprise two thirds of the entire AA sequence. The ligand binding sites are located at the C-terminus for most intracellular ligand-gated ion channels. The membrane regions of the channels are composed of all α-helices, and the intracellular domains consist of mostly β-sheets. Structurally, these channels can be divided into five parts: the selectivity filter, central cavity, gate, flexible linker, and cytoplasmic vestibule (Fig. F-1A). The selectivity filter is formed by four pore loops from the tetrameric channel, which determines the ion selectivity. The filter is so perfectly arranged that the K^+ channel allows the flow of only 1.33Å K^+ ions but not 0.95 Å Na^+ ions. The central cavity is the widest part of the pore region. The diameter of the cavity is ~10 Å in the closed state and can hold 20 water molecules. It is enlarged and can hold 27 water molecules in its open state. The greatest changes in the channel gating process come from the bundle-crossing region where the gate is likely to be located. The diameter of this region can vary from 3.5 Å to 12 Å during channel opening. A ring of hydrophobic residue, i.e., phenylalanine, restricts the pore size in its closed state and is thus acts as the activation gate. The linker region between the transmembrane domain and cytosolic domain is known to be flexible in the KirBac1.1 channel, although it is not resolved in

the MthK channel. Therefore it is unknown what its conformation would be during gating. The eight ligand binding domains of the MthK channel form a four-fold symmetric vestibule in the cytoplasm which is called the gating ring. The gating ring is ~20 Å after Ca^{2+} binding and provides a wide path for ions to flow through the pore. A comparison of the structure in open and closed states shows that gating of these channels includes changes in the selectivity filter, pore helices, central cavity volume, and gate.

F-II-2. Structure-function Characteristics Two characteristics of ion channels are ion-selective permeability and event-dependent gating. Ion selectivity is known to be mediated by the selectivity filter, while the gating mechanism is less clear. Most ion channels are composed of multiple subunits or multiple repeats from a single subunit. The interface among subunits or internal repeats lines the ion conductive pathway. Ionic flow through the pathway is controlled by two mechanisms: the selectivity filter located at the extracellular entrance of the channel, and the inner gate that controls the opening and closure of the ion permeable pathway, although the location of the gate is still under debate.

The ion selectivity filter determines which ions can pass through. All channels discriminate one or a few ions against others. The electrical signals and ion gradient cannot be generated without such discrimination. The mechanism for ion selectivity is much more complicated than ion radius, since the K^+ channels do not allow the flow of Na^+ ions although Na^+ is smaller than K^+. Based on the understanding of K^+ channels, the main chain carbonyl oxygen atoms of conserved AA in all K^+ channels, i.e., TXGYG or TXGFG (the signature AA sequence of K^+ channels), form the selectivity filter. The

bulky residue is critical for structural stability of the filter by packing against the aromatic residues in the pore loop, preventing it from collapse. The glycine provides rotational flexibility for the filter and allows all the carbonyl groups of the signature sequence to face toward the ion pathway. In an aquatic medium, K^+ exists as a complex with six to eight water molecules when they approach the selectivity filter. The positive charge of the K^+ ion attracts the negative end of the water molecules. The water molecules provide energy stability of the K^+, while together they cannot move through the selectivity filter. To solve the problem, a strategy is developed in ion channels to separate K^+ from water by creating an environment similar to aquatic media. The oxygen atoms of backbone carbonyl groups in the highly conserved Val-Gly-Tyr-Gly sequence point toward the center of the ion pathway. With 16 oxygen atoms from four subunits, the selectivity filter forms three K^+ cages with each of them having eight oxygen atoms that resemble water molecules surrounding a K^+. The dehydrated K^+ therefore can be easily transferred into the ion pathway with little or no energy barrier. This creates a mechanical bias against other ions because these carbonyl oxygen atoms are perfectly positioned for K^+ ions, but are too far or too close for other ions that are smaller or bigger (Mackinnon, 2004).

After passing the selectivity filter, the conduction of ions is controlled by the gating mechanism. The gating movement for different channels varies, although all channels share the same strategy by modifying the diameter of the ion conductive pathway. The pore lining helices move toward the center axis during channel closure. When they are close enough, the pore is blocked leading to channel closure, and vice versa for channel opening. During channel closure, accession of ions to the pore is

occluded by hydrophobic interactions of pore-lining residues. In the MscL channels and the nicotinic ACh receptor, two rings of hydrophobic side chains take part in the action (Perozo et al., 2001; Miyazawa et al., 2003). In KirBac1.1 and K_{ATP} channels, this gate may be formed by four phenylalanine residues from four subunits, referring to activation gate. This bulky residue in the K_{ATP} channel not only restricts the passage of the K^+ ions but also lowers the energy for the transition of the channel between open and closed states by preventing interaction of a series of hydrophobic residues surrounding Phe168 (Rojas et al. AJP in submission). Each type of channel exhibits different major movements during gating transition, and in all case the transmembrane helices move as rigid bodies. During channel gating, the pore lining TM1 helices of MscL channel are tilted from ~30º to ~70 º with respect to the central axis. The TM1 helices are widened from the central axis by an iris-like movement that changes the pore size from 2 Å to 35 Å. The channel conductance becomes ~2.5 nS when the channel is open (Cruickshank et al., 1997; Chang et al., 1998; Sukharev et al., 2001; Perozo et al., 2002). The pore lining TM2 helices of the ACh receptor undergo a ~15º clockwise rotation during channel opening (Unwin, 2003). A view into the gating movement of the two transmembrane domain-K^+ channels is obtained by comparing the crystal structure of the KirBac1.1 and MthK channel. A glycine in the inner helices serves as a hinge after the selectivity filter. The inner helices bend at the hinge after ligand binding and remove the hydrophobic gate from the ion permeable pathway (Jiang et al., 2002b; Kuo et al., 2003). It is possible that the inner helices also experience a rotational as well as translational movement during the gating process (Perozo et al., 1999).

F-II-3. Ligand binding domains The ligand binding domain constitutes a large part of the entire AA sequence of channels. In extracellular ligand-gated channels, ligand binding takes place at the N-terminus, for which the structure is best understood in the nicotinic Ach receptor (Sixma and Smit, 2003). Based on the crystal structure, the five subunits of the pentameric nicotinic Ach receptor assemble as a channel with αγαδβ subunits being arranged in a counterclockwise order. The extracellular ligand binding domain has been observed to form a doughnut-like structure with a radius of ~80 Å and height of 62 Å. The residues forming two Ach binding pockets have been revealed by mutagenesis and substitute cysteine accessibility method to be located at the interface of the α subunits and the neighboring γ or δ subunits. For each of the binding pocket, three loops (loop A-C) from the α subunit provide the principle binding sites and the neighboring subunits contribute another three loops (loop D-E). All these loops form a single pocket at the interface to hold the ligand. The aromatic residues from loop A to D line the pocket and the hydrophobic residues in loop E cover the pocket like a lid. Both ligand binding pockets are located toward the outside of the pentameric channel. The aromatic ligand cage has been suggested to contract after ligand binding. The β-sheets of the α subunits move with respect to each other to cause a conformational change. This conformational change propagates along the ligand binding domain like a wave with the change being largest at the ligand binding site and becoming gradually smaller during its propagation toward the gate. The movements of the non-ligand binding subunits are not clear, but they appear to be asymmetric. The structure of other extracellular ligand-gated

channels is less clear, but the tertiary structure of the binding domain is conserved even though their primary sequences show low similarity.

The binding domain for the intracellular ligand gated channels has been well studied in the prokaryotic cyclic nucleotide regulated K^+ channel (Clayton et al., 2004). This channel consists of six transmembrane domains with the C-terminus immediately after the last transmembrane region forming the cyclic nucleotide binding (CNB) domain. The CNB domain was crystallized in the presence and absence of ligands. The structure of CNB pocket is conserved, and includes a wide antiparallel β roll topped by three interacting helices. They are two C-linker helices $\alpha_{A'}$ and α_A and the C-terminal tail helix α_B. The mouth of the nucleotide cavity is large, and it is covered by the α_C helix from the C-terminal tail as a lid. Ligand binding is therefore stabilized by the lid. Interestingly, the two C-linker helices interact with the same region from different subunits by their hydrophobic residues and tend to dimerize the subunits. Without ligand binding, the structure of β rolls does not show any changes, while rearrangement of the helices following ligand binding has been revealed by the crystal structures. The αC helix moves away from the mouth of the nucleotide cavity, and the C-terminal end of the αB helix swings away from the β roll. The rearrangement also causes changes in the dimer interface and tetramers have been shown in the protein migration with ligand binding. As a result, the conformational change of all ligand binding domains may lead to an enlargement of the intracellular vestibule of the ion permeable pathway, similar to the MthK channel (Jiang, et al., 2002b).

F-II-4. Putative gates Ion flow through the channel is controlled by opening and closure of the pore. Based on the crystal structure of the KirBac1.1 channel, four strategies have been developed to restrict the conduction of ions. First, the ion is occluded from the permeable pathway by reduction of the activation gate (Kuo et al., 2003). Four hydrophobic residues, e.g., phenylalanine, move close enough to reduce the pore size to less than 4 Å, which shuts off the channel and prevents the passage of any ions. This hydrophobic gate has been widely identified in a variety of ion channels and is believed to be the major gating mechanism underlying the regulation by ligands and other signal molecules. Second, occlusion of the ion conduction pathway leads to a decrease in the volume of the central cavity, the largest water-filling part after the selectivity filter in the channel pore (Roux and Mackinnon, 1999). Ions are destabilized by reducing the number of water molecules during channel closure impeding the conduction of ions through the channel. Third, the pore helices of channels have been found to undergo rotational movement during the transition between channel open and closed states, which causes the misalignment of the pore helices and is unfavorable to ion passage (Kuo et al., 2003). Finally, evidence for the effect of misalignment in the pore helices on ion passage has been found in the selectivity filter (Liu and Siegelbaum, 2000; Kuo et al., 2003). The filter is such a delicate device whose geometric dimension and special AA residues determine what ions can pass through. A slight conformational change will affect the ion conduction pathway. Studies on other channels indicate that the selectivity filter may also serve as a second gate for the channel gating.

The potential role of the filter as a gating mechanism was first raised by studies of the voltage-gated K^+ channel (Kv). The selectivity filter in this channel has been suggested to be involved in the C-type inactivation (Lopez-Barneo et al., 1993). Further supporting evidence is found from the CNG, in which the selectivity filter changes its structure by rotating the pore helices by 100º to 180º during gating (Sun et al., 1996; Liu and Siegelbaum, 2000). Using the substituted-cysteine accessibility screening method, three of the pore helix residues are found to be only accessible to hydrophilic sulfhydryl-reactive methanethiosulfonate (MTS) reagent in the closed state, while one residue located at the opposite side of the pore helix is only accessible in the open state (Liu and Siegelbaum, 2000). A similar phenomenon has been found for the Kir6.2 channel modulation by Ba^{2+} (Proks et al., 2003). Ba^{2+} can still access its binding site at the selectivity filter when the channel is shut off. These studies can not be used as evidence against an inner gate, since the effect may result from the MTS regent or Ba^{2+} that is trapped in the inner cavity when the channel is closed. Further studies in the Kir channel indicate that gating of K_{ATP} channels includes multiple-components (Trapp et al., 1998b; Tucker et al., 1998; Loussouarn et al., 2000). Without a modulator, the channel undergoes spontaneous bursting separated by long closure states. Flickering activities characterized by rapid opening and closure are seen during the bursting. The transition between bursting and long closure refers to slow gate, and is regulated by ligands such as ATP, MgADP, and sulphonylureas (Alekseev et al., 1998; Trapp et al., 1998b). This gate is located at the inner mouth of the channel pore. The intraburst flickering activities are

controlled by fast gate which is affect by the voltage and extracellular K^+ ions, indicating a close correlation to the selectivity filter.

The gate in the extracellular ligand-gated channel is poorly studied. It is located below the filter in those channels that belong to the cys-loop superfamily, since both anions and cations can access the filter (Reeves et al., 2001). The role of the selectivity filter in channel gating is not known. Two rings of hydrophobic residues serve as gates in the nicotinic ACh receptor, which move toward the center of the channel pore during channel closure. The inner vestibule formed by the TM3 and TM4 loop may potentially serve as another gate. The length of this loop varies in different channels (Connolly and Wafford, 2004).

F-II-5. Events in channel gating In ligand-gated ion channels, the channel gating process starts with the binding of the ligand to its specific binding domain in the channel protein. In the MthK channel, eight ligand binding domains form the gating ring, which is enlarged after the Ca^{2+} binding. Ligand binding produces a lateral extension force to stretch open the ion permeable pathway (Jiang et al., 2002b). The gating is much more complex if the data obtained by other studies are considered. The formation of the ligand-channel complex causes a conformational change in the ligand binding domain. This signal is then transferred or coupled through a series of conformational changes and eventually causes the channel gating movement in the inner mouth of the pore. A number of events occur during signal transduction and coupling. According to the crystal structure of the KirBac1.1 channel, not only the C-terminus but also the N-terminus experiences movement during gating. The helix of the N-terminus moves laterally, and

the outer helix follows moving away from the central axis, making room for the inner helix to bend (Kuo et al., 2003). What causes these movements is unknown. The interaction of the slide helix with a conserved Arg at the end of the inner helix may make a contribution. Interaction between the N- and C-termini has also been demonstrated in a number of channels with different domains (Tucker and Ashcroft, 1999; Qu et al., 2000; Lin et al., 2003). Properties of these interactions have not been studied. It is supposed to be a dynamic event since the gating itself requires a fast, transient, and reversible transition between the opening and closure states.

Most channels are composed of multiple subunits. The gating transition is speeded up by this design, since subtle conformational changes in each subunit cause large alterations in the pore located at their interface, and the process can be easily reversed (Doyle, 2004). Multimeric channels with the pore located at the center have their advantages over monomeric proteins, e.g., transporters, but they also have problems. Coordination and cooperation are necessary for the movement of multiple subunits. Coordination may be critical especially for heteromeric channels since gating requires movement of all subunits at the pore region, while not every subunit carries a ligand binding site (Unwin, 1995). Synchronization of subunit movements during channel gating therefore requires subunit coordination. For some channels, the gating transition of individual subunits is not independent (Niu and Magleby, 2002; Drain et al., 2004). The activation of neighboring subunits may make the transition easier or more difficult, which refers to subunit cooperativity. Also it is likely that not all subunits are required to activate the channel gating. Subunit coordination and cooperativity may allow the

channel to be activated even though one or more subunits have defects. These transient events in binding-gating coupling are largely unknown. Even the differentiation of ligand binding from channel gating is not clear.

F-II-6. Functional subunit requirement for channel gating Because ion channels are encoded by genes on two alleles in the chromosome, mutations on these genes cause defects in these channels in various degrees. Mutations can cause defect in gene expression. For some of these mutations, heterozygote carrying mutant gene on one allele in the chromosome is enough to cause channel dysfunction, which refers to dominant trait. However, not all of the mutations have such an effect. For some channels, the protein expressed by one allele is enough to maintain normal function. Therefore subjects carrying the mutations on one allele of channel genes do not show the disease phenotype, referring to the recessive trait (Srivastava et al., 1999). For most mutations in ion channels, both alleles can be expressed in heterozygous individual, which is known as incomplete dominant or codominant trait and allows expression of channels in different combinations of mutant and wild-type subunits (Markworth, 2000). Certain gene mutations take place in protein domains that are so crucial that one subunit carrying the mutation is enough to silence an entire multimeric channel, known as dominant-negative effect. For instance, mutations at the selectivity filter region can completely eliminate the ion flow, which has been widely used in channel knockouts. One type of Bartter's syndrome found in humans is produced by dominant negative mutations in the Kir1.1 channel (Kunzelmann et al., 2000). In some other channels, patients carrying heteromeric

channel show weak or normal phenotype, producing partial or even full functional channels when one or more subunits are defective.

Functional channels with partial gating machineries in certain subunits are also found in the heteromeric channels. Heteromeric channels consist of asymmetric subunits. For the extracellular ligand gated ACh receptors, ligand binding sites are only located at the interface of α subunits with γ or δ subunits. However, the channel pore undergoes symmetric movement after ligand binding. The subunit that is free of ligand binding is activated by unknown mechanisms (Sixma and Smit, 2003). A similar phenomenon is also seen in intracellular ligand-gated heteromeric channels (Xu et al., 2000b; Pessia et al., 2001). Heteromeric Kir4.1 and Kir5.1 channels are inhibited by intracellular acidification. The pH sensitivity of the heteromer depends on a lysine residue located at the conjunction part of the N and C termini of the Kir4.1 subunits. Mutation of the Lys67 to a methionine eliminates the pH sensitivity of the heteromeric channel (Xu et al., 2000b). Switching these two lysine residues from Kir4.1 to Kir5.1 subunits keeps the pH sensitivity intact (Pessia et al., 2001). These data suggest that two subunits carrying intact pH-dependent gating machineries appear to be enough to operate the gating of the whole channel. Therefore, it is likely that some subunits may not make extra contributions to the gating of certain multimeric channels. It is not clear what underlies this phenomenon. Therefore questions arise as to what is the minimum requirement of functional subunits for the channel gating, and how many subunits are needed for full function of the gating mechanisms. The multimeric strategy may allow ion channels to function in the fast, transient and reversible gating process by operating with a few rather than all subunits.

Another benefit brought by this strategy may be the preservation of channel function when mutation occurs in some of the subunits

F-II-7. Subunit cooperativity of channels Cooperativity was first described by Bohr who studied the binding of oxygen to hemoglobin. He observed a sigmoid binding curve and explained that the binding of the first oxygen molecule made it easier for the second one to bind (Bohr, 1903). Several theories have been developed to describe the interaction between protein subunits. Hodgkin and Huxley developed a theory to describe the voltage-dependent channel gating. They postulated that there are four identical and independent voltage sensors in this channel. The channel opens only when all four subunits are in the open state. This model indicates that subunits are independent, and there is no cooperativity in the transition between different subunit conformations (Hodgkin and Huxley, 1952). The HH model has been successfully used in ion channel studies.

Another theory was developed by Monod, Wyman and Changeux (MWC model, Monod et al., 1965) in their study of enzymes. The interaction between the identical ligand binding sites of an enzyme is regarded as homotropic interaction, and that interaction between different ligand binding sites is designated as heterotropic interaction. The Allosteric interaction refers to the interaction of a ligand binding site with another functional site that is completely separate from the binding site. This separate site can function as another ligand binding domain in receptors, catalytic site in enzymes, and opening or closure control in ion channels. The heterotropic effect can be positive or negative in terms of changes in the second ligand binding, which could be

easier or more difficult (positive cooperativity and negative cooperativity respectively). Positive cooperativity is widely observed. Mutations altering the heterotropic interactions also spontaneously change homotropic interactions of the same binding sites. The MWC model of positive cooperativity is also known as “concerted” or “two state” model. This model assumes that a protein has two conformations, namely, T (tension) for the unliganded bound state and R (rest) for the ligand-bound state. There are no intermediate conformations. The whole system can be completely switched between T and R states depending on ligand binding. The model proposes that all subunits of a protein undergo a single concerted change to preserve the symmetry of the molecule when it transits from one conformation to another. The MWC model only considers positive cooperativity, which has been widely used to describe enzyme activity or receptor-ligand interactions.

An alternative theory described by Koshland, Nemethy and Filmer (KNF) model argues that the conformation of a protein can be changed by individual ligand binding, and each ligand binding distorts the conformation of the subunit. Conformational changes occur as a result of ligand binding to an individual subunit in an induced-fit fashion, which in turn causes consequential conformational changes of other subunits within an oligomer (Koshland et al., 1966). The KNF model allows the existence of mixed oligomers with individual subunits in either T or R states. Several intermediate states may exist with the combination of subunits at different states. However, there are only two states for each individual subunit. Negative cooperativity is suggested when the interaction of T-R states is stronger than the T-T or R-R interactions. On the other hand, positive cooperativity exists when the T-T and R-R interactions are stronger than the T-R

interaction (Koshland et al., 1966). Positive cooperativity amplifies the ligand sensitivity of the protein. The physiological significance of negative cooperativity is not clear, although a large number of negatively cooperative enzymes have been conserved during evolution (Koshland and Hamadani, 2002).

Cooperativity is usually considered as a specific case of allosteric interaction between binding sites. For channels with multiple binding sites, allosteric transition could be regarded as the transfer of information from a ligand-bound site to a non-bound site. This could result in a change in the intrinsic binding affinity of the second site (Harman, 2001). Subunit cooperativity may dampen or raise the energy barrier for reaching and stabilizing a particular state in the channel (Pugh, 1996). Similarly, cooperativity is likely to exist in the channel gating. Activation of the first subunit may change the energy requirement for the gating transition of the second one. Molecular mechanisms underlying the subunit coorperativity are not clear. Full understanding of these mechanisms may depend on information of the tertiary structure of proteins and on the functional assays.

F-II-8. Subunit coordination One benefit from multimerization is that the multimeric proteins may gain certain physiological advantages through subunit coordination. As shown in heteromeric channels, binding of a limited number of ligands activates all subunits whether with or without ligand binding sites. The molecular basis for the subunit coordination is subunit interaction. This interaction seldom depends on covalent bonds. Hydrophobic residues always form the interface of subunits and bring them together in plasma membranes. Hetero- or homomultimers have been demonstrated

in most ion channels and receptors. The multimerization of these channels undergoes regulation by ligand binding. Without ligand binding, dimers are obtained in the prokaryotic cyclic nucleotide dependent K^+ channel, while tetramers form in the presence of the ligand (Clayton et al., 2004). Subunits acting as functional dimers have also been suggested in the functional assays in the eukaryotic CNG, HCN, and Kir1.1 channels (Liu et al., 1998; Ulens and Siegelbaum, 2004; Wang et al. 2005b). It is possible that the coordination of subunits exists in channels as a cost-efficient way for ligand regulation and channel gating.

F-II-9. Potential coupling mechanisms Ligand binding and gating machineries are known to be separate in most ion channels. The ligand binding domain is located on the N or C termini, and the ligand-regulated channel gate is located at the intracellular end of the pore forming helices. Ligand binding needs to be coupled to the gating movement, which is carried out by a series of conformational changes. Rearrangement of the ligand binding domain and linker region has been demonstrated in a number of channels. Based on the crystal structure of the KcsA, Mthk, and KirBac1.1 channels (Roux and Mackinnon, 1999; Jiang et al., 2002b; Kuo et al., 2003), the binding of a ligand leads to the gating movement within the same subunit. This intrasubunit binding-gating coupling has also been reported in voltage sensing and channel opening of the Kv channel (Labro et al., 2005). However, intersubunit interaction may also exist in a number of channels. Also subunit coordination and cooperativity are always observed in channel kinetics. Therefore a question has been raised as to whether the coupling of

ligand binding to channel gating occurs within the same subunit or between adjacent subunits.

The problem of binding-gating coupling is far beyond the debate about inter- versus intrasubunit coupling. The ligand binding domain and the intrinsic gate are linked by a flexible peptide with the β-sheet as secondary structure (Kuo et al., 2003). It is thus unlikely that the force produced by the conformational change of the ligand binding domain will propagate to the pore lining helix directly and open the gate. The crystal structure of the KirBac1.1 channel supports the idea of transduction of the force through its TM1 helix. This transmembrane region located behind the pore lining TM2 helix is connected to the N terminus by the slide helix. Movement of the slide helix may stretch and swing the TM1 helix away from the central axis. The crystal structure shows that the N terminus directly contacts the C terminus of the neighboring subunit (Kuo et al., 2003). The original force to move the slide helix thus appears to come from the conformational change of the ligand binding domain. The slide helix interacts with a conserved arginine of the lower TM2 helix in the KirBac1.1 channel, which may eventually transfer the movement to the pore lining helix. Another possibility is that the lower TM1 and TM2 helices also interact with each other and help with the gate opening since they are so close around the bundle cross region. Further studies are needed to evaluate this possibility.

F-III. Insight with heteromeric subunit recombination

F-III-1. Problems and disadvantages of current approaches The most powerful method for understanding channel structure is X-ray crystallography. This method resolves the structure of proteins by analyzing the X-ray diffraction pattern when a beam of X-ray is directed onto the well-ordered crystal of proteins. Growth of crystals is essential for this method, which has been shown to be difficult for membrane proteins such as ion channels. The membrane regions of ion channels form the important part, e.g., the selectivity filter and gate. Without plasma membrane, the crystal structure of the channel may not grow correctly. Result explanation should consider the potential distortion of the crystal. X-ray crystallography has also been successfully used to understand channel gating mechanisms in MthK and KirBac1.1 channels (Jiang et al., 2002b; Kuo et al., 2003). Some basic information has been obtained. However, channel gating is much more complicated than that suggested by comparing crystal structure of the open and closed states. Gating is a dynamic process that involves a series of events from ligand binding to channel gating. The propagation of conformational changes starting with ligand binding is fast and transient. The transition between channel opening and closure occurs in microseconds, which makes it impossible to be detected by X-ray crystallography. Also, channel gating regulated by membrane lipids, proteins, and cytosolic signal molecules. The gating mechanism cannot be fully resolved without considering these factors.

This dynamic movement in channel gating can be approached by two other methods. The difficulty of growing crystals for X-ray crystallography is avoided with

nuclear magnetic resonance (NMR), which does not require crystal structure and can be used to obtain dynamic information about the ion channel. However, its resolution is far from satisfactory as X-ray crystallography is, and therefore structural details cannot be resolved by NMR. Besides, NMR is limited to proteins smaller than 35 kDa. Another approach developed recently is fluorescence resonance energy transfer (FRET). By detecting changes in fluorescence of protein labeled by the donor fluorophore transfers its energy to the protein labeled with the acceptor fluorophore, FRET can detect the respective movement of two protein domains occurring between 10-100 Å. The problem with this method is that the distance between two protein domains cannot be accurately quantified. Thus it only detects the presence or absence, but not the degree of protein interaction.

Channel opening and closure result in ionic currents. Patch-clamp and voltage-clamp are still the most efficient ways to detect changes in ion currents across membranes. Channel opening and closure can be revealed by single channel recordings using the patch-clamp technique (Hamill et al., 1981). The high frequency response of this technique allows detection of highly dynamic electrical changes with resolution of microseconds, which is necessary for the study of ion channel gating. The understanding of channel properties at present largely depends on data obtained by combination of patch-clamp and mutagenesis studies on the homomeric wild-type (wt) or mutant channels.

F-III-2. Advantage and potential pitfalls of heteromeric recombination The channel gating process involves asymmetric movement of multiple subunits. The

transition of the gating movement in asymmetric heteromeric channels is not expected to be completely symmetric. Even for the homomeric channels, not all ligand binding sites can be occupied when ligands levels are low. The asymmetric movement of subunits has also been indirectly demonstrated in some studies. Four subunits without ligand have been found to exist as dimers in protein purification experiments (Clayton et al., 2004). The assembly of the protein subunits is different in the presence or absence of ligands. This transient asymmetric movement may not be fully understood using the homomeric channels. Also studies on homomeric channels cannot address questions as to what is the minimum number of functional subunits required for channel gating; how subunits coordinate and cooperate with each other; and whether ligand binding is coupled to gating within the same or through an adjacent subunit. Heteromeric channels that lack ligand binding or gating machinery in different number of subunits are necessary for answering these questions.

The time course of this transient asymmetric movement of different subunits may be amplified by mutating ligand binding or gating machinery in part of the subunits. The contribution of each individual subunit can be evaluated by comparing the channel activity of heteromeric channels with different number of functional subunits. This comparison can also generate information about subunit coordination and cooperativity. However, heteromeric recombinant studies are difficult to be performed with X-ray crystallography since crystallization of dozens of heteromeric channels would be a great task when the researchers are still struggling with even a single one. NMR and FRET can be used, but the resolution is compromised. In addition, frequency response is also a

limitation for these two techniques. Patch-clamp therefore remains to be the most feasible and cost-efficient approach in studying heteromeric recombinant channels.

F-III-3. Kir channels as subject for the study in gating Kir channels were used in these studies for several reasons. First, Kir channels have the simplest structures among characterized eukaryotic channels. These channels are tetramers with each subunit having two transmembrane domains linked by the pore loop. The short N terminus and the long C terminus located in the cytosol are subject to regulation by intracellular signals. The protein sequences of these channels are only several hundreds of AAs, which makes them easier to be manipulated in DNA and RNA reconstruction. Second, high resolution X-ray crystal structures of bacterial channels with two transmembrane domains are available. The two transmembrane regions of the KcsA and MthK channels including the cytosolic N and C termini and the KirBac1.1 channel are resolved (Roux and Mackinnon, 1999; Jiang et al., 2002b; Kuo et al., 2003). The structure of the mammalian Kir3.1 cytoplasmic domain is also known (Nishida and Mackinnon, 2002). Sequence alignment of the KirBac1.1 channel with Kir channels has revealed high similarity, which makes it easier to link the functional study with relevant channel structure. Third, Kir channels are crucial for controlling cellular excitability, vascular tone, cardiac and skeleton muscle contraction, insulin secretion, and K^+ secretion and reabsorption in the kidney. Dysfunction of these channels causes diseases in the brain, ear, heart, muscle, and pancreas, and developmental abnormalities in crest-derived tissues (Andersen syndrome) (Ashcroft, 2000). Studies of these channels will improve the understanding of these diseases and shed light on their therapeutical potentials.

F-III-4. The Kir channel family and their regulatory mechanisms Kir channels are composed of seven subfamilies (Kir1-7, Fig. F-1B). Channels in the Kir family are characterized by their capability of allowing a greater influx of the K^+ ions than efflux. This inward rectification is caused by the rapid and voltage-dependent block of intracellular polyamine and Mg^{2+} ions. Strong inward rectifiers are sensitive to polyamine modification at high voltage levels such as Kir2.1 and Kir3.1. Weak rectifiers such as Kir1.1 and Kir6.2 are not so sensitive to polyamine, allowing relatively large outward currents. Heteromeric channels composed of Kir3.1/Kir3.4 (Krapivinsky et al., 1995) or Kir4.1/Kir5.1 (Pessia et al., 1996) have intermediate sensitivity to polyamine.

Kir channels are regulated by protein kinases. Protein kinase A (PKA) modulates almost all Kir channels by stimulating their currents, while the phosphorylation sites are not identified in their primary sequences. Regulation of the channel activity by PKA may be indirect through other messenger molecules. The Kir2.1 and Kir2.3, Kir3.1/Kir3.4 heteromer and Kir6.2 channels (Henry et al., 1996; Light et al., 2000; Mao et al., 2004) are also regulated by protein kinase C (PKC). The PKC phosphorylation sites have been identified in the Kir3.1, Kir3.4 and Kir6.2 channels.

In contrast to the indirect effect of protein kinases, most Kir channels are directly modulated by pH. Kir channels such as Kir1.1, Kir2.3, Kir4.1 and Kir4.1/Kir5.1 heteromer are inhibited by intracellular acidification, while the currents of Kir6 channels are stimulated by low pH (Jiang et al., 2002a). Kir6 channels are identified in pancreas, vascular smooth muscle, cardiac and skeleton muscle, and neurons (Seino, 1999). Activation of these channels during hypoxia inhibits the cellular excitability of these

cells, which may have protective effects. The heteromeric Kir3.1 and Kir3.4 have been found to be colocalized in postsynaptic membranes with inhibitory neurotransmitter receptors (Liao et al., 1996). The acidic pH resulted from transmitter release active these channels, which may enhance the effect of inhibitory neurotransmitters (Mao et al., 2002).

Another general regulator of Kir channels is phospholipids. Among them, the most important one is phosphatidylinositol-biphosphate (PIP_2). PIP_2 is broken down by PLC, which links the Kir channel activity to neurotransmitter receptors such as muscarinic Ach receptor, Substance P receptor, and other neurotransmitter and hormone receptors that can be coupled to G proteins (Jan and Jan, 1997; Lei et al., 2003). The spontaneous opening of Kir channels appears to depend on their PIP_2 sensitivities. The channels with high PIP_2 sensitivity are likely to have a higher opening probability such as Kir1.1, Kir2.1, Kir2.2, Kir 4.1 and Kir 4.1/Kir5.1 heteromer (Du et al., 2004). Low open probability (P_{open}) is shown for channels with low PIP_2 sensitivity, e.g., Kir6.2. Membrane lipids may activate channel gating by anchoring the intracellular domains on the cell membrane.

Some Kir channels have specific regulators. For instance, GIRK (Kir3.x) channels are activated by the βγ subunit of trimeric G proteins (Logothetis et al., 1987), and K_{ATP} channels are inhibited by intracellular ATP. The sulphonylurea receptor is an accessory subunit of K_{ATP} channels. With this subunit, ATP sensitivity of the channel is greatly increased. This subunit also underlies the mechanism of regulation of Kir6.2 channels by ADP and other blockers and openers (Seino, 1999). Kir 1.1 and Kir6.2

channels were used in the study since their regulatory mechanisms have been well studied. The following studies on channel gating mechanism thus can be based on this knowledge about ligand binding and gating sites.

G. SIGNIFICANCE

Ion channels are characterized by two functions: ion-selective permeability and event-dependent gating. Gating mechanisms are incompletely understood although progress has been made over past 5-6 years through X-ray crystallography and mutagenesis studies of homomeric channels. A number of questions remain to be addressed: what is the minimum number of subunits required for channel gating and ligand binding; how ligand binding can be differentiated from channel gating; whether four subunits act independently or cooperatively in ligand gating; whether there is specific subunit coordination between subunits in ligand binding and channel gating; how ligand binding is coupled to channel gating; and what determines gating after specific ligand binding. I proposed to address some of these questions using Kir1.1 and Kir6.2, because of their less complicated protein structures and well defined functional properties. We proposed to study 1) the stoichiometry for ligand binding and channel gating, 2) differences between ligand binding and channel gating and binding-gating coupling using the heteromeric Kir6.2 channel, and 3) the role of membrane helices in determining channel gating by manipulating two residues at the interface of the TM1 and TM2 of the Kir6.2 channel. I chose to use heteromeric channels, since the above questions can not be answered with homomeric channels that are currently widely used in ion channel studies. The subunit stoichiometry studies in heteromeric channels will also generate information about subunit coordination, cooperativity, and minimum requirement of functional subunits for ligand binding and channel gating. Since the mechanisms for channel gating may be shared by some channel families, results obtained

from Kir1.1 and Kir6.2 channels will have impact on our understanding of the function and modulation of other ion channels as well. My work will not only improve our understanding of ion channels but also may facilitate the design of therapeutical modalities to enhance or suppress the channel activity by targeting specific ligand binding, channel gating, or binding-gating coupling mechanisms.

H. METHODS AND MATERIALS

H-I. *Xenopus* oocyte and expression systems

Frog oocytes were obtained from *Xenopus* laevis as described in our previous study (Chanchevalap et al., 2000; Xu et al., 2000a; Mao et al., 2003). In brief, frogs were anesthetized by bathing them in 0.3% 3-aminobenzoic acid ethyl ester. A few lobes of ovaries were removed after a small abdominal incision (~5 mm). Then, the surgical incision was closed and the frogs were allowed to recover from the anesthesia. *Xenopus* oocytes were treated with 0.5mg/ml of collagenase (Type I, Sigma Chemicals, St Louis, MI) in the OR2 solution (in mM): NaCl 82, KCl 2, $MgCl_2$ 1 and HEPES 5, pH 7.4 for 90 min at room temperature. After 10-20 washes (2 min each) of the oocytes with the OR2 solution, cDNAs (25–50ng in 50nl water) were injected into the oocytes. The oocytes were then incubated at 18°C in the ND-96 solution containing (in mM) NaCl 96, KCl 2, $MgCl_2$ 1, $CaCl_2$ 1.8, HEPES 5, and sodium pyruvate 2.5 with 100mg/l geneticin added (pH 7.4).

H-II. Molecular biology

H-II-1.cDNA subcloning and expression Rat Kir1.1 (or ROMK1, Genbank accession number: X72341) cDNA was generously provided by Dr. Steven Hebert at Yale University. Mouse Kir2.1 (or IRK_1 Genbank accession #X73052) cDNA was a generous gift of Dr. L. Jan at California University at San Francisco. Mouse Kir6.2 (or mBIR, Genbank accession #D50581) cDNA was generously provided by Dr. S. Seino at Kobe University in Japan. The cDNA was subcloned into a eukaryotic expression vector

(pcDNA3.1, Invitrogen Inc., Carlsbad, CA), and used for *Xenopus* oocyte expression without cRNA synthesis.

H-II-2.Heteromeric channel construction To construct tandem-dimeric and tandem-tetrameric Kir1.1 channels, a cassette was constructed with the EcoR I restriction site introduced at the 5' end and an Mfe I site at the 3' end of the Kir1.1 cDNA using polymerase chain reaction (PCR). Based on the cassette, site-specific mutations of Lys80 to methionine and the stop codon to tyrosine were then prepared using a site-directed mutagenesis kit (Stratagene, La Jolla, CA). The cDNA of wild-type (wt) Kir1.1 without stop codon was linearized with the Mfe I restriction enzyme. The K80M mutant with stop codon was digested with EcoR I and Mfe I restriction enzymes. The isolated K80M mutant was then ligated to the linearized wt Kir1.1 to form dimeric wt-K80M. The same strategy was used to construct wt-wt and K80M-K80M tandem-dimers. Since the stop codon was removed in the first monomer, all tandem-dimers had only one open reading frame. There are 5 AAs (YGFPS) created between each monomer in these dimeric channels. To confirm correct mutations, the constructs were examined with DNA sequencing. Based on the appearance of single or double peaks at codon 80 (AAA vs. ATG), homomeric or heteromeric dimers were confirmed.

Cohesive ends of EcoR I and Mfe I restriction sites are complementary. Since both restriction sites are lost after ligation, each dimer still contains only one EcoR I site in front of the first ATG codon and one Mfe I site behind the stop codon. This allows a construction of tandem tetramers by joining two of the dimers. To do so, the first dimer was constructed with the stop codon eliminated, which was joined by another dimer with

intact stop codon. Using different combination of two sets of dimers, various tandem tetramers were generated (Table J-I-1). Correct orientation of the constructs was confirmed with DNA sequencing, and appropriate size was proved by isolation of the tetrameric DNA from the pcDNA3.1 using two restriction enzymes.

To construct the tandem-dimeric and tandem-tetrameric Kir6.2 channels, a cassette was generated with a BamH I restriction site introduced at the 5' end and a Bgl II site introduced at the 3' end of the Kir6.2ΔC36 open reading frame using PCR. Based on the cassette, site-specific mutation of Lys185 to glutamic acid and the stop codon to serine were then prepared using a site-directed mutagenesis kit (Stratagene, La Jolla, CA). The tandem-dimeric and tretrameric constructs were obtained as we did for the Kir1.1 dimers and tetramers. Similarly, the dimers and tretramers carrying H175K, C166S and T71Y mutations were constructed. Three AAs (Ser-Arg-Ser) were created to link the tandem dimeric and tetrameric channels.

H-II-3.Site directed mutagenesis Site specific mutations were made using the P*fu* DNA-polymerase-based site-directed mutagenesis kit (Quickchange, Stratagene, La Jolla, CA). Correct mutations were confirmed with DNA sequencing.

H-III. Electrophysiology recordings

Whole-cell currents were recorded with two-electrode voltage clamp 2–4 days after cDNA injection using an amplifier (Geneclamp 500, Axon Instruments Inc., Foster City, CA) at room temperature (~24°C). Experiments were performed in a semi-closed recording chamber (BSC-HT, Medical System, Greenvale, NY) in which oocytes were placed on a

supporting nylon mesh. The extracellular solution contained (in mM): KCl 90, $MgCl_2$ 3, and HEPES 5 (pH 7.4). At baseline, the chamber was ventilated with atmospheric air. The low pH exposure was produced by superfusing the bath solution with a gas mixture containing 15% CO_2 balanced with 21% O_2 and N_2 (Chanchevalap et al., 2000; Xu et al., 2000a; Zhu et al., 2000). The high dissolvability of CO_2 resulted in a detectable change in intra- or extracellular pH as fast as 10 s in the *Xenopus* oocytes, and the intracellular pH (pH_i) reached 6.6 within 3 minutes (Chanchevalap et al., 2000; Xu et al., 2000a; Zhu et al., 2000). Currents recorded were low-pass filtered (Bessel, 4-pole filter, 3 dB at 5 kHz), digitized at 5 kHz (12-bit resolution) and stored on computer disk for later analysis (pClamp 6, Axon Instruments).

For Kir1.1 channel, macroscopic and single-channel currents were recorded in excised inside-out patches as we described previously (Chanchevalap et al., 2000; Xu et al., 2000a; Yang et al., 2000; Wu et al., 2002a). The bath solution contain (in mM): 40 KCl, 75 potassium gluconate, 5 KF, 10 potassium pyrophosphate, 0.1 sodium vanadate, 5 EGTA, 10 glucose, 10 PIPES (pH = 7.4), 0.2 ADP and 0.1 spermine (Leung et al., 2000; Chanchevalap et al., 2000; Yang et al., 2000). The pipette was filled with the same solution. A parallel perfusion system was used to deliver low pH perfusates at a rate of ~1ml/min with no dead space (Yang et al., 2000; Wu et al., 2002a). Macroscopic and single-channel currents were analyzed using the Clampfit 9 software (Axon Instruments). Currents were expressed as a function of pH_i with Hill equation (Equation 2), SigmaPlot was used for data fitting with pH level for 50% inhibition (pKa) and h as two free parameters.

For the Kir6.2 channel, patch clamp was performed using solutions containing equal concentrations of K^+ applied to the bath and recording pipettes. The bath solution contained (in mM): 10 KCl, 105 potassium gluconate, 5 KF, 5 potassium pyrophosphate, 0.1 sodium vanadate, 5 EGTA, 5 glucose, and 10 HEPES (pH 7.4). The pipette was filled with the same solution (Yang et al., 2000). Pyrophosphate and vanadate are known to alleviate channel rundown. In several control experiments, we did not find any evident difference in current profile and channel responses to pH and ATP from those recorded in the absence of pyrophosphate and vanadate.

Single channel conductance was measured using ramp command potentials from 100 to –100mV. The open-state probability (P_{open}) was calculated by first measuring the time, t_j, spent at current levels corresponding to j = 0,1,2,·····N channels open, based on all evident openings during the entire period of record (Yang et al., 2000). The P_{open} was then obtained as

$$P_{open} = \frac{\sum_{j=1}^{N} t_j \bullet j}{T \bullet N} \qquad (1),$$

where N is the number of channels active in the patch and T is the duration of recordings. P_{open} values were calculated from at least four stretches of data acquired using the Clamfit 9.2 software (Axon Instruments Inc.) or the Fetchex6 software (Axon Instruments Inc.). Open and closed times were measured from records in which only a single active channel was active. Data were further filtered at 0-1,000Hz using Gaussian filter. The open- and closed-time distributions were fitted using the Marquardt-LSQ method in the PSTAT6 software (Axon Instruments Inc.) with datum duration >60 seconds. The current amplitude

was analyzed using all-point histograms. Each peak was described with the Gaussian distribution to indicate substate levels of conductance.

In the study of pH-dependent Kir1.1 channel gating, the amplitude of these inward rectifying currents is expressed as a function of pH_i using the Hill equation:

$$Y = \frac{1}{1+\left(\frac{pK_a}{pH_i}\right)^h} \quad (2),$$

where Y is the normalized current amplitude, pKa the midpoint pH value for channel inhibition, and *h* the Hill coefficient. The normalized current-response relationships in the studies of ATP sensitivity of Kir6.2 constructs were described with the Hill equation:

$$Y = \frac{I_m}{1+\left(\frac{IC_{50}}{[ATP]}\right)^h} \quad (3),$$

where [ATP] is the ATP concentration, EC_{50} the ATP concentration for 50% current stimulation, h the Hill coefficient, and I_m the maximal current activation.

In studies of the ligand binding, channel gating and the binding-gating coupling of the ATP-dependent Kir6.2 gating, the normalized current-response relationship was fitted with the equation of the operational model (Black and Leff, 1983)

$$P_{open} = P_{OP} - \frac{[ATP]^h \bullet \tau_A{}^h}{(K_A + [ATP])^h + \tau_A{}^h \bullet [ATP]^h} \quad (4),$$

for the K185E tandem tetramers, and

$$P_{open} = P_{OP} - \frac{[ATP]^h \bullet \tau_C{}^h}{(K_C + [ATP])^h + \tau_C{}^h \bullet [ATP]^h} \quad (5)$$

for the C166S and T71Y tandem tetramers. P_{open} is the open state probability, P_{OP} is the baseline P_{open} with no inhibition by ATP, and τ is the inverse of the fraction of receptors needed to be occupied to produce half of the maximum inhibition. The percentage of receptors need to be occupied to produce the half of the maximum inhibition is 50% if $\tau = 2$. K_A is the equilibrium dissociation constant for ATP binding to the K_{ATP} channel. The working range of the channel activity and the ATP concentration for 50% inhibition (IC_{50}) are determined with

$$P_{OP} - P_{OT} = \frac{\tau^h}{\tau^h + 1} \quad (6),$$

and

$$IC_{50} = \frac{K_A}{\left(2 + \tau_A{}^h\right)^{1/h} - 1} \quad (7).$$

for the K185E tandem tetramers, as well as

$$IC_{50} = \frac{K_C}{\left(2 + \tau_C{}^h\right)^{1/h} - 1} \quad (8)$$

for the C166S and T71Y tandem tetramers. The P_{OT} is the trough of P_{open} at the plateau level of the inhibition.

H-IV. Ligand exposures

Adenosine 5'-triphosphate (ATP in K^+ salt) was purchased from Sigma (St. Louis, MO). ATP solution was freshly made each time before experiments. The ATP was dissolved as 30 mM concentration in the solution contained (in mM): 10 KCl, 40 potassium gluconate, 5 KF, 5 potassium pyrophosphate, 0.1 sodium vanadate, 5 EGTA, 5

glucose, and 10 HEPES (pH 7.4). The solution is then diluted by the perfusion solution in a series of concentration gradient as indicated in the Results. A parallel perfusion system was used to deliver solutions containing channel regulators at a rate of ~1ml/min with no dead space.

H-V. Statistics and data analysis

Data are presented as means ± s.e. (standard error). All patch data reported were based on four or more patches obtained from at least two oocytes. The difference in channel sensitivities to a given regulator was examined using single factor ANOVA or Student t tests. The dose-response relationship was described with different models. The quality of the regression was tested with R square test. The statistical significance between regressions was examined with F test. Differences were considered to be statistically significant if $P \leq 0.05$

H-VI. Theoretic modeling

Two classes of models were used in the study to predict independent or concerted action of individual subunits. The predictions were based on the ATP (or H^+) concentration for 50% channel inhibition (IC_{50} or pKa) and baseline P_{open} of channels with four wt or four mutant subunits. No free parameter was needed. We assumed that the subunits underwent inhibitory gating by a transition between an open state (O) and close state (C). The prediction of the IC_{50} was firstly performed for tetramers with disruption at the ligand binding. The Hill coefficients of all constructs were fixed as 1 since it varied from 0.9 to 1.2. The Monod, Wyman and Changeux (MWC) model

describes the single concerted transition of four subunits between two states. In the Kir6.2 channel, the ATP-dependent gating without ligand binding was characterized by allosteric equilibrium constant L_0. The dissociation constants for a ligand to bind to the resting state and inactive state were K_O and K_C respectively. The closing equilibrium constant for a functional subunit with ligand binding was given as $L_0 \bullet f$, with $f = K_C / K_O$. Each functional subunit stabilized the channel at close state with a factor f. Therefore the channel with n functional subunits shifted the close equilibrium with a factor f^n. The channel activity with all subunits disrupted can be expressed:

$$P_{open(0)} = \frac{1}{1+L_0} = \frac{1}{1+\frac{x}{IC_{50(0)}}} \qquad (9).$$

With n functional subunits it is

$$P_{open(n)} = \frac{1}{1+L_0 \bullet f^n} = \frac{1}{1+\frac{x}{IC_{50(0)}} \bullet f^n} = \frac{1}{1+\frac{x}{IC_{50(0)} \bullet \left(\frac{1}{f}\right)^n}} \qquad (10).$$

The $IC_{50(0)}$ value obtained from the tetramer 4K185E was 21.7mM, and the f therefore calculated based on the data from 4wt with equation 8 was 0.385, assuming n = 4. Consequently the IC_{50} levels for tetramers with 1, 2 and 3 wt subunits were 6.249, 1.797 and 0.517 mM, respectively. Similarly, the IC_{50} values for channels with disruption at the channel gating were predicted. The IC_{50} values for C166S tetramers with 1, 2 or 3 wt subunits were 2.593, 0.997 and 0.384 mM, and the corresponding IC_{50} obtained for T71Y tetramers were 12.99, 2.92 and 0.66 mM. Baseline P_{open} was predicted according to equations 7 and 8. The L_0 was calculated first based on the baseline P_{open} of the channel

carrying four disrupted subunits. With the value of L_0 and baseline P_{open} of the 4wt channel, the f was obtained. The baseline P_{open} for channels with 1, 2 and 3 wt subunits was predicted using equation 8, and the values were 0.553, 0.369 and 0.217 for C166S tetramers, and 0.567, 0.378 and 0.217 for T71Y tetramers.

The Hodgkin-Huxley (HH) model describes independent transition of all subunits between the opening and close states. The channel is open only when all four subunits are in the open state. The activity of all subunits in a tetrameric channel is a parallel rather than serial event. Channel activation is calculated by assuming that the probability for a subunit with ligand binding to be in the active state is m_a, and the probability for a subunit with no ligand binding to be in the active state is m_o. The probability for a channel with four ligand binding sites to be in the open state is:

$$P_{open(4)} = (m_a)^4 = \left[\frac{1}{1 + \left(\frac{x}{IC_{50(a)}} \right)} \right]^4 \qquad (11),$$

and the probability for a channel with no ligand binding site to be in the open state is:

$$P_{open(0)} = (m_0)^4 = \left[\frac{1}{1 + \left(\frac{x}{IC_{50(0)}} \right)} \right]^4 \qquad (12).$$

The $IC_{50(a)}$ and $IC_{50(0)}$ were calculated by fitting the fourth root of the experimental dose-response relationship of 4wt and 4K185E with hill equation. Finally, the open state probability for channels with n binding sites is

$$P_{open(n)} = (m_a)^n \bullet (m_0)^{(4-n)} = \left[\frac{1}{1+\left(\frac{x}{IC_{50(a)}}\right)}\right]^n \bullet \left[\frac{1}{1+\left(\frac{x}{IC_{50(0)}}\right)}\right]^{(4-n)} = \frac{1}{1+\left(\frac{x}{IC_{50}}\right)} \quad (13).$$

With the $IC_{50(a)}$ and $IC_{50(0)}$, the dose-response relationship for the channel with n functional subunits were obtained at each concentration of ATP. This dose-response relationship was then fitted with Hill equation to get the predicted IC_{50} of the model. The predicted IC_{50} values for K185E tetramers with 1, 2 and 3 wt subunits were 1.50, 0.45 and 0.24mM. Similarly, the corresponding IC_{50} values for tetramers with disruption of channel gating were obtained, and the values for C166S tetramers were 1.20, 0.42 and 0.23mM, and the ones for T71Y tetramers were 1.8, 0.48, 0.24mM. The baseline P_{open} of channels with n functional subunits was calculated with equation 10, 11 and 12 with the m_a and m_o obtained firstly from the baseline activity of the channel carrying four wt and four disrupted subunits respectively. The predicted P_{open} for tetramers with 1, 2 or 3 disrupted Cys166 subunits was 0.183, 0.289 and 0.457, and the corresponding baseline P_{open} for T71Y tetramers was 0.184, 0.293 and 0.465.

I. EXPERIMENTAL DESIGN AND RESULTS

I-I. Subunit Stoichiometry of the Kir1.1 Channel in Proton-dependent Gating

Results from this study have been published:

Wang, R., Su,J., Wang,X., Piao,H., Zhang,X., Adams,C.Y., Cui,N., and Jiang,C. (2005). Subunit stoichiometry of the Kir1.1 channel in proton-dependent gating. J.Biol.Chem. *280*, 13433-13441.

Acknowledgement: This study includes three parts, e.g., the cDNA construction, the whole cell voltage clamp, and patch clamp, with each part contributing to one third efforts. I discussed with my collaborators and Dr. Jiang, who all agreed with this effort proportions. I designed the experiments with Dr. Jiang. I performed all patch-clamp experiments and most (80-90%) of the cDNA constructions. Furthermore, I drafted the manuscript. Dr. Junda Su, Dr. Xueren Wang and Dr. Ningren Cui performed the whole cell recording with Dr. Junda Su contributing ~25% efforts, and Dr. Xueren Wang and Dr. Ningren Cui to ~5% efforts to the experiments. Dr. Hailan Piao did one cDNA construct, Xiaoli Zhang, Carmen Y. Adams helped me with some mini and midi preparations of cDNA constructions. Together they made ~5% contribution to the experiments. Here I would like to express my appreciation.

I-I-1. Introduction

Kir1.1 (ROMK1) is a member in the Kir channel family. A functional channel consists of four Kir subunits, and each Kir subunit has two membrane-spanning helices and a pore-forming sequence (Nichols et al., 1997; Bichet et al., 2003). The Kir1.1 channel was originally cloned from the outer medulla of the kidney and later found in several other tissues (Ho et al., 1993; Wang, 1999). The channel regulates K^+ recycling in the thick ascending limb of the loop of Henle, and K^+ secretion in the cortical collecting duct (Wang, 1999; Hebert, 2003). Dysfunction of the Kir1.1 channel is one of major causes for Bartter syndrome that is characterized by decreased salt transport in the thick ascending limb of the loop of Henle (Hebert, 2003). Surface expression and trafficking of Kir1.1 rely on PKA and PKC (Yoo et al., 2003; Lin et al., 2002). Activity of the Kir1.1 channel is directly regulated by intracellular pH, PKA, PKC, PIP_2, and WNK4 (serine-threonine kinase 4 with no Lysine) (Tsai et al., 1995; McNicholas et al., 1994; Kahle et al., 2003; Huang, 2001). Inhibition of PKA activity or PIP_2 production shifts the channel sensitivity toward more alkaline pH levels (Leipziger et al., 2000; Leung et al., 2000).

Studies over the past few years have revealed several AA residues that contribute to the control of the channel opening and closure known as channel gating, although the gating mechanisms are still unclear (Fakler et al., 1996; Choe et al., 1997; Schulte et al., 1999; Xu et al., 2000a; Xu et al., 2000c; Chanchevalap et al., 2000). Among them is a lysine residue (Lys80) at the boundary between the TM1 and the N terminus of the Kir1.1 channel. Mutation of this residue to a methionine disrupts the pH-dependent channel gating (Fakler et al., 1996). Similar effect has been found in several other Kir channels

that have such a lysine residue (Choe et al., 1997; McNicholas et al., 1998; Yang et al., 2000; Pessia et al., 2001).

Like all other ion channels, how the gating mechanism of the Kir1.1 channel is not well understood. One approach is to disrupt one or more functional subunits in a tetrameric channel. How an individual subunit contributes to the channel gating can then be evaluated. Such a subunit-disruption intervention may yield information about subunit coordination, cooperativity, dominant-negative effect, and minimal requirement of functional subunits for channel gating. To elucidate the subunit stoichiometry in the pH-dependent Kir1.1 channel gating, therefore, we performed these studies on tandem-dimeric and tandem-tetrameric channels in which a predetermined number of subunits carrying the K80M mutation was introduced. The channel pH sensitivity was studied as we have documented previously (Xu et al., 2000a; Xu et al., 2000c; Chanchevalap et al., 2000). Our results showed that the Kir1.1 channel gating requires specific subunit configuration and coordination.

I-I-2. Results

I-I-2-a. Proton-dependent gating of monomeric Kir1.1 and its K80M mutant

The Kir1.1 channel was expressed in *Xenopus* oocytes. Whole-cell K^+ currents were recorded with two-electrode voltage clamp in a bath solution (KD90) containing 90 mM K^+. Consistent with previous reports (Xu et al., 2000a; Xu et al., 2000c; Chanchevalap et al., 2000), the Kir1.1 currents showed clear inward rectification with average amplitude of -13.3±2.7 μA (n=8, measured at -160 mV). Injection of the expression vector alone did not yield inward rectifying currents, and the currents measured at -160mV were 0.5 ± 0.1 μA (n=9).

Exposure of the oocytes to 15% CO_2 produced strong and reversible inhibition of the inward rectifying currents (–76.7 ± 2.0%, n=8). The effect was mediated by pH rather than molecular CO_2, as intracellular, but not extracellular, acidification to the same pH levels as seen during CO_2 exposures produced the same degree of current inhibition (Zhu et al., 2000; Xu et al., 2000a). Mutation of Lys80 to methionine (K80M), a residue found in the pH-insensitive Kir2.1 channel, totally eliminated the inhibitory effect of CO_2 on the whole-cell currents (0.7±1.5%, n=5).

The pH sensitivity was also studied in excised inside-out patches. In these experiments, expression of the Kir1.1 channel was first screened in whole-cell recording. Then, macroscopic currents consisting of over five active channels were recorded in excised patches using recording pipettes with tip diameter of 4-5 μm.

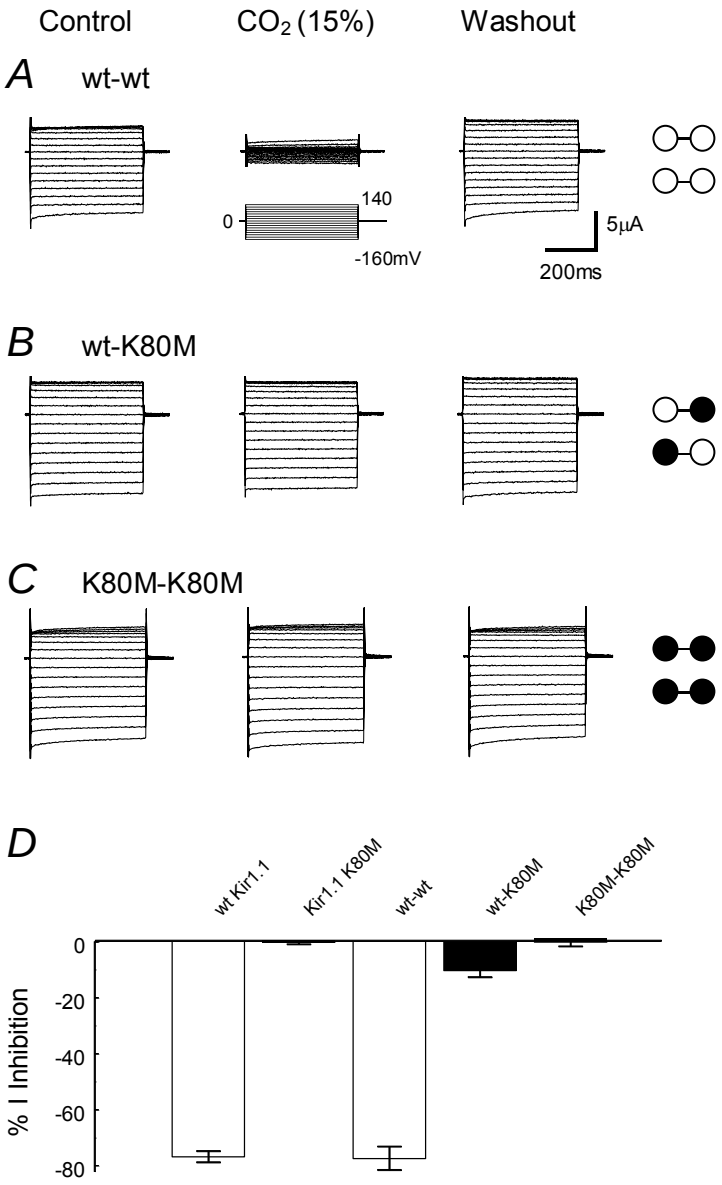

Fig. I-I-1. The effect of hypercapnic acidosis on dimeric Kir1.1 channels. ***A.*** Whole-cell voltage clamp in a *Xenopus* oocyte that received an injection of the tandem dimer of wild-type Kir1.1. A series of voltage commands (from –160mV to 140mV with 20mV increments at a holding potential of 0mV) was applied to the cell in a bath solution containing 90mM K^+. Under this condition, clear inward rectifying currents were seen in the oocyte 3 days after the injection. These currents were strongly and reversibly inhibited when the cell was exposed to 15% CO_2. ***B.*** Similar experiments were performed on another oocyte expressing the wt-K80M dimer. The currents were modestly inhibited with 15% CO_2. ***C.*** The K80M-K80M dimer was unaffected by the same concentration of CO_2. ***D.*** Percentage inhibition of the inward rectifying currents of monomeric and dimeric Kir1.1 channels. Data are presented as means ± s.e. (n = 4 or 5). The whole cell recordings were performed by Dr. Junda Su (***A-C***).

Exposure of the intracellular membrane to low pH perfusates produced concentration-dependent inhibition of the currents. The pH_i dependent response of the Kir1.1 currents was described with the Hill equation, and the pKa value (pH_i level at 50% current inhibition) and the Hill coefficient (h) were subsequently obtained (see Equation 1 in Methods), which were 6.75±0.01 (n=5) and 4.1±0.5 (n=5), respectively. The pH_i sensitivity of the K80M mutant was very low with pKa 5.70±0.03 (n=4) and h 1.2±0.1 (n=4) (Table I-I-1). These observations are thus consistent with previous studies (Tsai et al., 1995; Fakler et al., 1996; Choe et al., 1997; Schulte et al., 1999; Xu et al., 2000a; Xu et al., 2000c; Chanchevalap et al., 2000)

I-I-2-b. Effect of subunit disruption on the pH sensitivity of tandem-dimeric channels

To determine how each subunit contributes to the pH-dependent channel gating, three tandem-dimeric channels were constructed using wt Kir1.1 and the K80M mutant, i.e., wt-wt, wt-K80M and K80M-K80M. All of them expressed inward rectifying currents with amplitude of –10 to –25μA (Fig. I-I-1; Table I-I-1). Exposure to 15% CO_2 led to inhibition of the wt-wt currents by 77.3 ± 4.2% (n=4), to the same degree as the monomeric Kir1.1 ($P>0.05$). Like the monomeric K80M, the K80M-K80M totally lost its CO_2 sensitivity (Fig. I-I-1 C; Table I-I-1). In contrast, the wt-K80M was inhibited by only 10.2±2.4% (n=12) when exposed to 15% CO_2 (Fig. I-I-1B,D).

Table I-I-1. Current responses to CO_2 and pH

Name	BL I (μA)	CO_2 Effect (%)	pKa	h
Monomer				
Kir1.1	–13.3 ± 2.7	–76.7 ± 2.0 (8)	6.75 ± 0.01 (5)	4.1 ± 0.5
K80M	–16.5 ± 12.0	0.7 ± 1.5 (5)	5.70 ± 0.03 (4)	1.2± 0.1
Tandem dimer				
wt-wt	–13.0 ± 3.4	–77.3 ± 4.2 (4)	6.78 ± 0.02 (4)	4.0 ± 1.0
wt-K80M	–13.7 ± 5.6	–10.2 ± 2.4 (12)	6.22 ± 0.01 (4)	3.0 ± 0.2
K80M-K80M	–22.9 ± 1.8	1.4 ± 3.0 (6)	5.75 ± 0.03 (4)	1.2 ± 0.1
Tandem tetramer				
4wt	–4.3 ± 1.7	–79.3 ± 4.2 (6)	6.81 ± 0.01 (4)	3.7 ± 0.2
3wt-K80M	–5.4 ± 2.0	–37.7 ± 3.9 (10)	6. 59 ± 0.01 (5)	3.3 ± 0.1
trans 2wt-2K80M	–6.1 ± 1.4	–12.8 ± 1.5 (14)	6.23 ± 0.01 (5)	2.8 ± 0.2
cis 2wt-2K80M	–5.9 ± 1.1	–12.5 ± 0.7 (6)	6.22 ± 0.01 (5)	2.8 ± 0.1
wt-3K80M	–7.5 ± 3.6	–2.3 ± 3.1 (5)	6.01 ± 0.02 (5)	2.0± 0.2
4K80M	–5.4 ± 1.0	0.2 ± 3.8 (5)	5.80 ± 0.05 (4)	1.2 ± 0.2

Abbreviation: BL I, whole-cell baseline current measured at –160mV; h, Hill coefficient; n, number of observation; pKa, pH_i value at 50% current inhibition; wt, wild type. Data are presented as means ± s.e. The baseline currents and the CO_2 effects for tandem dimers and tetramers were obtained by Dr. Junda Su. Drs. Xueren Wang and Ningren Cui recorded the baseline currents and CO_2 effects for monomers and dimeric wt-wt.

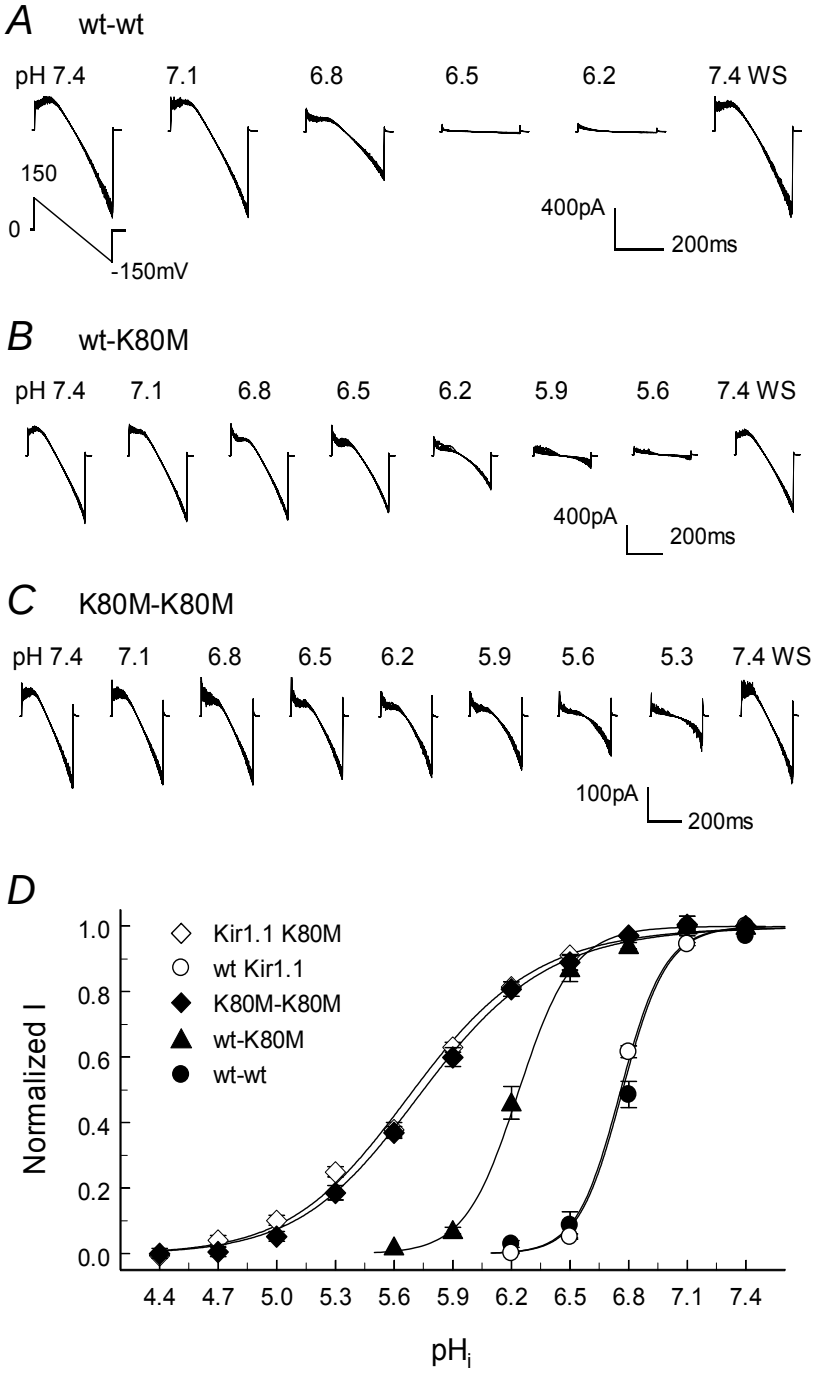

Fig. I-I-2. Inhibition of the tandem-dimeric Kir1.1 channels by intracellular protons. ***A.*** Macroscopic currents were recorded in inside-out patches using symmetric concentrations of K^+ (150mM) on both sides of the patch membranes. Exposures of the internal membranes to solutions of acidic pH produced a fast and reversible inhibition of inward rectifying currents. ***B.*** Similar experiments were done in the wt-K80M dimer that was also inhibited by acidic pH though to a lesser degree. ***C.*** The K80M-K80M was inhibited only when intracellular pH (pH_i) was very low. Note that eight superimposed traces are shown in each panel of A, B and C. ***D.*** The amplitude of these inward rectifying currents is expressed as a function of pH_i using the equation 2 (Methods). See Table I-I-1 for pKa and *h* values. The titration curves of homomeric wt-wt and K80M-K80M are almost identical to their monomeric counterparts, while the wt-K80M has intermediate pH sensitivity. Data are presented as means ± s.e.

Macroscopic currents of the dimeric wt-wt channel were completely inhibited at pH_i 6.2 with pKa 6.78±0.02 (n=4) (Fig. I-I-2A; Table I-I-1). The pH sensitivity of the dimeric K80M-K80M was greatly reduced with pKa 5.75±0.03 (n=4) (Fig. I-I-2C). The concentration-response curves from the dimeric wt-wt and K80M-K80M nicely match those obtained from monomeric wt and K80M-mutant channels (Fig. I-I-2D), indicating that the pH sensitivity of the dimers is well retained. In contrast to the dominant-negative effect of certain residues in the selectivity filter, the K80M-disrupted subunit did not completely eliminate the pH sensitivity of the heteromeric channel. The pH_i response of the heteromeric wt-K80M dimer lay in between of those of the homomeric wt and K80M-mutant channels (Fig. I-I-2B). In comparison to the wt channel the titration curve of the wt-K80M was left-shifted by 0.56 pH units (pKa 6.22±0.01, n=4). Such a change was not a parallel shift, as the Hill coefficient was lowered from 4.0 in wt-wt to 3.0 in wt-K80M (Table I-I-1).

I-I-2-c. Stoichiometry of tandem-tetrameric K80M channels in pH-dependent channel gating

To elucidate the contribution of two functional subunits (in adjacent and diagonal positions) to the pH-dependent Kir1.1 channel gating and the effect of one or three subunit disruptions on a tetrameric channel, tandem-tetrameric channels were constructed. The homomeric wt and K80M-mutant tandem tetramers are named 4wt and 4K80M, respectively. Tandem tetramers with one and three mutant subunits refer to 3wt-K80M and wt-3K80M. Heteromeric tandem tetramers with two mutant subunits at the diagonal and adjacent positions are *trans* 2wt-2K80M and *cis* 2wt-2K80M.

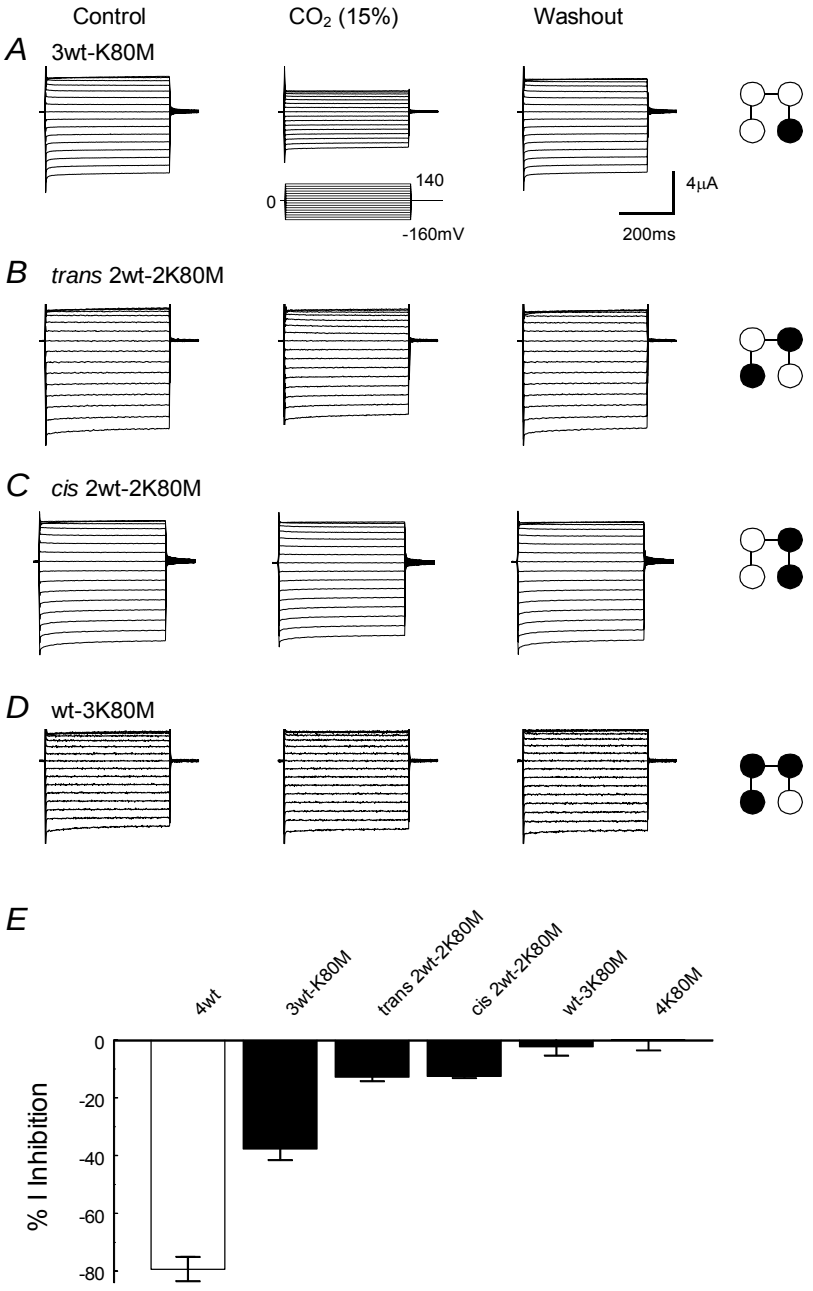

Fig. I-I-3. CO_2 sensitivity of tandem tetramers. ***A.*** The 3wt-K80M was inhibited moderately by hypercapnic acidosis. ***B,C.*** The *trans* 2wt-2K80M responded to CO_2 to the same extent as the *cis* 2wt-2K80M. ***D.*** The wt-3K80M lost its CO_2 sensitivity. ***E.*** The graded decrease in CO_2 sensitivity is revealed when the percentage inhibition of the inward rectifying currents (I) is plotted out. Note that the same levels of inhibition in *cis* and *trans* 2wt-2K80M. The whole cell recording was carried out by Dr. Junda Su (***A-D***).

Baseline whole-cell currents of the tandem-tetrameric channels remained the same as the wt Kir1.1 channel, although the current amplitude was smaller (Table I-I-1). The 4wt and 4K80M responded to 15% CO_2 to almost the same extent as their monomeric counterparts (Table I-I-1) indicating that the pH-dependent channel gating is unaffected by the tandem construction. Introduction of one K80M-disrupted subunit to a tandem-tetrameric channel (3wt-K80M) markedly reduced the CO_2 sensitivity in comparison to the 4wt (Fig. I-I-3A,E). Further decrease in the CO_2 sensitivity was seen in 2wt-2K80M tetramers. Interestingly, both *trans* and *cis* forms of 2wt-2K80M showed the same level of inhibition by 15% CO_2 (Fig. I-I-3B,C,E). CO_2 (15%) did not produce evident inhibition in the wt-3K80M (Fig. I-I-3D,E)

In inside-out patches, the pH sensitivity of homomeric 4wt and 4K80M were comparable to corresponding monomeric and dimeric channels (Table I-I-1). One subunit disruption (3wt-K80M) reduced the pH sensitivity by 0.22 units (Fig. I-I-4A,E). The pH sensitivity of the *cis* 2wt-2K80M shifted by 0.59 pH units toward acidic pH in comparison to the 4wt. The pKa shift of the *cis* 2wt-2K80M was almost identical to that of the *trans* 2wt-2K80M (0.58 pH units, Fig. I-I-4B,C,E; Table I-I-1). The h value was identical in both of them as well (Table I-I-1). With three mutant subunits, the pH sensitivity of the wt-3K80M was 0.80 units lower than the 4wt (Fig. I-I-4D,E). Thus, these patch data are consistent with our whole-cell recordings, indicating that subunit disruptions cause graded loss of the pH-dependent channel gating.

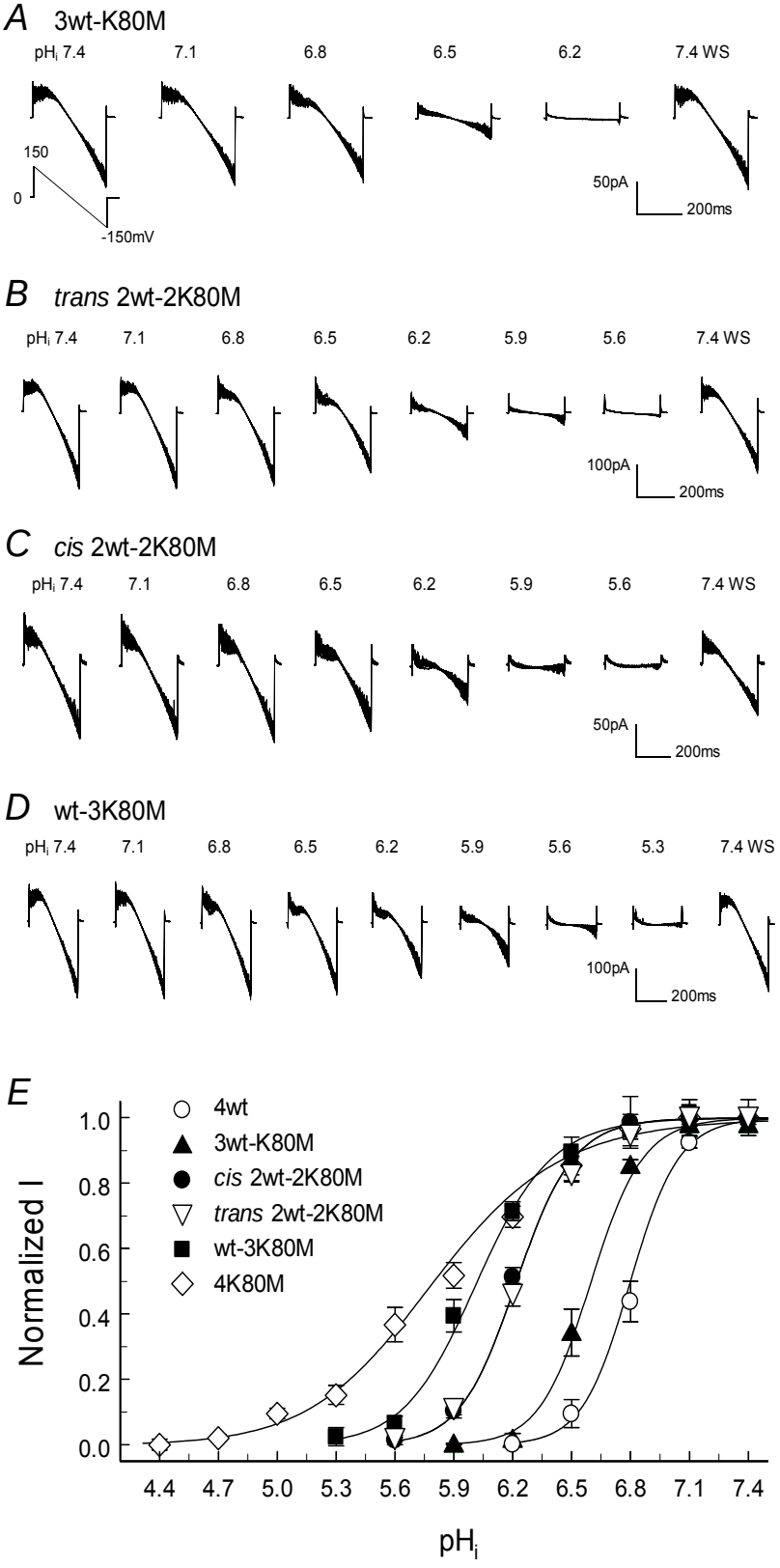
A 3wt-K80M
pH$_i$ 7.4
7.1
6.8
6.5
6.2
7.4 WS
150
0
-150mV
50pA
200ms
B trans 2wt-2K80M
pH$_i$ 7.4
7.1
6.8
6.5
6.2
5.9
5.6
7.4 WS
100pA
200ms
C cis 2wt-2K80M
pH$_i$ 7.4
7.1
6.8
6.5
6.2
5.9
5.6
7.4 WS
50pA
200ms
D wt-3K80M
pH$_i$ 7.4
7.1
6.8
6.5
6.2
5.9
5.6
5.3
7.4 WS
100pA
200ms
E
4wt
3wt-K80M
cis 2wt-2K80M
trans 2wt-2K80M
wt-3K80M
4K80M
Normalized I
1.0
0.8
0.6
0.4
0.2
0.0
4.4
4.7
5.0
5.3
5.6
5.9
6.2
6.5
6.8
7.1
7.4
pH$_i$

Fig. I-I-4. Response of tandem-tetrameric channels to intracellular protons in inside-out patches. ***A-D.*** Experiments were done in the same condition as Fig. I-I-2. Concentration-dependent inhibition of the tetrameric Kir1.1 channels was seen when internal patch membranes were exposed to acidic perfusates. All tetramers were reversibly inhibited by acidic pH_i although their pH sensitivity was different. Note that eight superimposed traces are shown in each panel of ***A-D***. ***E.*** The pH sensitivity of the tetramers is compared by plotting their current-pH_i relationship in the same x-y axis system. The curves were obtained as described in Fig. I-I-2D.

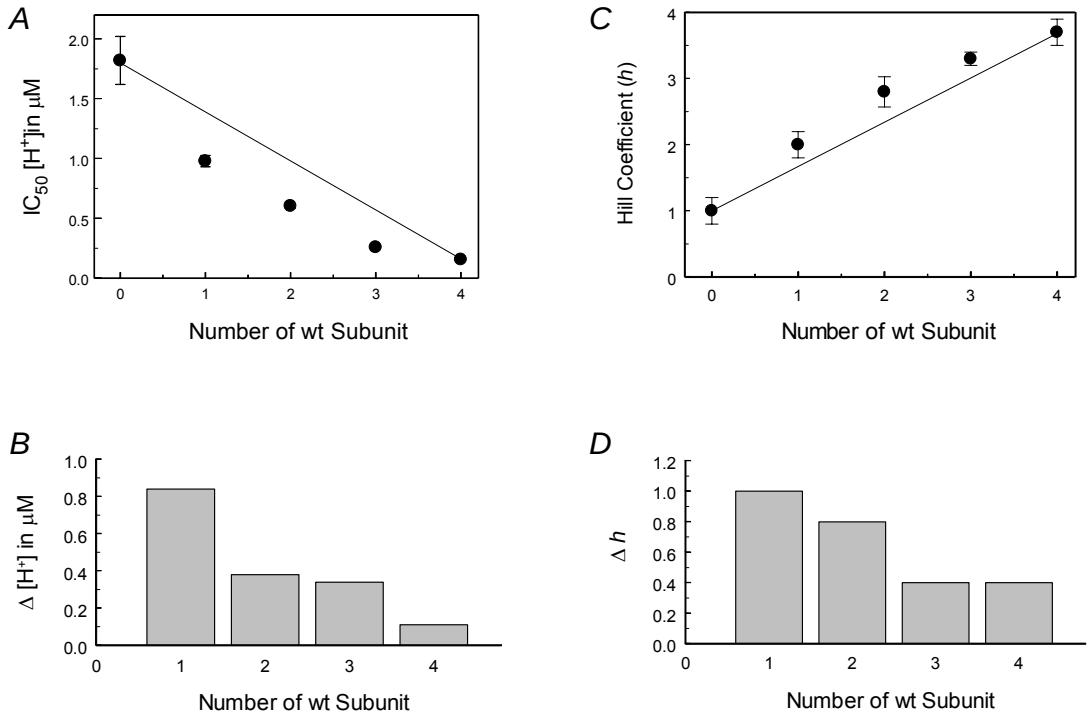

Fig. I-I-5. Changes in IC_{50} and h with the number of wt subunit in tandem-tetrameric Kir1.1 channels. ***A.*** The pKa values are converted to H^+ concentrations and shown as the H^+ concentration for 50% channel inhibition (IC_{50}). The relationship of IC_{50} with the number of wt subunit is not linear in comparison to the straight line. While a great effect is produced by the recruitment of the first wt subunit, much smaller effects are seen with successive subunits. ***B.*** Changes in IC_{50} with number of wt subunits. The IC_{50} value decreases by 0.61 μM with introduction of the first wt subunit, while the second wt subunit shifts IC_{50} by 0.37 μM. The IC_{50} shifts further by 0.35 μM with the third wt subunit introduced, and a small change occurs with the fourth one. ***C,D.*** Similar nonlinear changes in h values are revealed in the tandem-tetrameric channels.

To show the relationship of current response with the number of wt subunit, pKa values were converted to proton concentrations and shown as the IC_{50}. The relationship of IC_{50} with the number of wt subunit was not linear (Fig. I-I-5A). The most prominent shift in IC_{50} was produced by the first wt subunit with much smaller effects contributed by each additional subunit. With the first wt subunit the IC_{50} of H^+ concentration dropped by 0.61μM, while each following subunit reduced the IC_{50} by 0.37, 0.35 and 0.10μM, respectively (Fig. I-I-5B). Similar trend was also observed for h values (Fig. I-I-5C,D).

I-I-2-d. Effects of the heteromeric recombination on single-channel properties

Single channel properties of the tandem-tetrameric channels were studied in inside-out patches using recording pipettes of ~1μm in tip diameter. The homomeric 4wt channel was fully open with brief periods of closures at baseline (pH_i 7.4, not shown). The channel was inhibited at acidic pH_i. Consistent with previous studies on monomeric Kir1 channels (Choe et al., 1997; McNicholas et al., 1998), the inhibition was due to enhancement of longer period closures with moderate effect on openings (Fig. I-I-6A). In contrast, the homomeric K80M and 4K80M showed high-frequency flicking activity at acidic pH_i (Fig. I-I-6F). The changes in single-channel activity of each tandem-tetrameric channel were compared at their pKa levels. Similar to the wt channel (Choe et al., 1997) and the 4wt, tandem-tetrameric channels with one or two disrupted subunits (i.e., 3wt-K80M, *cis* 2wt-2K80M and *trans* 2wt-2K80M) showed long periods of closures (Fig. I-I-6B-D).

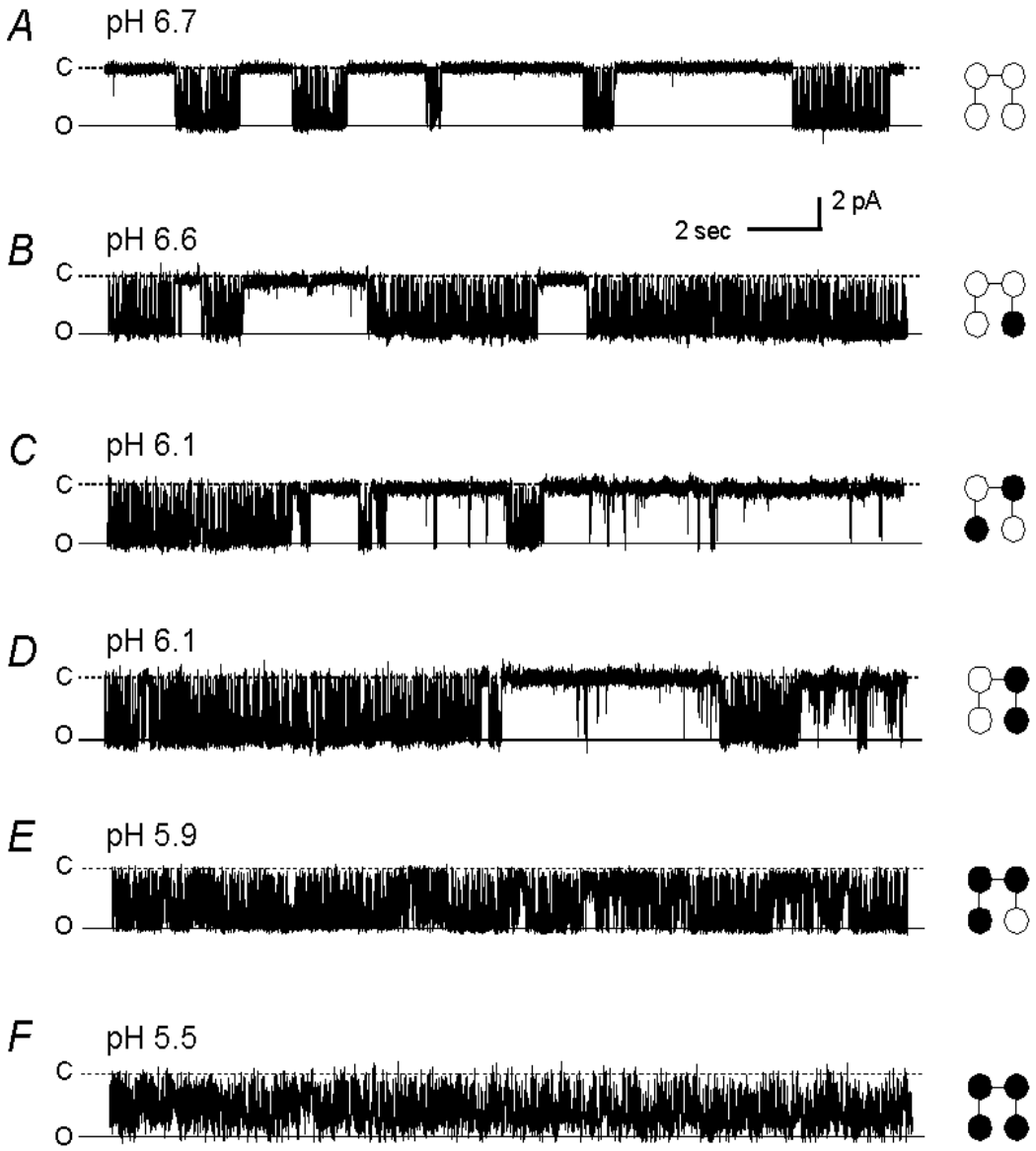

Fig. I-I-6. Single-channel recording of tetrameric Kir1.1 at their pKa levels. Single-channel currents were recorded in inside-out patches that showed only one active channel. Equal concentrations of K^+ (150mM) were applied to both sides of the patch membranes with the membrane potential held at -80mV. To show changes in single-channel activity, each channel was studied at a pH level near to its pKa. ***A.*** At pH_i 6.7, the 4wt showed long periods of closures in between with bursting openings. ***B-D.*** Similar single-channel activity was seen in the 3wt-K80M as well as *trans* and *cis* 2wt-2K80M channels. ***E,F.*** In contrast, the long periods of closured were absent in the wt-3K80M and 4K80M. Instead, high-frequency flicking activity was observed in these two tandem-tetrameric channels.

However, the acid-induced long periods of closures were not seen in the wt-3K80M (Fig. I-I-6E), suggesting a similarity to the 4K80M (Fig. I-I-6F). With extremel acidification (pH<5.3) we did found the long-lasting closures in the wt-3K80M and 4K80M that were mostly associated with channel rundown (not shown).

Dwell-time histograms were studied on patches that showed only one active channel. At pH 7.4, the dwell-time histograms were similar among all constructs with a long period of opening and two short periods of closures revealed (Table I-I-2). The mean open time of these currents varied from 12 to 15ms, and their mean close times were ~1ms (Figs. I-I-7A-D; I-I-8A-D; Table I-I-2). Clear differences were found at the pKa levels. At such pH levels, the inhibition of the channel P_{open} is mostly due to the increase in mean close time for 4wt, 3wt-K80M, *trans* 2wt-2K80M and *cis* 2wt-2K80M (Table I-I-2), while both the reduction in the mean open time and the extension of the mean close time contributed to the inhibition of the 3wt-K80M and 4K80M at their pKa levels (Table I-I-2). The dwell-time histograms for channel openings were well described with two exponentials in the 4wt, 3wt-K80M, *trans* 2wt-2K80M and *cis* 2wt-2K80M (Fig. I-I-7A-D; Table I-I-2), while they were poorly described in the wt-3K80M by two exponentials but better fitted with three (Fig. I-I-7K). The dwell-time histogram of 4K80M can only be fitted with three exponentials (Fig. I-I-7L; Table I-I-2). Although dwell-time histograms for channel closures of all tandem tetramers can be expressed with three exponentials, long-lasting closures were seen in the 4wt, 3wt-K80M, *trans* 2wt-2K80M and *cis* 2wt-2K80M (Fig. I-I-8A-D; Table I-I-2), but not in the wt-3K80M and 4K80M at their pKa levels (Fig. I-I-8E,F; Table I-I-2). Thus, the dwell-time analysis

suggests that the 3wt-K80M, *trans* 2wt-2K80M and *cis* 2wt-2K80M resemble the wt channel, while the wt-3K80M is more like the 4K80M.

Consistent with previous studies on monomeric Kir1.2 (McNicholas et al., 1998), a substate conductance at 40.8±2.0% (n=5) of full conductance level was seen in the homomeric 4wt, especially at pKa level (41.6±1.5% of the full conductance, n=4, Fig. I-I-9A; Table I-I-3). Such a substate conductance was also observed in 3wt-K80M, *cis* 2wt-2K80M and *trans* 2wt-2K80M at neutral pH, and was more obvious at acidic pH (41.0±0.9%~43.2±2.3% of the full conductance, n=4, Fig. I-I-9B-D; Table I-I-3). However, the wt-3K80M and 4K80M showed completely different sublevels of conductance at a pH near to their pKa. In the wt-3K80M, two substates of conductance were seen with the amplitude 23.1±0.8% and 76.5±1.0% of the full conductance, respectively (Fig. I-I-9E). In the 4K80M, sublevels of conductance of as many as three with about equal amplitude were observed (S1=20.5±1.5%, S2=47.6±2.1% and S3=76.2±2.1% of the full conductance level. (Fig. I-I-9F; Table I-I-3). All those sublevels of conductance found in wt-3K80M and 4K80M at pH close to pKa were detected at neutral pH except the small one at ~20% of full conductance level (Fig. I-I-9E, F; Table I-I-3).

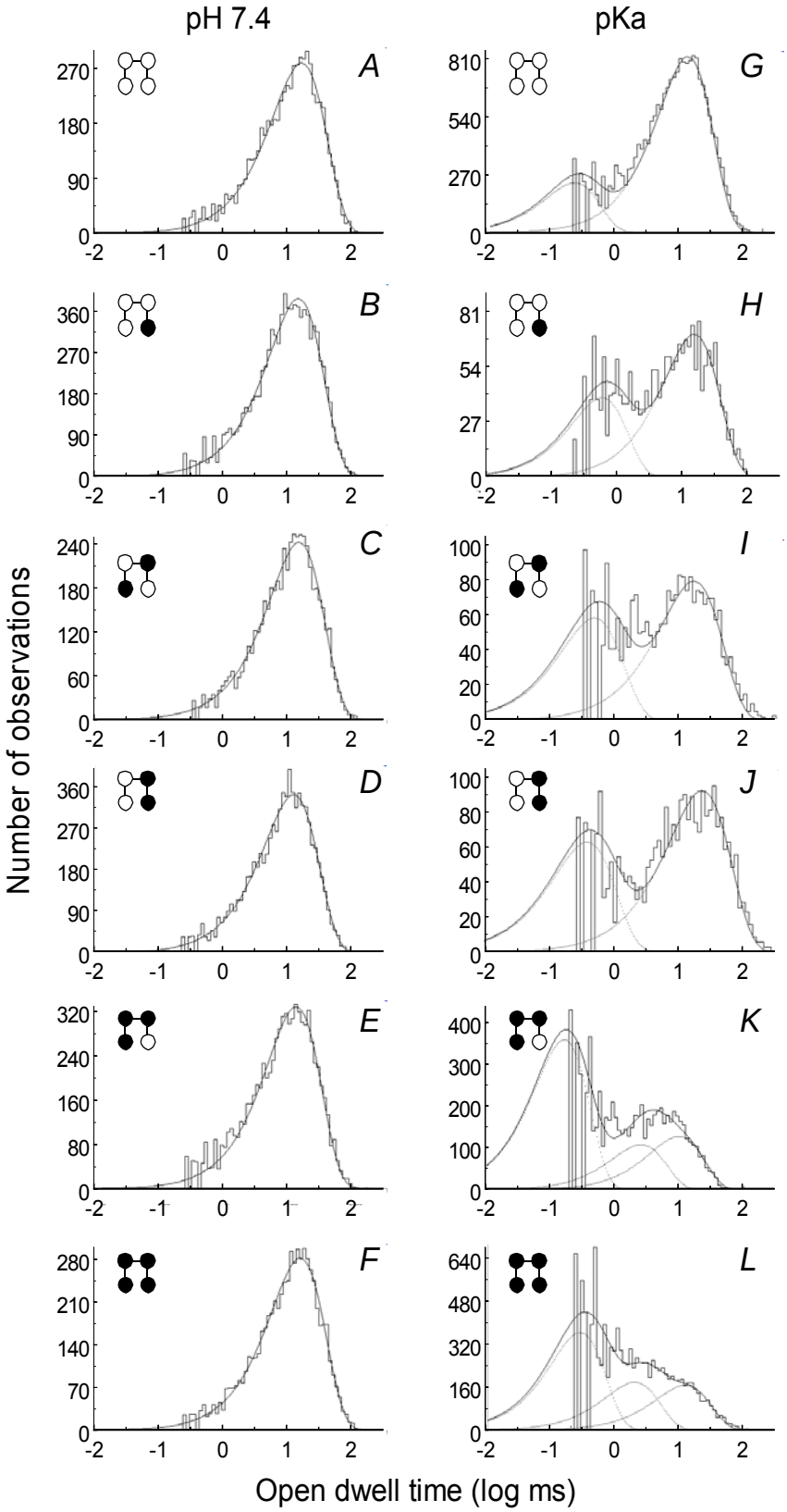
pH 7.4
pKa
A
B
C
D
E
F
G
H
I
J
K
L
Number of observations
Open dwell time (log ms)

Fig. I-I-7. Open-state dwell-time histograms of tandem-tetrameric channels. One active channel was recorded from each inside-out patch in the same condition as Fig. I-I-6. At pH 7.4, the open-state dwell-time histograms of all tetrameric channels are well fitted with one exponential. Differences are shown at pH close to pKa. ***A-D.*** The dwell-time histograms of 4wt, 3wt-K80M, *trans* 2wt-2K80M and *cis* 2wt-2K80M can be fitted using two exponentials with time constants τ_{O1} 0.2ms and τ_{O2} 13.7ms for ***A*** at pH 6.7**,** 0.6ms and 18.8ms for ***B*** at pH 6.6**,** 0.3ms and 8.7ms for ***C*** at pH 6.1**,** and 0.4ms and 10.8ms for ***D*** at pH 6.1***. E,F.*** Dwell-time histograms of wt-3K80M and 4K80M are fitted better with three time constants, i.e., τ_{O1} 0.2ms, τ_{O2} 2.9ms and τ_{O3} 11.1ms for ***E*** at pH 5.9**,** and 0.3ms, 1.9ms and 11.8ms for ***F*** at pH 5.5***.***

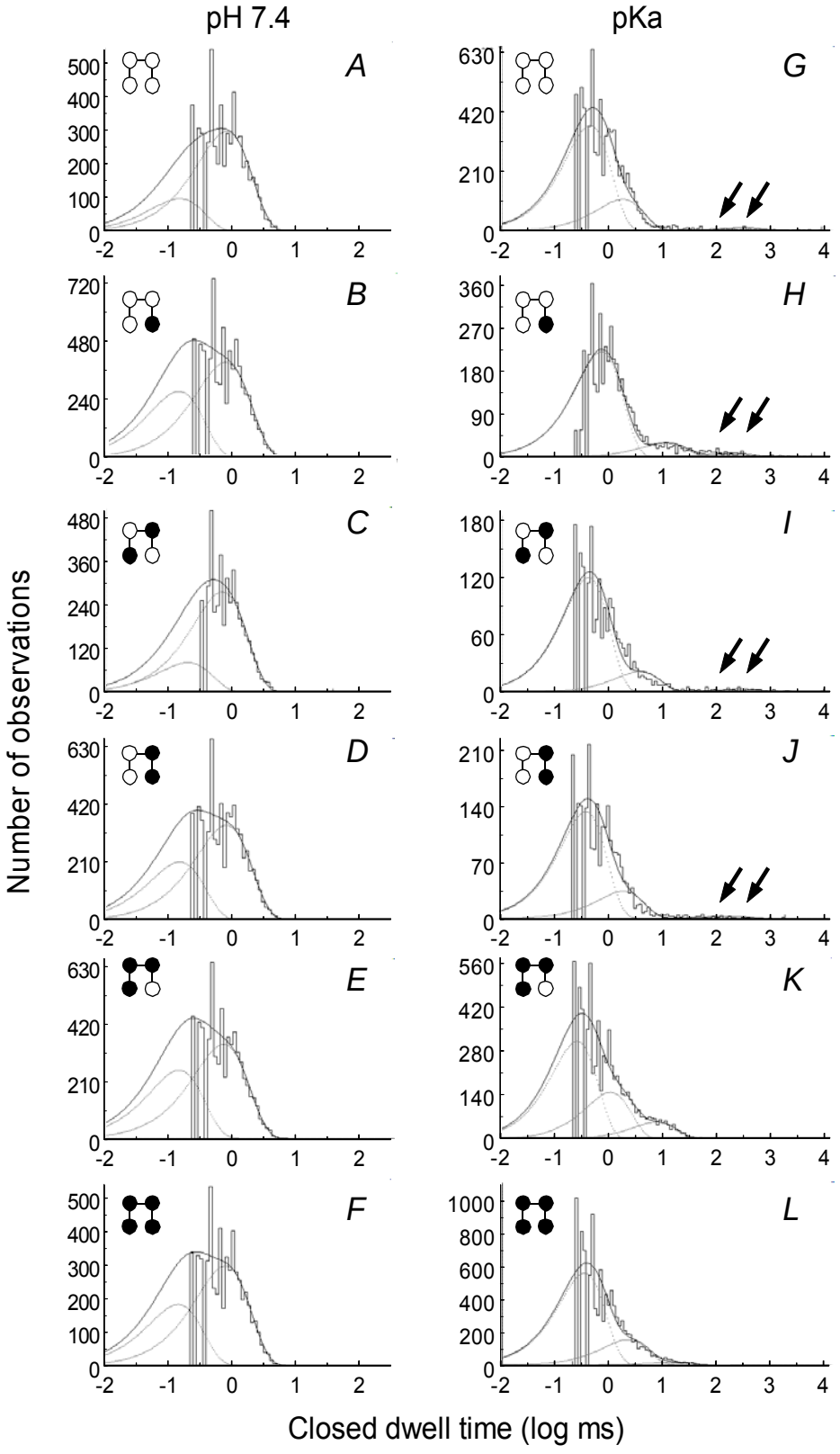
pH 7.4
pKa
A
B
C
D
E
F
G
H
I
J
K
L
Number of observations
Closed dwell time (log ms)

Fig. I-I-8. Closed-state dwell-time histograms of tandem-tetrameric channels. The closed-state histograms are obtained using the same patch data in Fig. I-I-7. The time constants are described with two exponentials at pH 7.4 with τ_{C1} 0.2~0.3 ms and τ_{C2} 0.8~1.0 ms (*A*–*F*). *G*–*J*, three exponentials are used to fit the closed-state dwell-time histograms at their p*Ka* levels with τ_{C1} 0.2 ms, τ_{C2} 1.0 ms, and τ_{C3} 45.0 ms at pH 6.7 for 4wt (*G*); 0.3, 9.9, and 55.1 ms at pH 6.6 for 3wt-K80M (*H*); 0.2, 1.3, and 89.4 ms at pH 6.1 for *trans* 2wt-2K80M (*I*); 0.2, 9.9, and 35.5 ms at pH 6.1 for *cis* 2wt-2K80M (*J*) 0.2, 0.8, and 8.4 ms at pH 5.9 for wt-3K80M (*K*), and 0.2, 1.0, and 8.3 ms at pH 5.5 for 4K80M (*L*). Note that the long periods of closures indicated by *arrows* in *G*–*J* disappear in *K* and *L.*

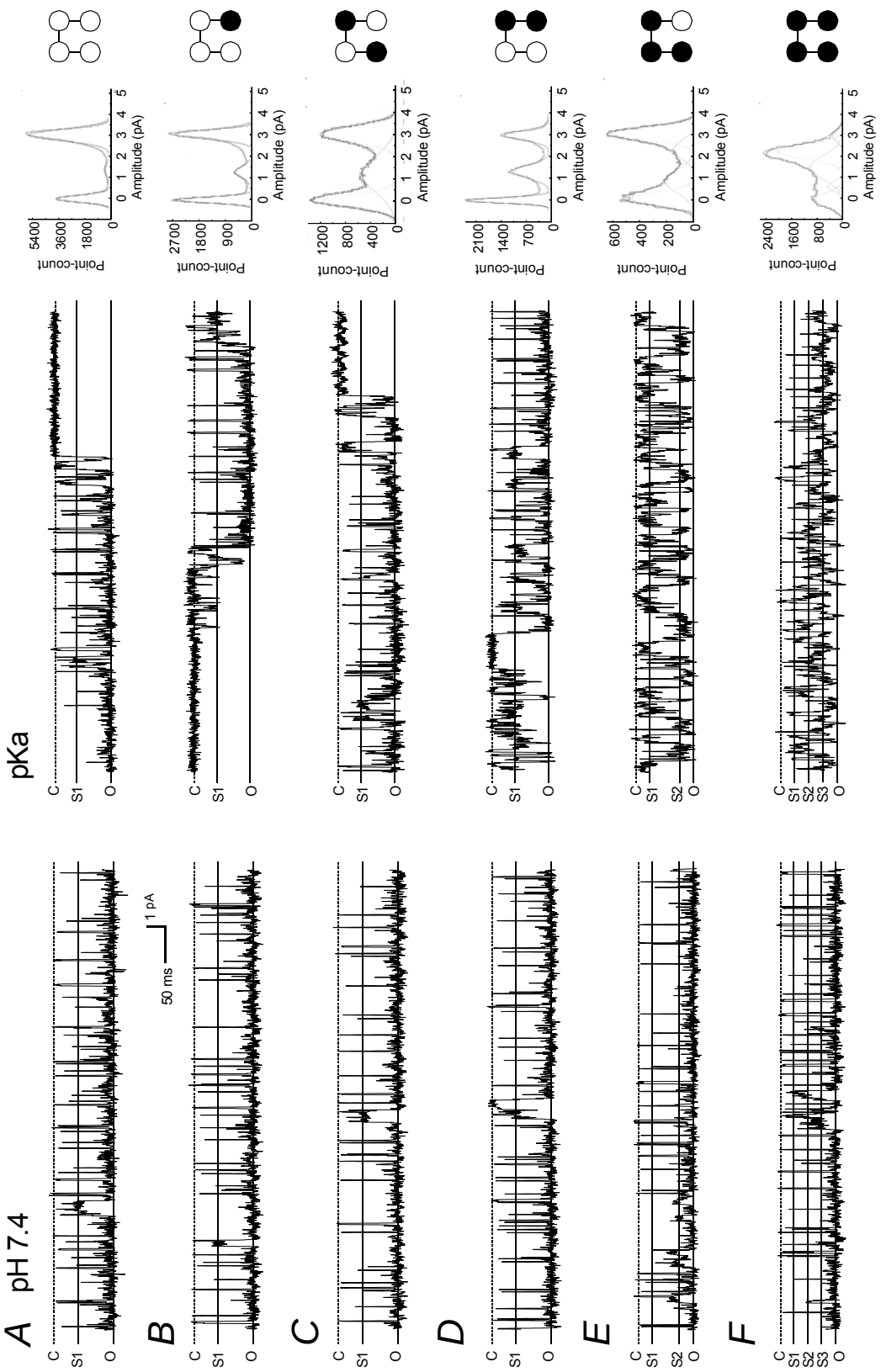
A pH 7.4
B
C
D
E
F
C
S1
S2
S3
O
50 ms
1 pA
pKa
Point-count
Amplitude (pA)
0 1 2 3 4 5
5400
3600
1800
2700
1800
900
1200
800
400
2100
1400
700
600
400
200
2400
1600
800

Fig. I-I-9. Substate conductance of tandem-tetrameric Kir1.1 channels. Each row shows single-channel currents at pH 7.4 and pH levels close to pKa, all-point histogram, and tetrameric sample, from left to right respectively. The substate conductance is 40.9% of the full conductance at pH 7.4, and 41.5% at pH 6.7 for 4wt, (***A***), 43.3% at pH 7.4, and 40.8% at pH 6.1 for 3wt-K80M (***B***), 42.3% at pH 7.4, and 41.1% at pH 6.1 for *trans* 2wt-2K80M (***C***), 37.7% at pH 7.4, and 42.6% at pH 6.1 for *cis* 2wt-2K80M (***D***). In the wt-3K80M one substate of conductance is observed at pH 7.4 with amplitude 74.0% of the full conductance, and two sublevels of conductance at 22.5% and ~75.2% are shown at pH 5.9. (***E***). In the 4K80M, two substates of conductance at 38.0% and 70.4% of full conductance are seen at pH 7.4, and three are observed at pH 5.5 with amplitude of 22.2%, 53.8% and 79.7% of full conductance. (***F***). Note that the full-state conductance remains the same in all tandem-tetramers.

Table I-I-2. Single channel kinetics of tetrameric constructs studied at pH 7.4 and at the pKa level for each channel.

pKa	MTo	MTc	τ_{c1}	τ_{c2}	τ_{c3}	τ_{o1}	τ_{o2}	τ_{o3}	n
4wt	12.8±0.9	22.4±8.7	0.5±0.0	2.3±0.2	243.4±32.4	0.2±0.0	13.3±0.7	—	4
3wt-m	11.3±1.3	11.3±2.5	0.4±0.1	3.4±1.8	187.4±14.8	0.4±0.1	12.4±1.4	—	4
trans	6.7±1.1	13.3±3.7	0.4±0.1	2.6±0.7	200.1±58.2	0.3±0.0	7.5±1.3	—	4
cis	8.1±0.8	11.4±1.9	0.5±0.1	3.0±0.4	191.3±7.9	0.3±0.1	10.1±0.6	—	4
wt-3m	4.2±0.6	3.0±0.3	0.3±0.0	1.1±0.1	8.8±1.0	0.2±0.0	1.8±0.3	8.8±0.9	5
4m	2.5±1.0	5.1±1.5	0.2±0.0	1.4±0.3	11.7±1.8	0.2±0.0	1.2±0.3	6.1±2.0	4
pH 7.4									
4wt	14.7±0.3	1.0±0.0	0.3±0.1	0.9±0.3	—	14.6±0.3	—	—	5
3wt-m	14.1±0.6	1.0±0.0	0.2±0.0	0.8±0.0	—	13.9±0.5	—	—	4
trans	15.2±0.4	1.1±0.0	0.3±0.1	1.0±0.3	—	14.8±0.4	—	—	4
cis	12.5±0.2	0.9±0.0	0.2±0.0	0.8±0.0	—	12.4±0.1	—	—	4
wt-3m	13.5±0.9	1.0±0.0	0.2±0.0	0.8±0.1	—	13.5±0.9	—	—	6
4m	13.4±0.6	0.9±0.0	0.2±0.0	0.8±0.1	—	13.2±0.6	—	—	4

Abbreviation: MTo, mean open time; MTc, mean closed time; τ_{c1}, time constant of the first closure; τ_{o1}, time constant for the first opening; n, number of patches. Data are shown as means±s.e.

Table I-I-3. Substate conductance of tetrameric constructs studied at pH 7.4 and at the pKa level for each channel.

pKa	Full g (pS)	S1 (pS)	S1 % of full g	S2	S2 % of full g	S3	S3 % of full g	n
4wt	39.7±0.6	–	–	16.5±0.6	41.6±1.5%	–	–	4
3wt-m	37.2±1.0	–	–	15.8±1.0	42.6±2.3%	–	–	5
trans	35.8±0.6	–	–	14.8±0.5	41.0±0.9%	–	–	4
cis	36.5±0.3	–	–	15.8±0.8	43.2±2.3%	–	–	4
wt-3m	36.2±2.1	7.8±0.8	23.1±0.8%			27.2±1.3	76.5±1.0%	4
4m	37.8±1.3	7.8±0.5	20.5±1.5%	18.0±1.2	47.6±2.1%	29.4±1.3	76.2±2.1%	4
pH 7.4								
4wt	39.5±0.7	–	–	16.1±0.8	40.8±2.0%	–	–	5
3wt-m	40.6±0.7	–	–	17.4±0.3	43.7±1.0%	–	–	4
trans	40.5±1.7	–	–	15.4±1.3	37.9±2.1%	–	–	4
cis	39.6±0.7	–	–	16.0±0.4	40.5±1.7%	–	–	4
wt-3m	38.9±0.9	–	–	–	–	29.6±1.3	75.9±1.7%	5
4m	39.6±0.7	–	–	17.8±1.5	44.8±3.0%	33.0±1.1	78.2±3.4%	4

Abbreviation: g, unitary conductance; S1, the 1st substate conductance; S2, the 2nd substate conductance; S3, the 3rd substate conductance. Data are shown as means±s.e. Note that "–" indicates substate conductance undetectable.

I-I-3. Discussion

By selective disruption of one or more subunits, we have studied subunit stoichiometry for the Kir1.1 channel gating by intracellular protons. Although the K80M mutation severely disrupts the pH-dependent channel gating of homomeric Kir1.1 channels, it does not have a dominant-negative effect on the heteromeric channels. Instead, the heteromeric dimers and tetramers show graded reduction in their pH sensitivity with increasing number of the K80M-mutant subunits. Although the full pH sensitivity requires all four functional subunits, one wt subunit is sufficient to enable significant pH sensitivity. Among these subunits a coordination of two subunits in either *trans* or *cis* pair appears important for the pH-dependent gating of Kir1.1 channel.

Kir1 channels including ROMK1 and ROMK2 are expressed in the ascending limb of Henle and the cortical collecting duct, and play an important role in K^+ homeostasis (Wang, 1999; Hebert, 2003). Although they are modulated by several intracellular messengers such as PIP_2, PKA, PKC and WNK4 (McNicholas et al., 1994; Kahle et al., 2003; Huang, 2001), proton is the major regulator (Tsai et al., 1995; Fakler et al., 1996; Choe et al., 1997; Schulte et al., 1999; Xu et al., 2000a; Xu et al., 2000c; Chanchevalap et al., 2000; McNicholas et al., 1998). While the Kir1 channels are widely open at physiological pH levels, intracellular acidosis causes strong inhibition of these channels (Fakler et al., 1996; Choe et al., 1997; Schulte et al., 1999; Xu et al., 2000a; Xu et al., 2000c; Chanchevalap et al., 2000; McNicholas et al., 1998). Genetic mutations of the Kir1 channels which were found in patients with Bartter syndrome affect the channel sensitivity to pH_i (Schulte et al., 1999; Flagg et al., 2002). The Lys80 has been shown to

be a critical player in the pH sensitivity, as mutation of this residue to a methionine greatly reduces the pH sensitivity of Kir1 channels (Fakler et al., 1996; McNicholas et al., 1998). Creation of this residue makes the Kir2.1 channel pH-sensitive (Fakler et al., 1996). Such a lysine residue is also found in Kir1.2, Kir4.1 and Kir4.2 channels, in which similar disruption of the pH sensitivity has been observed following site-specific mutation (Choe et al., 1997; McNicholas et al., 1998; Yang et al., 2000; Pessia et al., 2001). In addition to the Lys80, several other residues are involved in the pH sensitivity of the Kir1 channels. Four of six histidine residues located in the C terminus (His225, Hir274, His342 and His354) have been shown to play a part in the channel sensitivity to pH_i. Mutation of any of them reduced the pH sensitivity by 0.2-0.3 pH units (Chanchevalap et al., 2000). Arg41, Thr51 (in Kir1.2), Val66, Asn171 and Arg311 all contribute to the pH sensitivity of Kir1 channels (Choe et al., 1997; Schulte et al., 1999; Xu et al., 2000a; Xu et al., 2000c). These residues are either non-titratable or titrated at high pH levels, and are believed to shift the pKa of Lys80 to physiological pH levels (Choe et al., 1997; Schulte et al., 1999). Although a number of other residues and protein domains are also involved, the Lys80 is a determinant player in the pH sensitivity of homomeric Kir1.1 channel.

The subunit functional stoichiometry has been studied previously in several Kir channels. Mutation on the signature sequence of the selectivity filter GYG to AAA results in none conductive K^+ channel (Kubo et al., 1993; Kuzhikandathil et al., 2000). This has been widely used in transgenic mice to suppress certain Kir currents because of its dominant negative effect (McLerie et al., 2003). Some other naturally occurring

mutations in Kir channels that cause diseases also show dominant-negative effect (Flagg et al., 1999; Kunzelmann et al., 2000). However, systematic studies reveal more complicated situations with regard to subunit contributions. The closure of the ATP-sensitive K^+ channels has been shown to be produced by occupation of one of the SUR subunits (Dorschner et al., 1999). The tetrameric Kir2.1 channel largely retains its sensitivity to Mg^{2+} and polyamine when there are three subunits carrying mutations that abolish Mg^{2+} and polyamine blockade (Yang et al. 1995). Activation of the GIRK channels by $G_{\beta\gamma}$ results from graded effects, requiring at least three $G_{\beta\gamma}$ to bind to the channel protein to achieve full channel activation (Sadja et al., 2002).

The subunit stoichiometry is well demonstrated in several other intracellular-ligand-gated ion channels. Ruiz and Karpen (1997) have found that the opening of CNG channels requires at least two cyclic nucleotide molecules, while the binding of each successive cyclic nucleotide can further enhance the channel opening. Similar observations were made by Rosenmund et al. (1998) in AMPA type glutamate receptor. In contrast, Liu et al. (1998) and Ulens et al. (Ulens and Siegelbaum, 2003) have shown that the binding of a single cyclic nucleotide molecule is enough to increase the channel opening of the CNG and the hyperpolarization- and cyclic nucleotide-activated HCN channels. They have also found that the successive binding of more ligands provides a none linear enhancement of the channel activation, and two ligands bound in *trans* configuration produce a greater effect than in *cis* configuration (Liu et al., 1998; Ulens and Siegelbaum, 2003). Their studies suggest that ligand binding to four subunits of the

CNG and HCN channels promote the formation of dimer of dimers and activate the gating mechanisms.

Our stoichiometric studies of the Kir1.1 channel reveal that the K80M mutation does not have a dominant-negative effect on the heteromeric channels. Indeed, our results suggest that each individual subunit contributes to pH dependent gating of the Kir1.1 channel. The pH sensitivity of the heteromeric channels drops with a decrease in the number of wt subunits. A reduction of 1 pH units is found when all Lys80 are mutated in a tandem-tetrameric channel. These results thus suggest that one functional subunit is sufficient to act on the pH-dependent gating of the Kir1.1 channel, although the full pH sensitivity requires contributions of all four subunits. This result is in agreement with previous observations on the CNG and HCN channels (Liu et al., 1998; Ulens and Siegelbaum, 2003; Labarca et al., 1995; Schonherr et al., 1999).

These subunit stoichiometric studies allow us to appreciate an interesting finding: most of shifts in pKa and h values results from the introduction of the first single wt subunit, whereas additions of an extra subunit have smaller effects. This result does not support positive cooperativity as suggested by the steep titration curve with high h value in Kir1 channels (Tsai et al., 1995; Fakler et al., 1996; Xu et al., 2000c; McNicholas et al., 1998). Although this finding by itself may not be adequate to indicate negative cooperativity that has been observed previously in several other ion channels and receptors (Gentet and Clements, 2002; MacGregor et al., 2002; Gunderson et al., 1994), it demonstrates a feasibility for further studies. The function attributed to the negative

cooperativity is unclear. It may be involved in subunit coordination in a tetrameric channel.

The pH-dependent gating of Kir1.1 channel relies on specific subunit coordination. The wt Kir1.1 shows a single substate conductance at ~40% of the full conductance level. Disruption of all four subunits results in two new substates of conductance, likely to result from the relieved independence of individual subunits. It is worth noting that the newly appeared substates of conductance cannot be explained with flickering activity, since no second full conductance is seen in these recordings, since a single-substate conductance should not produce two or three substates with amplitudes distinct from the original one. Both these new substates disappear when there are two or more wt subunits in a tetrameric channel, suggesting that the four subunits are coordinated in pairs. Supporting this idea are our data indicating that channels with less than two wt subunits show flickering activity (Fig. I-I-6E,F), new opening events (Fig. I-I-7K,L), and a loss of the long-lasting closures (Fig. I-I-8K,L) during intracellular acidification. Thus, it is possible that four subunits are coordinated in functional dimers as suggested previously in CNG and HCN channels (Liu et al., 1998; Ulens and Siegelbaum, 2003). Although each subunit has significant contribution to the gating process, a bigger step is achieved when the potential functional dimer is recruited. Interestingly, the subunit coordination in the Kir1.1 channel does not require specific conformation of the functional dimers. Both *cis* and *trans* conformations have identical effects, which makes a clear contrast to that found in the CNG and HCN channels (Liu et al., 1998; Ulens and Siegelbaum, 2003). Since the Lys80 is located behind the TM2

bundle of crossing, the interaction site for the dimers does not seem to occur at this location, perhaps in the C terminal instead. With the functional dimers, the wild types of channel closures, substate conductance and pH sensitivity may be largely maintained when one or two of the subunits are disrupted.

In conclusion, the Kir1.1 gating by intracellular protons requires special subunit stoichiometry. While all four subunits are needed for full strength of channel inhibition, a single subunit is sufficient to activate the pH-dependent gating mechanism. These subunits appear to act as two dynamic functional dimers in the pH-dependent gating of Kir1.1 channel, and the coordination between two subunits can occur in either *trans* or *cis* configuration.

I-I-4. Summary and Conclusions

Kir1.1 channel regulates membrane potential and K^+ secretion in renal tubular cells. This channel is gated by intracellular protons, in which a lysine residue (Lys80) plays a critical role. Mutation of the Lys80 to a methionine (K80M) disrupts the pH-dependent channel gating. To understand how and individual subunits in a tetrameric channel are involved in pH-dependent channel gating, we performed these studies by introducing K80M-disrupted subunits to tandem-tetrameric channels. The pH sensitivity was studied in whole-cell voltage clamp and inside-out patches. Homomeric tetramers of the wt and K80M-disrupted channels showed pH sensitivity almost identical to their monomeric counterparts. In heteromeric tetramers and dimers, the pH sensitivity was a function of the number of wt subunits. Recruitment of the first single wt subunit shifts the pKa greatly, whereas additions of any extra wt subunit had smaller effects. Single-channel analysis revealed that the tetrameric channel with two or more wt subunits showed one substate conductance at ~40% of the full conductance, suggesting that four subunits act as two pairs. However, three and four substates of conductance were seen in the tetrameric wt-3K80M and 4K80M channels. Acidic pH increased long-time closures when there were two or more wt subunits. Disruption of more than two subunits led to flickering activity with appearance of a new opening event and loss of the long period of closures. Interestingly, the channel with two wt subunits at diagonal and adjacent configurations showed the same pH sensitivity, substate conductance and long-time closure. These results thus suggest that one functional subunit is sufficient to act in the pH-dependent gating of the Kir1.1 channel, the channel sensitivity to pH increases with

additional subunit, the full pH sensitivity requires contributions of all four subunits, and two subunits may be coordinated in functional dimers of either *trans* or *cis* configuration.

I-II. Kir6.2 Channel Gating by Intracellular Protons: Subunit Stoichiometry for Ligand Binding and Channel Gating

Manuscript in submission:

Wang, R*., Su,J*., Zhang,X., Piao,H., Wang,X., Shi.Y., Cui,N., Onyebuchi,VA., and Jiang,C. Kir6.2 Channel Gating by Intracellular Protons: Subunit Stoichiometry for Ligand Binding and Channel Gating.

Acknowledgement: Experiments in this study were made of molecular construction and whole cell recording in equal proportions of efforts. The project was designed by Dr. Jiang and me. I constructed most (~80%) of the cDNA, performed the data analysis for modeling, and drafted the paper. Dr. Junda Su performed most (~80%) whole-cell voltage clamp and the whole-cell data analysis. Drs. Xueren Wang and Ninren Cui also performed some whole-cell recordings (~20%). Dr. Hailan Piao, Xiaoli Zhang and Vivian A. Onyebuchi helped me with the mini and midi preparations, who contributed ~20% efforts to the molecular constructions. I am grateful for their assistance.

I-II-1. Introduction

The K_{ATP} channels play a role in cellular responses to metabolic status (Ashcroft and Gribble, 1998; Seino, 1999). The K_{ATP} channel is an octamer consisting of four pore-lining Kir6.x subunits and four peripheral SURx subunits. Each Kir6.x subunit has two TM1, TM2 and a pore-forming (P) loop. The K_{ATP} channel activity is controlled by ATP, ADP and phospholipids (Ashcroft and Gribble, 1998; Seino, 1999). In addition, these channels are gated by intracellular protons (Davies, 1990). The pH-dependent activation of K_{ATP} channels has a profound impact on cellular function and responses to metabolic stress, as a significant drop in intracellular pH is more frequently seen under a number of physiological and pathophysiological conditions than a sole decrease in intracellular ATP levels (Davies et al. 1991). The protonation site has been identified to be His175 in the Kir6.2 (Xu et al. 2001a,b), allowing further studies of the pH-dependent channel gating. Several other AA residues are known to be critical for the Kir6.2 channel gating. Cys166 in the TM2 region is one of them, mutation of which to serine or alanine eliminates K_{ATP} channel gating by multiple channel regulators including ATP, protons and sulfonylurea (Trapp et al. 1998a; Piao et al. 2001). A threonine residue (Thr71) located at the boundary of the TM1 and N terminus has a similar effect. Mutation of the Thr71 to a bulky AA (phenylalanine, tyrosine or arginine) abolishes channel gating by both ATP and protons (Trapp et al. 1998a; Piao et al. 2001). The ubiquitous effects on channel sensitivity to more than one ligand molecule indicate that Cys166 and Thr71 participate in channel gating rather than ligand binding (Trapp et al. 1998a; Piao et al. 2001; Cui et al. 2003).

In contrast to the rich information of AA residues and protein domains in K_{ATP} channel sensitivities to specific ligand molecules, the channel gating mechanisms are still elusive. Since site-specific mutation of either His175, Cys166 or Thr71 is sufficient to disrupt the proton-dependent gating of the homomeric Kir6.2 channel, it is possible that studies can be designed using these identified residues to target proton binding and channel gating in a given number of subunits. Such studies may yield information about how proton binding to the C terminus is coupled to membrane helices. Moreover, the stoichiometric studies may shed insight into ligand binding, channel gating, binding-gating coupling, subunit coordination, cooperativity, dominant-negative effect and minimal number of functional subunits required for channel gating. The above information cannot be obtained by studying the homomeric channels. One alternative approach is to construct dimeric and tetrameric concatemers carrying one or more of H175K, C166S and T71Y mutations. Our study may improve the understanding about those transient events in ligand binding and channel gating. To simplify our experimental subjects we chose to use the Kir6.2 with 36 AAs truncated at the C terminus, i.e., Kir6.2ΔC36, because it expresses ATP- and pH-dependent currents without the SUR subunit (Tucker et al. 1997; Xu et al. 2001a, b), and the SUR subunit is not required for the pH sensitivity (Xu et al. 2001a; Wu et al. 2002b). The pH-dependent Kir6.2 channel gating was studied in whole-cell recordings using 15% CO_2, since low pH causes rapid Kir6.2 channel rundown in excised patches (Xu et al. 2001a, 2001b; Piao et al. 2001; Wu et al. 2002b) and since we have characterized the CO_2 effect on intra- and extracellular pH (Zhu et al. 2000; Xu et al. 2000b, 2001a).

I-II-2. Results

I-II-2-a.Proton-dependent gating of monomeric and tandem-dimeric Kir6.2 channels

Kir6.2ΔC36 was expressed in *Xenopus* oocytes. The whole-cell currents were recorded as reported previously (Tucker et al. 1997; Xu et al. 2001a). The Kir6.2 currents showed strong inward rectification with the current amplitude averaging 2.1±0.4 μA (n=14, measured at -160mV). Injection of the vector alone did not yield the inward rectification currents. Exposure of the oocyte to 15% CO_2 produced strong and reversible activation of the inward rectifying currents (Fig. I-II-1A). The effect was mediated by pH rather than molecular CO_2, as intracellular, but not extracellular, acidification to the same levels as seen during CO_2 exposures produced the same degrees of channel activation (Xu et al. 2001a). The proton sensor for the acid induced activation has been demonstrated to be His175 in our previous studies (Xu et al. 2001a, 2001b; Wu et al. 2002b). Mutation of this residue to alanine or lysine (H175A, H175K) totally eliminated the CO_2 effect on the whole-cell currents, and the channel was inhibited during acidification. (Table I-II-1; Fig. I-II-1B). Cys166 and Thr71 are two non-titratable sites that are also critical for the pH sensitivity of the Kir6.2 channel. Mutation of Cys166 to serine and Thr71 to tyrosine has been reported to stabilize the channel at open conformation (Trapp et al., 1998a; Cui et al., 2003), and the mutant channels were no longer sensitive to acidification (Piao et al. 2001; Cui et al., 2003). Instead, the C166S and T71Y mutant channels were inhibited during acidosis by 13.5±1.1% (n=9) and 5.0±1.3% (n=5), respectively (Table I-II-1; Fig I-II-2C, D).

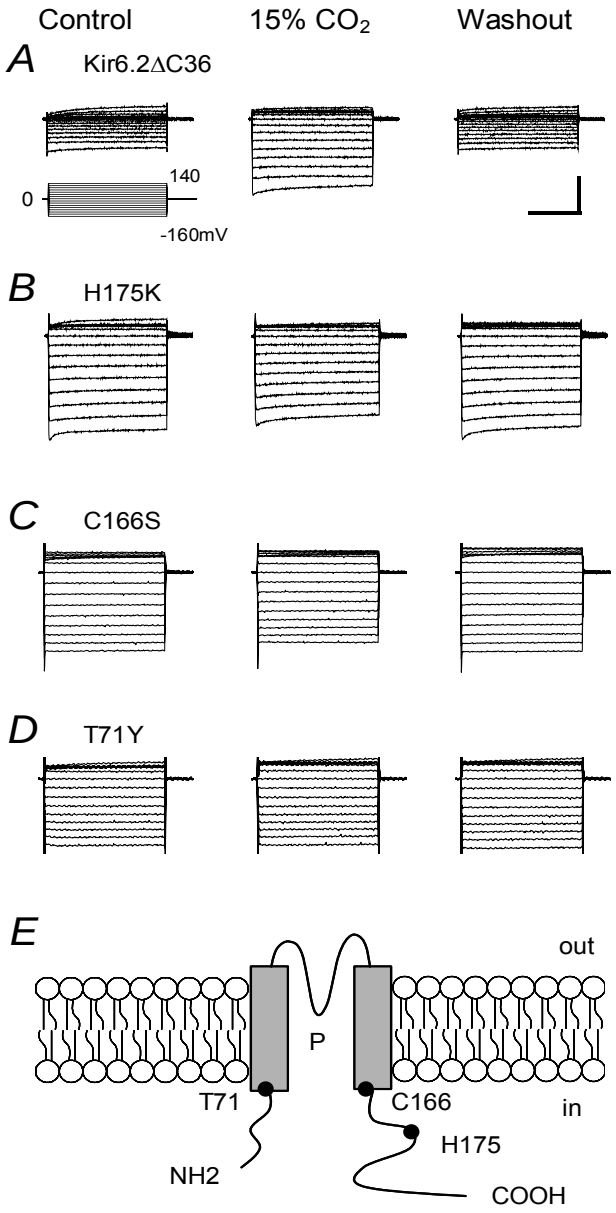

Fig. I-II-1. The effect of hypercapnic acidosis on monomeric Kir6.2 channels. Whole-cell currents were studied in two-electrode voltage clamp in *Xenopus* oocytes that received an injection of the wild-type Kir6.2ΔC36 or its mutants. A series of voltage commands (from –160mV to 140mV with 20mV increments at a holding potential of 0mV) was applied to the cells in a bath solution containing 90 mM K^+. ***A.*** Under this condition, clear inward rectifying currents were seen in the oocyte 3 days after the injection of the wild-type Kir6.2ΔC36. These currents were strongly and reversibly activated when the cell was exposed to 15% CO_2***.*** Similar experiments were performed on the H175K (***B***), C166S (***C***) and T71Y (***D***), all of which lost the pH sensitivity. The currents instead were inhibited during CO_2 exposure. Calibration: 200ms/2μA for A, B; 200ms/4μA for the rest. ***E***. Schematic of transmembrane topology of the Kir6.2 channel and locations of His175K, Cys166 and Thr71. The whole cell recordings were performed by Dr. Ningren Cui.

Table I-II-1. CO_2 sensitivity of all Kir6.2 constructs.

Construct	WBL Current (μA)	CO_2 Effect (%)
Monomer		
Kir6.2ΔC36	2.1 ± 0.4 (14)	130.3 ± 12.2 (14)
H175K	9.1 ± 3.0 (6)	–18.6 ± 2.7 (6)
C166S	14.1 ± 2.4 (9)	–13.5 ± 1.4 (9)
T71Y	9.1 ± 3.1 (5)	–5.0 ± 1.3 (5)
Tandem-dimer		
wt-wt	1.4 ± 0.2 (8)	123.3 ± 8.2 (8)
wt-H175K	4.2 ± 0.4 (7)	30.5 ± 1.6 (5)
H175K-H175K	7.2 ± 1.0 (5)	–19.2 ± 0.9 (5)
wt-C166S	8.3 ± 3.5 (4)	35.6 ± 6.9 (4)
C166S-C166S	13.4 ± 1.3 (5)	–13.1 ± 1.6 (5)
wt-T71Y	3.9 ± 0.4 (5)	74.1 ± 9.4 (5)
T71Y-T71Y	2.5 ± 0.4 (5)	– 5.5 ± 1.8 (5)
Tandem-tetramer		
4wt	1.4 ± 0.1 (4)	120.4 ± 9.9 (4)
H175K		
3wt-H175K	2.7 ± 0.5 (10)	58.1 ± 4.2 (6)
trans 2wt-2H175K	1.7 ± 0.2 (11)	25.9 ± 1.4 (11)
cis 2wt-2H175K	2.2 ± 0.2 (9)	24.5 ± 2.2 (9)
wt-3H175K	7.2 ± 0.2 (6)	–6.5 ± 0.4 (6)
4H175K	3.4 ± 0.3 (7)	–24.0 ± 2.7 (7)
C166S		
3wt-C166S	2.3 ± 0.3 (4)	65.1 ± 9.7 (4)
trans 2wt-2C166S	3.0 ± 0.4 (5)	35.7 ± 2.4 (5)
cis 2wt-2C166S	3.9 ± 0.4 (5)	36.3 ± 4.4 (5)
wt-3C166S	19.0 ± 3.7 (4)	–0.9 ± 0.5 (4)
4C166S	14.2 ± 0.9 (4)	–15.6 ± 1.6 (4)
T71Y		
3wt-T71Y	2.8 ± 0.6 (6)	90.1 ± 6.1 (6)
trans 2wt-2T71Y	2.8 ± 0.5 (7)	62.3 ± 9.4 (7)
cis 2wt-2T71Y	6.8 ± 1.1 (9)	61.6 ± 3.4 (9)
wt-3T71Y	5.8 ± 1.3 (4)	16.1 ± 1.2 (4)
4T71Y	3.4 ± 0.4 (6)	–3.8 ± 2.8 (6)

All mutant channels were constructed on Kir6.2ΔC36. Abbreviation: WBL, whole-cell baseline; m, mutant; w/wt, wild type. Data are presented as means ± s.e. with number of observation in parentheses. The whole cell recordings for monomers were performed by Dr. Ningren Cui. The dimers and tetramers were performed by Dr. Junda Su, with the 4wt finished by Drs. Xueren Wang, Junda Su and Mr. Yun Shi together. Dr. Xueren Wang also contributed to some of the recording *trans* 2wt-2H175K and *trans* 2wt-2T71Y.

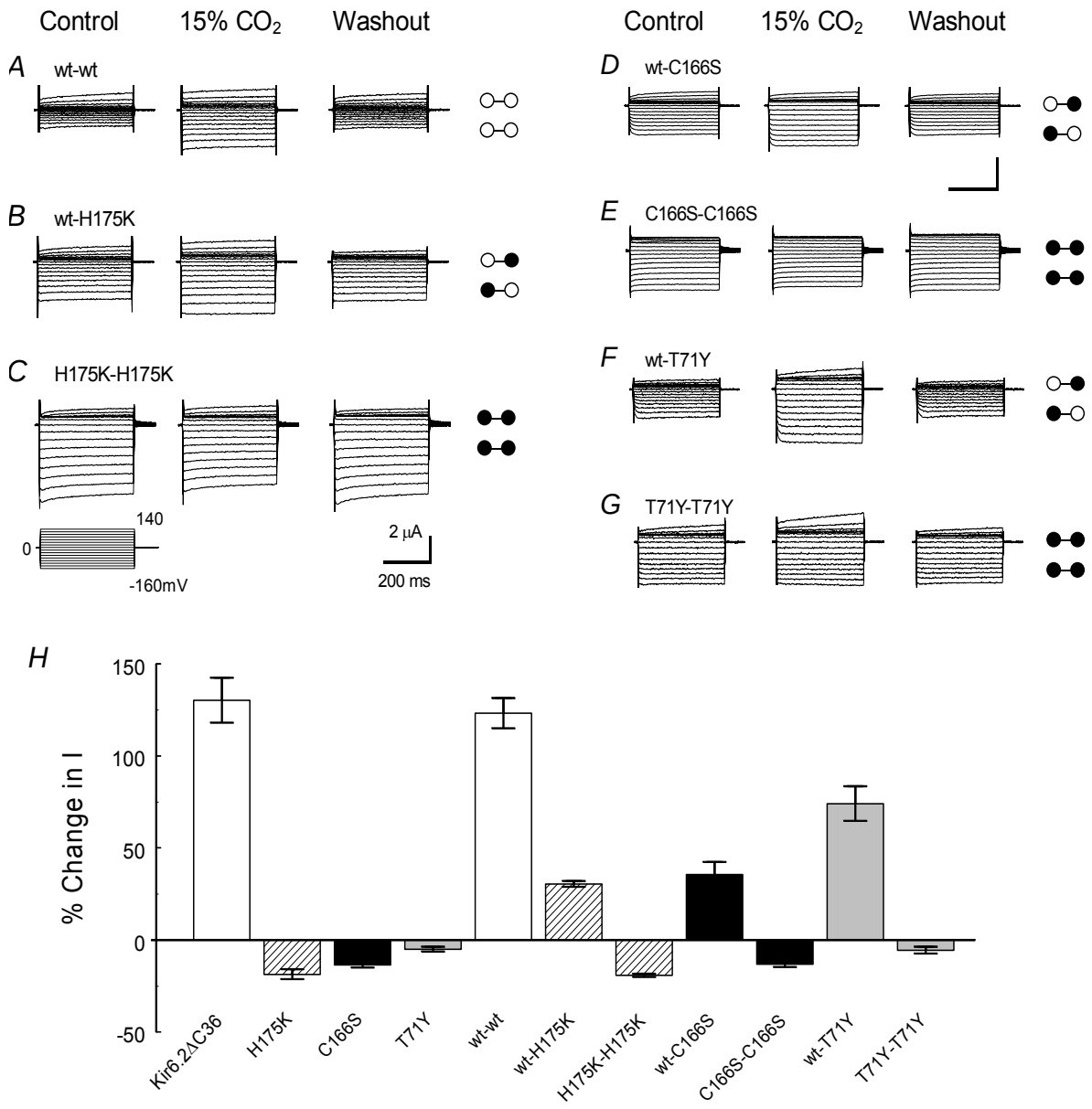

Fig. I-II-2. Response of concatenated-dimeric Kir6.2 channels to acidic pH. ***A.*** Concatenated dimer made of two wt subunits remained to be activated by acidic pH to a similar degree as the monomeric Kir6.2ΔC36. The pH sensitivity was completely eliminated in concatenated dimers with both subunits disrupted with the H175K (***C***), C166S (***E***) or T71Y (***G***) mutation. Intermediate response to 15% CO_2 was seen in heteromeric dimers containing the H175K (***B***), C166S (***D***) or T71Y (***F***) mutation. Calibration: 200ms/2μA for A-C; 200ms/8μA for D, E; 200ms/4μA for the rest. ***H.*** Percentage activation and inhibition of the inward rectifying currents of monomeric and dimeric Kir6.2 channel and its mutants. Data are presented as means ± s.e. (n =4-8). Dr. Junda Su performed the whole cell recording (***A-G***).

To determine how the proton sensor in each subunit contributes to the pH-dependent channel gating, three dimeric concatemers were constructed based on the Kir6.2ΔC36 (referring to the wild-type or wt in the present study) and the H175K, i.e., wt-wt, wt-H175K and H175K-H175K. All of the dimers expressed inward rectification currents with amplitude of 1.4 to 7.2 μA (Table I-II-1; Fig. I-II-2A-C). Exposure of the oocytes to 15% CO_2 led to activation of wt-wt channel by 123.3±8.2% (n=8) similar to the homomeric Kir6.2ΔC36 (Fig. I-II-2H). Like the monomeric H175K channel, the dimeric H175K-H175K totally lost the channel activation by CO_2. Instead, the channel was inhibited during hypercapnic acidosis (Table I-II-1; Fig. I-II-2C, H). The currents of heteromeric wt-H175K were inhibited by 30.5±1.6% (n=5) during CO_2 exposure (Table I-II-1; Fig. I-II-2B,H).

The dimeric T71Y-T71Y and C166S-C166S behaved like their monomeric counterparts, which were both inhibited to the same degree during CO_2 exposure as monomeric T71Y and C166S (Table I-II-1; Fig. I-II-2E,G,H). In contrast, the heteromeric wt-C166S was activated to about the same level as the wt-H175K when exposed to 15% CO_2 (Table I-II-1; Fig. I-II-2D,H). The stimulatory effect of CO_2 was doubled and reached 74.1±9.4% (n=5) in the heteromeric wt-T71Y (Table I-II-1; Fig. I-II-2F,H). The partial pH sensitivity of the heteromeric channels indicates that none of His175, Cys166 and Thr71 has a dominant negative effect.

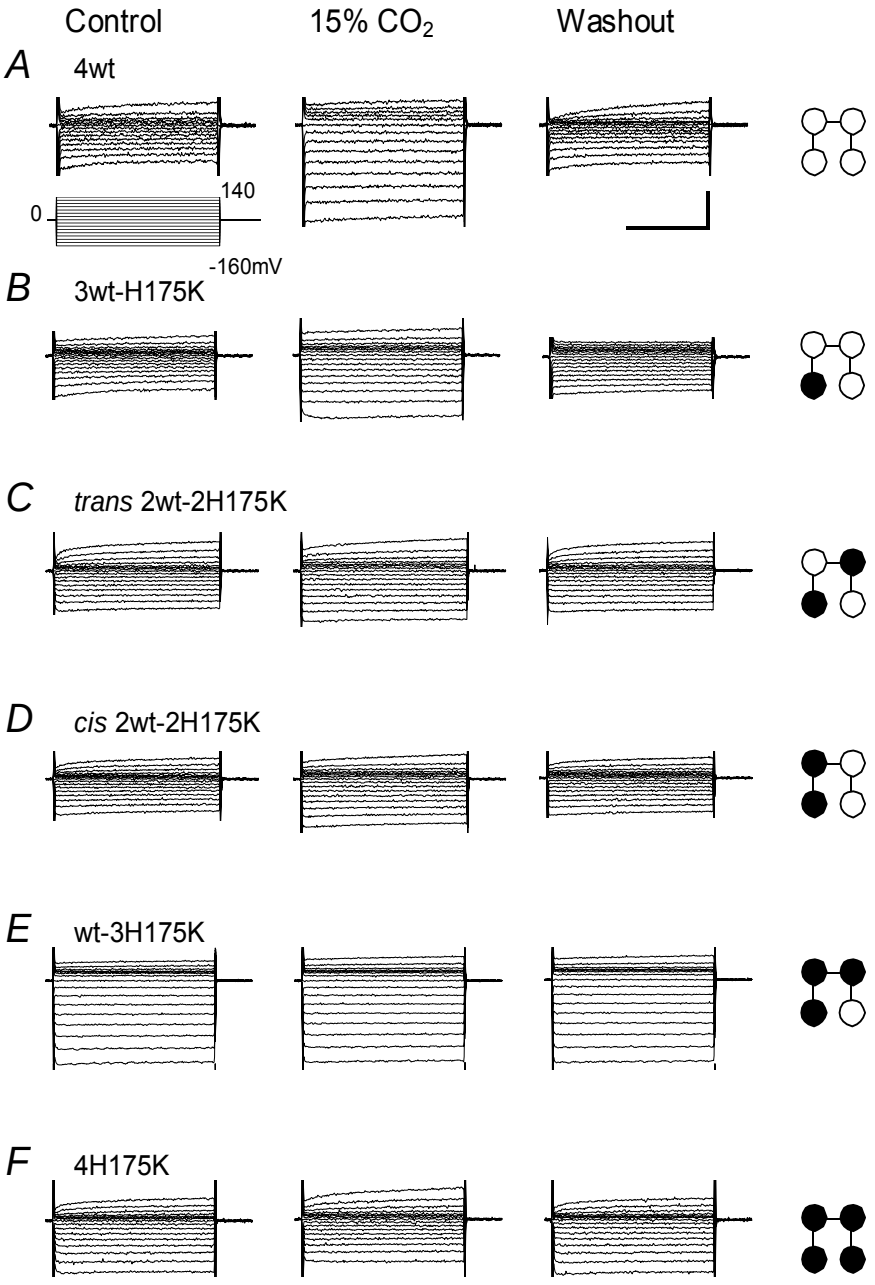

Fig. I-II-3. CO_2 sensitivity of H175K concatenated tetramers. ***A.*** The concatenated tetramer with 4 wt subunits (4wt) was augmented by hypercapnic acidosis to the same degree as its monomeric and dimeric counterparts. ***B.*** The 3wt-H175K was stimulated during CO_2 exposure. ***C,D.*** The *trans* 2wt-2H175K responded to CO_2 similarly as the *cis* 2wt-2H175K. ***E.*** The wt-3H175K lost its CO_2 sensitivity. ***F.*** The 4H175K was even inhibited with CO_2 exposure. Calibration: 200ms/2μA for A; 200ms/3μA for the rest. The whole cell recording for 4wt channel was conducted by Dr. Xueren Wang, Junda Su and Yun Shi. Others were performed by Dr. Junda Su.

I-II-2-b. Stoichiometry of proton binding

To understand the subunit stoichiometry for the proton binding, tetrameric concatemers were constructed with the wt and H175-disrupted subunits. The channels with two functional subunits located at adjacent and diagonal positions were named *cis* and *trans* 2wt-2 H175K, respectively. All concatenated-tetrameric constructs were functionally expressed with properties, such as inward rectification, current amplitude and time-dependent activation and inactivation kinetics, indistinguishable from the monomeric and dimeric wt channels (Fig. I-II-3). Also similar to the wt channel was the pH sensitivity of the 4wt, which was augmented by 120.4±9.9% (n=4, P>0.05) during 15% CO_2 exposure (Fig. I-II-3A; Table I-II-1). Disruption of one functional subunit caused a loss of the pH sensitivity by ~50% in the 3wt-H175K (Fig. I-II-3B). Both *cis* and *trans* 2wt-2 H175K were activated moderately by acidic pH by ~25%, levels that did not show any statistical difference between the*se* two configurations (P>0.05, n=8) (Fig. I-II-3C,D; Table I-II-1) With three subunits disrupted, the wt-3H175K became completely insensitive to hypercapnic acidosis, and was even slightly inhibited during CO_2 exposure (Fig. I-II-3E). Like its monomeric dimeric counterparts, the 4H175K was inhibited by 24.0±2.7% (n=7) during the CO_2 exposure (Fig. I–II-3F). This inhibition is known to be caused by protonation of three histidine residues located further downstream the H175 (His186, His193 and His216) (Xu et al. 2001b). Since these histidine residues exist in all constructs, we tentatively considered the small inhibition produced to be constant and normalized them to zero when performing current normalization (see below).

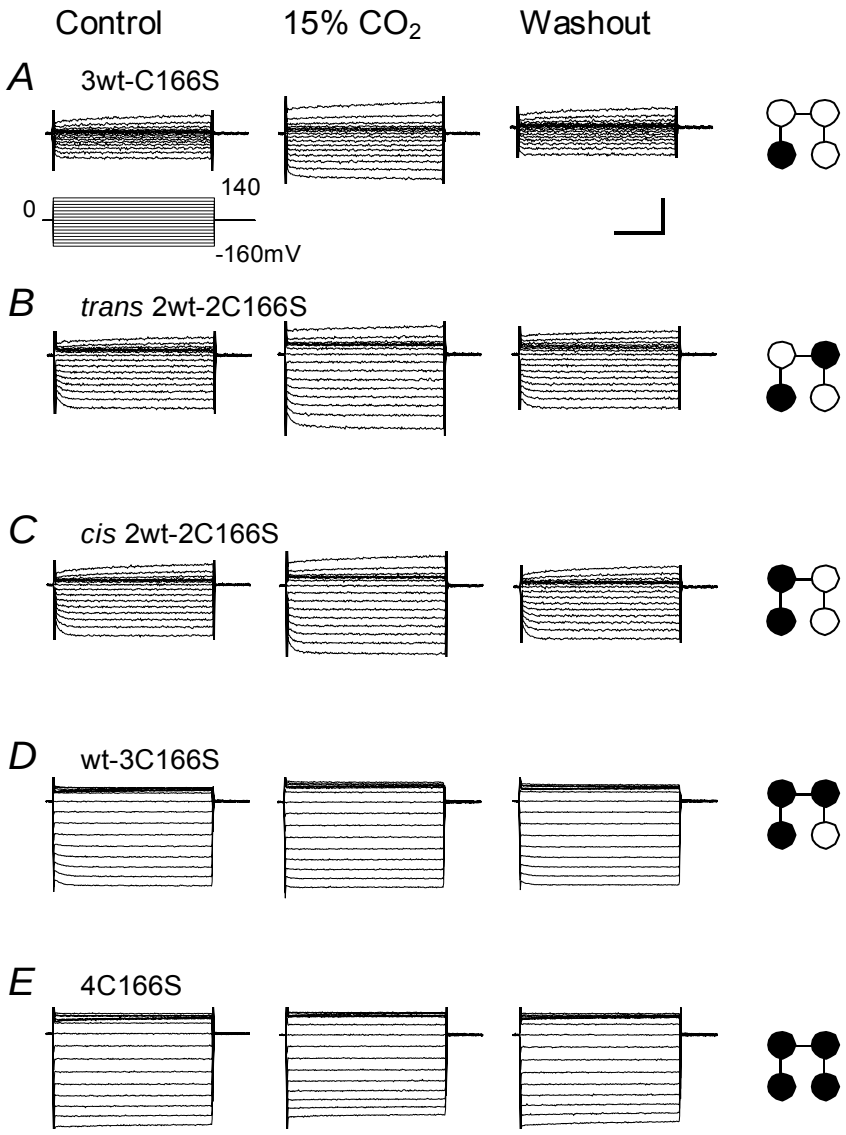

Fig. I-II-4. Responses of the C166S concatenated tetramers to CO_2. While the 3wt-C166S (***A***), *trans* 2wt-2C166S (***B***) and *cis* 2wt-2C166S (***C***) were stimulated, the wt-3C166S (***D***) and 4C166S (***E***) lost their CO_2 sensitivity. Calibration: 100ms/3μA for A-C; 100ms/6μA for the rest. Dr. Junda Su performed the whole cell recording.

I-II-2-c. Stoichiometry of channel gating

In contrast to His175, Cys166 and Tyr71 are not titratable, and their role in the pH sensitivity of Kir6.2 channel is very likely to be related to channel gating or the coupling of ligand binding to channel gating. To understand the stoichiometry of channel gating, therefore, we constructed tetrameric concatemers using the C166S and T71Y to disrupt functional subunits. Baseline properties of the concatenated tetramers with C166S-disrupted subunits were almost the same as the monomeric and dimeric channels of the C166S. Similar to H175K subunit disruption, tetrameric concatemers with C166S-disrupted subunits showed graded losses of the pH sensitivity. Disruption of one functional subunit reduced the pH-dependent channel activation to 65.1 ± 9.7% (n=4) (Fig. I-II-4A). With two subunits disrupted, the *trans* 2wt-2C166S was still augmented by 35.7 ± 2.4% (n=5) which was almost identical to the level of the *cis* 2wt-2C166S channel activation (Fig. I-II-4B,C; Table I-II-1). Also similar to the H175K constructs, the wt-3C166S and 4C166S were slightly and markedly inhibited during CO_2 exposure, respectively (Fig. I-II-4D,E; Table I-II-1). These results suggest that the channel gating stoichiometry revealed with C166S subunit disruption is similar to that produced with H175K.

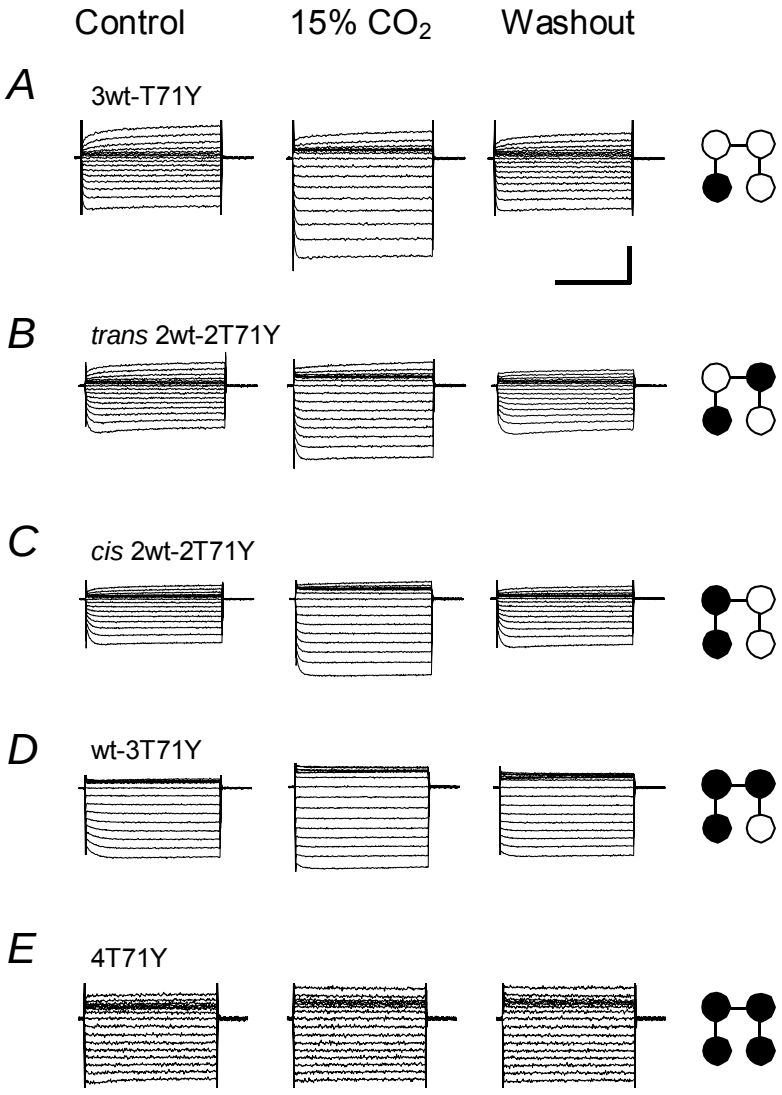

Fig. I-II-5. Effects of CO_2 on T71Y concatenated tetramers. ***A.*** The 3wt-T71Y was stimulated during CO_2 exposure. ***B,C.*** The *trans* 2wt-2T71Y responded to CO_2 to the same extent as the *cis* 2wt-2T71Y. ***D.*** The wt-T71Y was insensitive to CO_2. ***E.*** The 4 T71Y was even inhibited during CO_2 exposure. Calibration: 100ms/4μA for A, B; 200ms/3μA for e; 200ms/6μA for the rest. Dr. Junda Su conducted the whole cell recording.

Tetrameric concatemers with T71Y-disrupted subunits showed a similar pattern as the C166S constructs. Although the *trans* 2wt-2T71Y had slightly higher pH sensitivity than the *cis*, the difference was statistically insignificant ($P>0.05$). These concatemers were more sensitive to pH than the H175K and C166S constructs. The 3wt-T71Y was augmented by 90.1 ± 6.1% (n=6) during CO_2 exposure, which was significantly higher than that of the H175K and C166S ($P<0.05$) (Fig. I-II-5A). Also more strongly activated were the *trans* and *cis* 2wt-2T71Y constructs (Fig. I-II-5B,C; Table I-II-1). The wt-3T71Y remained to be activated, while the 4T71Y was modestly inhibited with hypercapnia (Fig. I-II-5D,E; Table I-II-1).

I-II-2-d. Subunit cooperativity and coordination

To reveal subunit cooperativity, the percentage channel activation was plotted against number of disrupted subunits. The inhibition seen in 4H175K, 4C166S and 4T71Y was normalized to 0.01, and the maximum activation was normalized to 0.99. The plots were then compared to two classes of models with and without cooperativity (see Methods). The HH model describes channel gating process produced by independent action of individual subunits (Hodgkin and Huxley, 1952; Liu et al., 1998; Ulens and Siegelbaum, 2003), whereas the MWC model describes positive cooperativity, in which four subunits undergo a single concerted transition between channel opening and closure (Monod et al., 1965; Liu et al., 1998; Ulens and Siegelbaum, 2003). All H175K, C166S and T71K constructs resembled the MWC model but not the HH model (Fig. I-II-6B-D), suggesting the existence of positive cooperativity for the proton-dependent Kir6.2

channel gating. The normalized activations of the constructs with H175K mutation were compared with the corresponding constructs carrying C166S or T71K mutations. Significant differences were found between all H175K and T71Y tetramers except 4175K and 4T71Y ($P<0.05$), but not between H175K and C166S constructions ($P>0.05$).

Introduction of the first functional subunit had a rather small effect on the pH sensitivity. Such an effect was much more evident with the joining by the second functional subunit. Indeed, the channels gained about 30% of the pH sensitivity with two functional subunits (Fig. I-II-6A). This was more evident for the T71Y constructs. Although two functional subunits enabled significant pH sensitivity, the full scale channel gating by intracellular protons required all four subunits (Fig. I-II-6A). The step increases in the pH sensitivity also suggest special subunit coordination. The increase in pH sensitivity mostly occurred with the introduction of the second and fourth subunits except the 4T71Y (Fig. I-II-6E-F). Thus, these observations suggest that the subunits may work as two pairs of functional dimers in the pH-dependent channel gating.

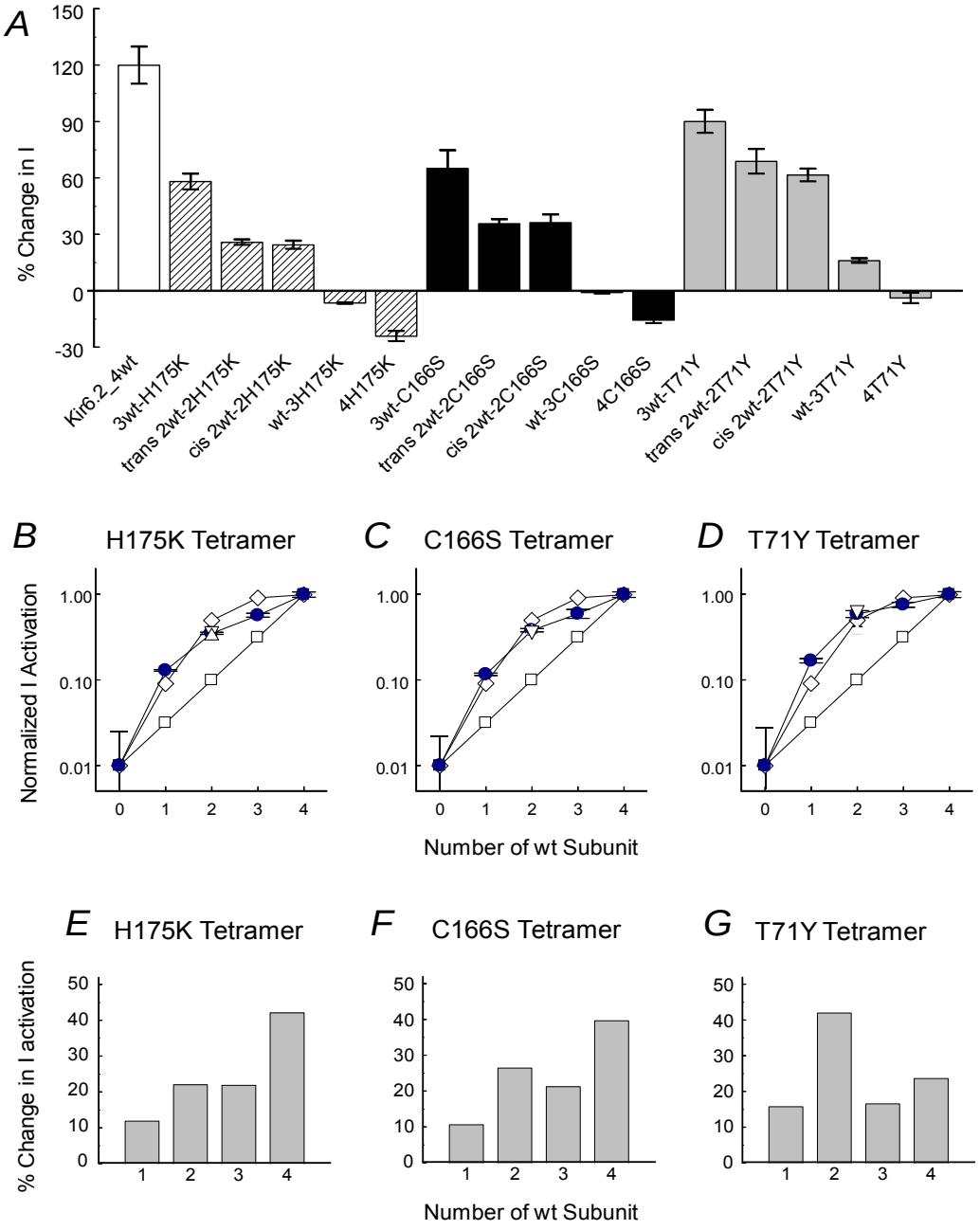

Fig. I-II-6. Subunit coordination and cooperativity in the pH-dependent Kir6.2 channel gating. ***A.*** Percentage effect of 15% CO_2 on concatenated tetramers. Data are presented as means ± s.e. (n = 4-11). ***B-D.*** Plots of current activation versus the number of wt subunits. Open square, data prediction based on the HH model; open diamond, prediction with the MWC model (see text for details). ***B.*** The plot of tetrameric H175K (solid circle) closely resembles the MWC model. Similar results are seen in the C166S (***C***) and T71Y plots (***D***). Upper triangle, the *cis* tetramers; down triangle, heteromeric dimers. ***E-F.*** Percentage changes in current activation in the presence of different numbers of wt subunits. Although the introduction of every new wt subunit leads to a leap in the channel activation, greater effects were seen with the second one. Similar effects were also seen with the fourth wt subunit except the 4T71Y.

I-II-3. Discussion

This is the first demonstration on the subunit stoichiometry of Kir6.2 channel gating by a specific ligand molecule. The proton-binding and channel-gating mechanisms were selectively disrupted in different number of subunits. Our data have shown that such a channel gating requires all four subunits although two of them can produce significant pH sensitivity. There is strong positive cooperativity among subunits in proton binding and channel gating. The similarity in subunit stoichiometry for proton binding and channel gating suggests that the channel gating signal or movement comes directly from the C terminus where protons bind to.

I-II-3-a. Channel sensitivity to intracellular pH

While most Kir channels (Kir1.1, Kir1.2, Kir2.3, Kir2.4, Kir4.1, Kir4.2 and the heteromeric Kir4.1-Kir5.1) are inhibited by acidic pH, the K_{ATP} channels are activated followed by strong inhibition with intracellular acidification (Coulter et al., 1995; Shuck et al., 1997; Tsai et al., 1995; Hughes et al., 2000; Fakler et al., 1996; Zhu et al., 1999; Pessia et al., 2001; Yang et al., 1999; Yang et al., 2000; Xu et al., 2001a, b). The channel inhibition is not seen in whole-cell recording and has been shown to be related to channel rundown (Xu et al., 2001a, b). Therefore, the channel activation by acidic pH is an important regulatory mechanism of the channels. In fact, the pH sensitivity has been shown to allow the channels to regulate skeletal muscle excitability and vascular tone (Davis, 1991; Chrissobolis et al., 2003). We have previously shown that the pH sensitivity of the K_{ATP} channels is an inherent property of the channel that depends on the Kir6 subunit but not the SUR1 (Xu et al. 2001a). More importantly, we have identified

the protonation site (His175) in the Kir6.2 subunit (Xu et al. 2001b). The fact that the His175 is the only protonation site in the Kir6.2 subunit has allowed us to further identify critical protein domains and AA residues that play a role in channel gating but not in proton binding (Piao et al. 2001; Cui et al. 2003). These include Cys166 and Thr71, both of which are involved in the Kir6.2 channel gating by multiple ligand molecules (Trapp et al., 1998a; Cui et al., 2003; Piao et al., 2001; Wu et al., 2004).

I-II-3-b. Proton binding versus channel gating

The demonstration of specific sites that play a critical role in ligand binding and channel gating makes it possible to study subunit stoichiometry for these channel functions. Although we have recently shown subunit stoichiometry for Kir1.1 channel gating using the K80M to disrupt individual subunits (Wang et al., 2005b), there are still uncertainties as to whether the Lys80 in Kir1.1 is a protonation site, a site for channel gating or both. Therefore, the Kir6.2 with the well defined proton sensor (His175) and gating sites (Cys166 and Thr71) appears more helpful to understand the ligand-binding, channel gating and binding-gating coupling. By selectively disrupting proton binding in a given number of subunits, we have seen graded losses of the pH sensitivity with a decrease in wt subunits. The stoichiometric pattern is quite similar to that revealed by channel gating disruption with the C166S mutation. The similarity as well as the close location of these two residues suggests that the signal of conformational change produced by proton binding to His175 is directly coupled to the membrane helices where the Cys166 is found. Although the T71Y constructs also show stepwise reductions in the pH sensitivity, the degree is significantly less for every concatenated constructs than that for

H175K and C166S constructs. These results suggest that the conformational change produced by protonation of a C-terminal residue is also coupled to the base of the N terminus or the TM1 helix whose conformational change is equally important for the channel gating. Recent studies in CNG, Kir and Kv channels have shown that protein domains at near the membrane-spanning sequences play an important role in channel gating (Varnum and Zagotta, 1997; Meera et al. 1997; Drain et al. 1998; Schulte et al. 1999; Tucker et al. 1998; Minor et al. 2000; Qu et al. 2000). During the gating process, these protein domains may move or interact with each other leading to a change in protein conformation and channel activity. Certain physical interaction between these intracellular termini as well as between the TM1 and TM2 has been demonstrated (Tucker and Ashcroft, 1999; Wang et al. 2005a). Such interaction has been shown not only to affect the channel opening and closure but also to determine how the channel gating movement is proceeded (Wang et al. 2005a). Therefore, it is possible that proton binding to the C terminus initiates a cascade of conformational changes involving the C terminus, N terminus and their linked membrane helices.

I-II-3-c. Cooperativity and coordination

These studies allow us to have a close look at several stoichiometric mechanisms that have not been seen previously in the monomeric channels. First, none of the His175, Cys166 and Thr71 has a dominant negative effect, although mutation of each of them completely eliminates the pH-dependent Kir6.2 gating (Xu et al., 2001b; Trapp et al., 1998a; Cui et al., 2003). Second, there is extensive positive cooperativity among the subunits for proton binding as well as channel gating. Such a positive cooperativity is

consistent with previous studies on the wt channel showing a high value of the Hill coefficient in excised patches (Xu et al., 2001a, 2001b). In the close vicinity of the Cys166, another residue Thr171 has been found to play also an important role in Kir6.2 channel gating (Drain et al. 2004). Co-injection of the T171A and wt cRNAs reveals that the Thr171 forms an inhibition gate and its movements require the concerted, rather than independent, action of all four Thr171 regions (Drain et al. 2004), consistent with our finding in the C166S constructs. Third, subunits appear to be coordinated in functional dimers during channel gating. The existence of functional dimers, which is in agreement with several previous studies in other tetrameric ion channels (Liu et al., 1998; Ulens and Siegelbaum, 2003; Wang et al., 2005b), seems to lead to higher pH sensitivity and greater response in channel activity to acidic pH. Fourth, two subunits in *trans* configuration may interact as a functional dimer as those in *cis* configuration, consistent with our previous observations in the Kir1.1 channel (Wang et al. 2005b). Finally, the pH-dependent gating can be fulfilled by two functional subunits, although the full pH sensitivity requires all four subunits in the channel. With these subunit coordination and cooperativity, the pH-dependent Kir6.2 channel gating can be largely preserved even with disruptions of one or two functional subunits.

In conclusion, the pH-dependent Kir6.2 channel gating has been studied by selective disruptions of proton binding and channel gating mechanisms. Several novel findings have been made including the stoichiometry for proton binding and channel gating, subunit coordination and cooperativity. Such information may help understand the ligand-dependent gating of the K_{ATP} channels as well as other ligand-gated ion channels.

I-II-4. Summary and Conclusions

The K_{ATP} channels are gated by several metabolites, whereas the gating mechanism remains poorly understood. Kir6.2, a subunit of the pancreatic and striated muscular K_{ATP} channels, has all machineries for ligand binding and channel gating. In the Kir6.2, His175 is the protonation site, and Thr71 and Cys166 are involved in channel gating. Here we show subunit stoichiometry for proton binding and channel gating by selectively disrupting functional subunits in a tetrameric channel using mutations of these residues. All homomeric dimers and tetramers showed pH sensitivity similar to the monomeric channels. Heteromerization with the wild-type and disrupted subunits revealed that none of these sites had a dominant-negative effect on proton-dependent channel gating. Subunit stoichiometry for proton binding was almost identical to that for channel gating involving the Cys166, suggesting a one-to-one coupling from the proton binding to the channel gating between the C terminus and TM2 helix. The gating stoichiometry for the Thr71 region was different from that for the Cys166 suggesting distinct contributions of TM1 and TM2 helices to channel gating. In the pH-dependent channel gating, the subunits underwent concerted rather than independent action. Two wild-type subunits appeared to form a functional dimer in both *cis* and *trans* configurations. The subunit stoichiometric studies thus provide novel insight into the Kir6.2 channel gating by intracellular protons.

I-III. Subunit-Stoichiometric Evidence for Kir6.2 Channel Gating, ATP Binding and Binding-Gating Coupling

Manuscript in submission:

Wang, R., Zhang,X., Cui,N., Wu, J., and Jiang,C. Subunit-stoichiometric evidence for Kir6.2 channel gating, ATP binding and binding-gating coupling.

Acknowledgement: In this study, the cDNA construction and patch-clamp recording each took 50% efforts, and I did most of the work for both, assuming to be 80-85%. Other people contributed to 15-20%. Also I drafted the manuscript. Xiaoli Zhang helped me with the mini and midi preparation and has constructed four dimers. Dr. Ninren Cui helped me with several patch-clamp experiments. Dr. Jianping Wu also tested on construct. I appreciate all the helps.

I-III-1. Introduction

K_{ATP} channels play an important role in insulin secretion, glucose uptake, myocardium excitability and neuronal responses to metabolic stress (Ashcroft and Gribble 1998; Seino, 1999). Such functions rely on the sensitivity of the channels to intracellular ligand molecules, by which these channels couple intermediary metabolites to cellular excitability. The K_{ATP} channel activity is inhibited by intracellular ATP and activated by ADP, protons and phospholipids (Noma, 1983; Cook and Hales, 1984; Aschcroft et. al., 1984; Lederer and Nichols, 1989; Davies, 1990; Baukrowitz et al., 1998; Shyng and Nichols, 1998; Xu et al., 2001a). Like other ligand-gated ion channels, the interaction of the K_{ATP} channel protein with the ligand (*ligand binding*) is believed to trigger a cascade of conformational changes and concerted movements of individual subunits, leading to channel opening or closure. The latter step is known as *channel gating*, and intermediate steps refer to signal transduction or *coupling*. Although this scenario has been supported by a number of previous studies (Armstrong et al., 1966; Enkvetchakul et al., 2001; Perozo et al., 1999; Flynn and Zagotta, 2001; Johnson and Zagotta, 2001; Jiang et al. 2002b; Jin et al., 2002; Phillips et al., 2003), the differentiation of ligand binding from channel gating and coupling has been challenging with current experimental approaches and has led to widespread misinterpretation (Colquhoun, 1998).

Since most of the previous studies were done on homomeric channels of wt or mutants, further understanding of how individual subunits in a multimeric channel act in ligand binding, channel gating and their couplings, and how they are coordinated in ligand-dependent gating depends on information from heteromeric channels. We thus

performed studies on tandem-dimeric and tandem-tetrameric channels constructed with a predetermined number of subunits disrupted with T71Y, C166S and K185E mutations. Although a number of residues are involved in ATP sensitivity, Lys185 is outstanding. The K185E mutation causes an over 100-fold reduction in ATP sensitivity (Drain et al. 1998; Tucker et al. 1998; Reimann et al., 1999), while this residue is not involved in sensing sulfonylurea, protons and lipid metabolites (Xu et al., 2001b; Wu et al., 2002b; Ribalet et al., 2003; Manning Fox et al., 2004), indicating that it plays a role in the ATP-dependent but not ATP-independent gating. Further studies have shown that Lys185 indeed contributes to ATP binding at the Kir6.2 protein (Tanabe et al., 1999; Trapp et al., 2003; Dong et al., 2005). In contrast, Cys166 is known to participate in channel gating or the final stage of signal transduction from ligand binding to channel gating, as the C166S mutation disrupts K_{ATP} channel gating by ATP, protons and sulfonylurea (Trapp et. al., 1998a; Piao et al., 2001; Wu et al., 2004). Similarly Thr71 is likely to act in channel gating by ATP and protons as well (Cui et al., 2003; Wang et al. 2005a). Studies on the subunit stoichiometry of K_{ATP} channels whose ATP binding or channel gating is disrupted with these residues thus may generate information about the subunit coordination, cooperativity and minimal number of functional subunits required for ATP-dependent gating. They may also shed insight into subunit contributions to ligand binding, channel gating and potential coupling mechanism of ligand binding to channel gating.

I-III-2. Results

I-III-2-a. Selective suppression of ATP-dependent channel gating.

The Kir6.2ΔC36 channel was expressed in *Xenopus* oocytes. The rationale for choosing this form of K_{ATP} channels was 1) the truncation of 36 residues at the C terminus allows the Kir6.2 to be expressed without the SUR subunit with much of the ATP sensitivity retained (Tucker *et al.,* 1997), and 2) it can simplify the studies of ATP-dependent channel gating by dissecting the contribution from the SUR subunit. Expression of the channel was screened by two-electrode voltage clamp using a bath solution (KD90) containing 90mM K^+. Cells showing clear inward rectifying K^+ currents were used for further patch-clamp studies. Injection of the expression vector alone did not yield inward rectifying currents. Macroscopic currents with multiple active channels were recorded in excised inside-out patches using giant recording pipettes. Exposure of intracellular membranes to perfusates with various ATP levels produced a concentration-dependent inhibition of the currents. The ATP–current relationship was described with the Hill equation. The IC_{50} value was 110 μM (n = 12) and the h value was 1.2 (n = 12) (Fig. I-III-1A,E). The ATP sensitivity was mostly eliminated with either C166S, K185E or T71Y mutation (Fig. I-III-1B-D; Table I-III-1).

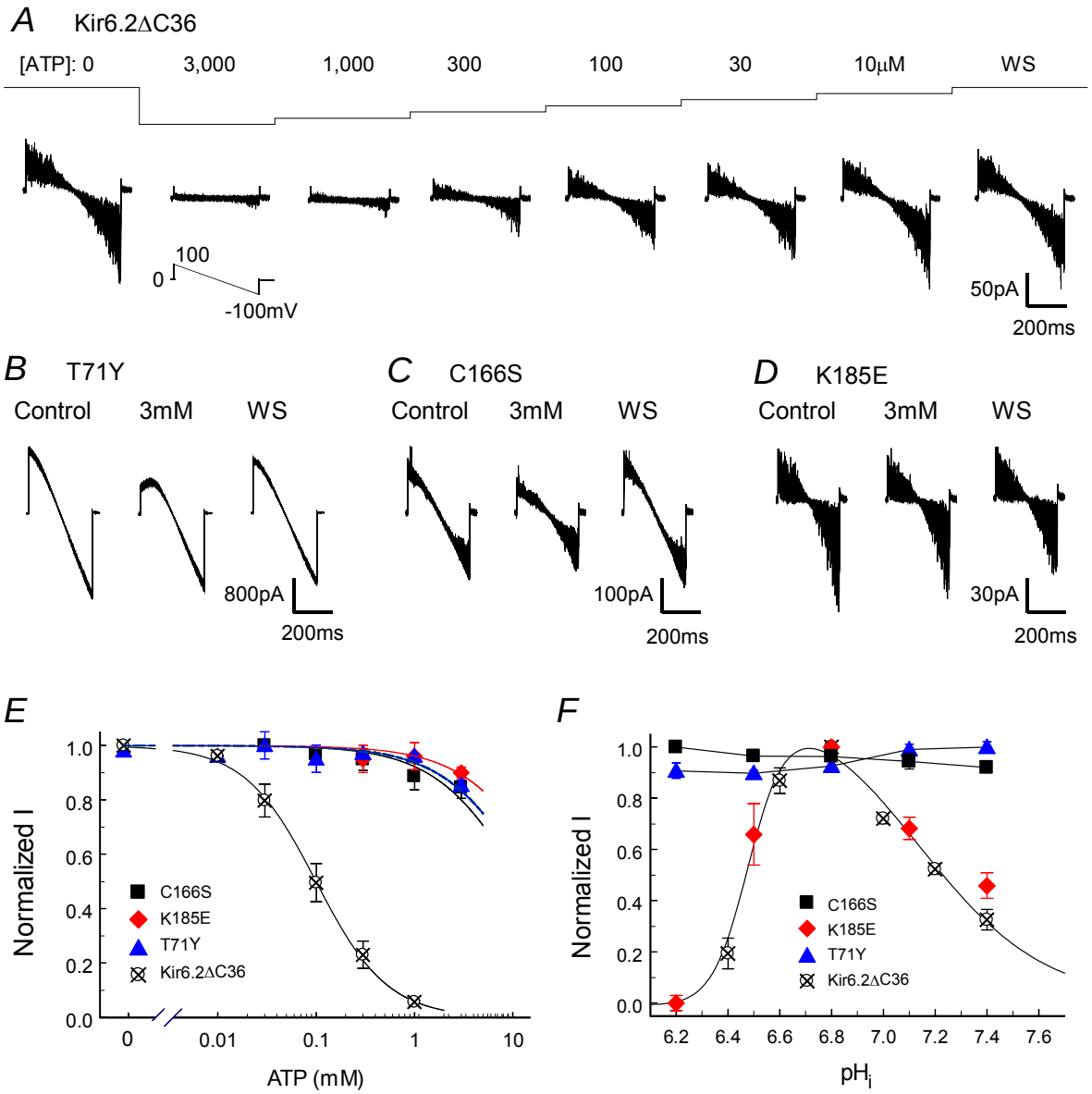

Fig. I-III-1. The ATP and pH sensitivity of the wt and mutant homomeric monomers. Currents were recorded from inside-out patches with symmetric concentration of K^+ across the patch membrane. ***A.*** In the wt Kir6.2ΔC36 channel, exposure of the internal membrane to ATP produced fast and reversible inhibition of the inward rectifying currents with a half-current inhibition by 100 μM ATP. ***B-D.*** High concentration of ATP (3 mM) only slightly inhibits the T71Y (***B***), C166S (***C***) and K185E (***D***) mutants. ***E.*** The ATP-current relationship is expressed using the Hill equation. The dose-response curves show that all channels carrying T71Y, C166S or K185E mutations lose their ATP sensitivity. ***F.*** The pH-current relationship shows that the pH sensitivity of the K185E is the same as the wt Kir6.2ΔC36, while the T71Y and C166S mutant do not respond to acidic pH. Data are presented as means ± s.e. The recordings were performed by Dr. Jianping Wu.

Table I-III-1. Measurements and predictions of Kir6.2 constructs.

Construct	Baseline P_{open}	Residual I (%)	Hill equation IC_{50} ATP (mM)	Hill equation h	n	Operational model τ_A / τ_C	Operational model K_A / K_C (mM)	Operational model IC_{50} ATP (mM)
Monomer								
Kir6.2ΔC36	–	0.0	0.11	1.2	12	–	–	–
K185E	–	–	>20	1.2	4	–	–	–
C166S	–	–	>10	–	4	–	–	–
T71Y	–	–	>20	–	4	–	–	–
Tandem-dimer								
wt-wt	–	0.0	0.15	1.1	7	–	–	–
wt-K185E	–	9.7	0.22	1.1	5	–	–	–
K185E-K185E		–	>20		4			
wt-C166S	–	0.0	0.62	1.0	4	–	–	–
C166S-C166S	–	–	>10	1.0	5	–	–	–
wt-T71Y	–	0.0	1.00	1.2	4	–	–	–
T71Y-T71Y	–	–	>20	1.1	5	–	–	–
Tandem-tetramer								
4wt	0.116	0.0	0.15	1.2	10	0.19	0.13	0.15
K185E								
3wt-K185E	0.118	0.0	0.17	1.1	4	0.16	0.18	0.18
cis 2wt-2K185E	0.127	4.4	0.18	1.1	4	0.15	0.18	0.18
trans 2wt-2K185E	0.116	12.7	0.23	1.1	6	0.14	0.23	0.24
wt-3K185E	0.120	19.7	0.60	0.9	7	0.08	0.65	0.53
4K185E	0.120	–	>20	0.9	5	0.03	>20	>20
C166S								
3wt-C166S	0.180	0.0	0.17	1.2	5	0.28	0.18	0.19
cis 2wt-2C166S	0.514	0.8	0.72	1.2	4	1.05	1.15	0.75
trans 2wt-2C166S	0.497	0.8	0.72	1.2	5	1.05	1.15	0.75
wt-3C166S	0.556	–	1.80	1.1	4	1.29	3.60	1.82
4C166S	0.723	–	7.00	1.1	4	2.50	>20	6.74
T71Y								
3wt-T71Y	0.490	0.0	0.25	1.1	4	1.00	0.38	0.22
cis 2wt-2T71Y	0.540	0.8	1.10	1.2	4	1.10	1.80	1.14
trans 2wt-2T71Y	0.511	0.8	1.10	1.2	4	1.10	1.80	1.14
wt-3T71Y	0.736	–	6.00	1.1	4	2.50	18.00	5.78
4T71Y	0.738	–	>20	1.1	4	2.50	>20	>20
Coupling dimer								
wt-K185/C166	0.538	27.8	0.78	1.0	5	0.65	1.40	0.85
K185-C166	0.542	50.6	1.10	1.0	5	0.42	1.70	1.20
wt-K185/T71	0.545	46.6	1.10	1.0	4	0.42	1.70	1.20
K185-T71	0.581	51.8	1.10	1.0	4	0.42	1.70	1.20

All mutant channels were constructed on Kir6.2ΔC36. Residue currents (I) were measured as a portion of maximal channel activity in the presence of 30mM ATP. Data are presented as means ± s.e. Abbreviation: h, Hill coefficient; n, number of observation; –, not available.

The Kir6.2ΔC36 channel is also gated by intracellular protons, in which a protonation site (His175) has been previously identified (Xu *et al.,* 2001b). The pH-dependent channel gating was lost with the T71Y or C166S mutation, suggesting a role of these residues in channel gating (Fig. I-III-1E,F). In contrast, the K185E mutation disrupted the ATP-dependent but not the pH-dependent channel gating (Fig. I-III-1E,F), supporting that the Lys185 contributes to ATP binding as reported in several previous studies (Drain et al. 1998; Reimann *et al.,* 1999; Tanabe *et al.,* 1999; Trapp *et al.,* 2003; Dong *et al.,* 2005).

I-III-2-b. Effects of heteromeric recombination of tandem-dimeric channels

To understand the subunit stoichiometry of Kir6.2 channel gating by intracellular ATP, we first constructed tandem-dimeric channels by linking the wt Kir6.2ΔC36 and C166S-mutant subunits in wt-wt, wt-C166S and C166S-C166S configurations. All dimeric concatemers expressed functional currents without significant changes in inward rectification, current amplitude and other single channel properties in comparison to their monomeric counterparts. Macroscopic currents of the wt-wt channel were dose-dependently inhibited by ATP with an IC_{50} value of 150 μM (n = 7) and h value of 1.2 (n = 7). Complete current inhibition was reached with 3mM ATP (Fig. I-III-2D; Table I-III-1). The ATP sensitivity was eliminated in the C166S-C166S dimer with IC_{50} greater than 10 mM, consistent with the monomeric C166S (Fig. I-III-2D; Table I-III-1). The ATP sensitivity of the heteromeric wt-C166S dimer lay in between the homomeric wt-wt and C166S-C166S channels. The ATP-current relationship of the wt-C166S was closer to that

of the wt-wt dimer with IC_{50} of 0.62 mM and h value of 1.0 (Fig. I-III-2A,D; Table I-III-1).

Similar constructions were also performed for the Thr71. The ATP sensitivity of the T71Y-T71Y dimer was comparable to the monomeric T71Y channel (Fig. I-III-2D). Like the C166S dimers, the ATP sensitivity of the wt-T71Y was closer to the wt-wt channel than the T71Y-T71Y dimer, in which a parallel shift of the ATP-current relationship curve was observed. The IC_{50} value increased to 1.0 mM with h value of 1.2 (Fig. I-III-2A,D; Table I-III-1).

To determine the contribution of each subunit to the ATP binding, a group of dimers was created with the mutation at Lys185. The homomeric K185E-K185E responded to intracellular ATP like the corresponding monomer. Interestingly, the wt-K185E currents were not totally inhibited even with high concentrations of ATP and the plateau level of inhibition was reached at 3 mM (Fig. I-III-2C,D). In contrast to the wt-T71Y and wt-C166S channels, there were still ~9.7% residue currents left uninhibited under 30 mM ATP in the wt-K185E (Table I-III-1), suggesting a different stoichiometry for ligand binding from that for channel gating. The dose-response curve showed that the IC_{50} of ATP was only 70 μM higher in the wt-K185E than in the wt-wt channel with no change in the h values (Fig. I-III-2D; Table I-III-1). The ATP-dependent gating was well retained and began to manifest itself in these dimeric constructs.

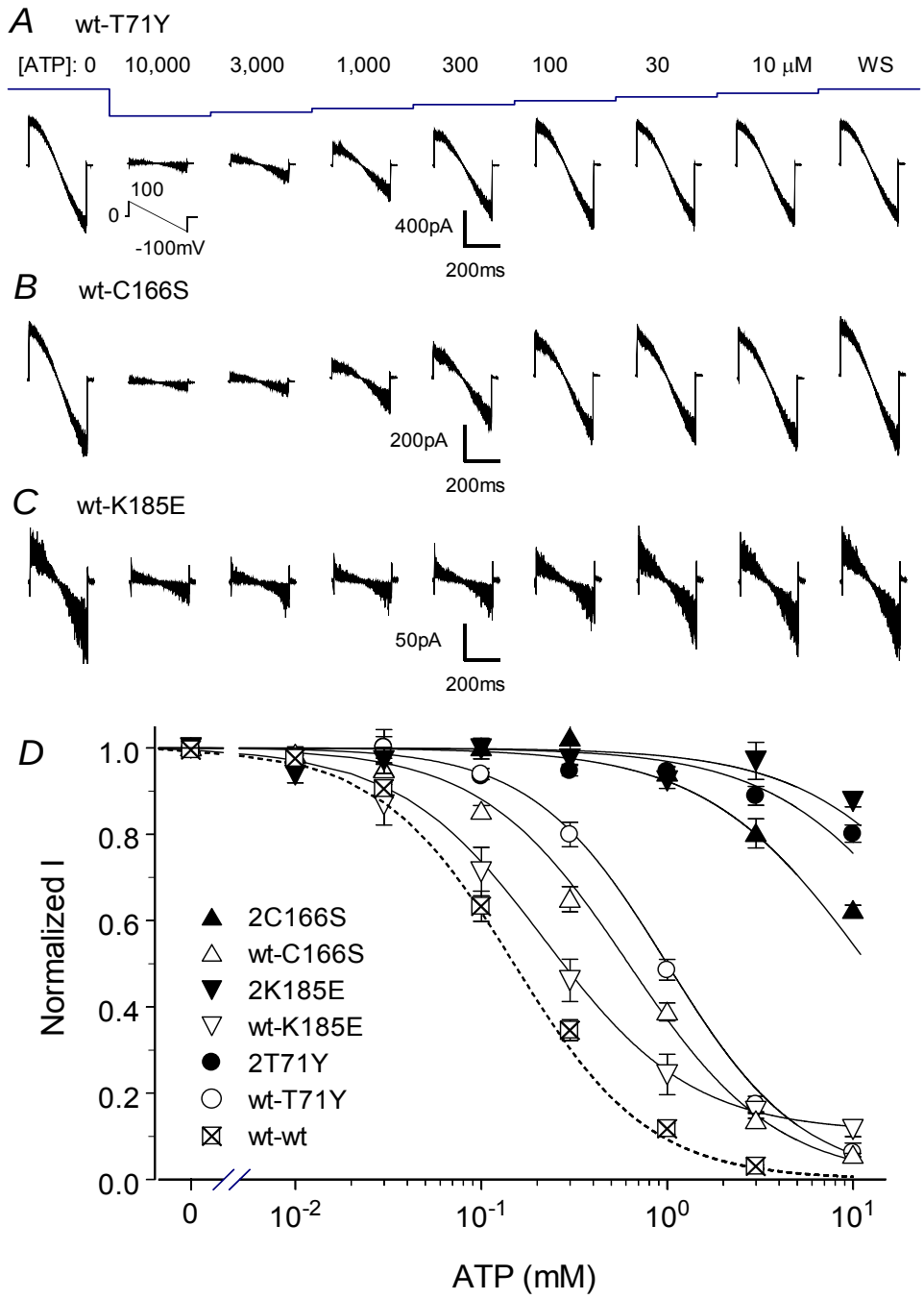

Fig. I-III-2. ATP response of the tandem-dimeric Kir6.2 channels. Intracellular ATP produced dose-dependent inhibition in the heteromeric wt-T71Y (***A.***) and wt-C166S (***B.***) dimers. The currents were almost completely inhibited by 10 mM ATP. ***C.*** Although the wt-K185E currents were also inhibited, the inhibitory effect reached the plateau with 1 mM ATP and there were still substantial currents uninhibited. ***D.*** The dose-response curves of the homomeric wt and mutant dimers show the same ATP sensitivity to their monomeric counterparts. The curves of the heteromeric wt-C166S and wt-T71Y dimers lay in between the wt-wt and mutant dimers with the curves more close to the wt-wt channel. The ATP-current relationship for the wt-K185E dimer was special, as there were ~10% of currents left uninhibited with 10 mM ATP.

I-III-2-c. Subunit stoichiometry for ATP binding

To understand further the subunit stoichiometry of the ATP binding, tetrameric concatemers were constructed with the wt and K185E-disrupted subunits. The channels with two functional subunits located at adjacent and diagonal positions were named *cis* and *trans* 2wt-2K185E. Similar to the dimeric wt-K185E, the P_{open} of several K185E-concatenated tetramers were not fully inhibited with 30 mM ATP, although their IC_{50} levels were rather low (Fig. I-III-3,4). In the presence of substantial uninhibited channel activity, the concentration-response relationship of these K185E-concatenated tetramers can no longer be described using the conventional Hill equation without counting the levels of maximum inhibition. Indeed, the ATP-current relationship resembles partial antagonism for ligand-receptor interactions (Kenakin, 2004), suggesting that the subunit disruption causes a loss of not only ligand binding potency but also efficacy. Therefore, we employed the operational model for the ligand-receptor interaction to describe the subunit stoichiometry of the K185E-concatenated tetramers (see Equation 4 in Methods). Two constants are introduced in the equation, i.e., dissociation constant K_A and allosteric constant τ_A. According to Black et al. (1985), Colquhoun (1998), Trzeciakowski (1999a) and Kenakin, (2004), K_A and τ_A are measures of the binding affinity of the ligand-receptor complex and the magnitude of the first step of conformational change after ligand binding, respectively. The model has been used to describe multiple steps of events of the ligand-receptor interaction, i.e., formation of ligand-receptor complex, the consequent conformational change of the ligand binding domain and signal transduction

(Black *et al.,* 1985; Colquhoun, 1998; Trzeciakowski, 1999a; Kenakin, 2004). The IC_{50} can also be calculated using these two factors (Equation 7).

Since there is no significant difference in the spontaneous P_{open} of all K185E constructs (Table I-III-1), an average of P_{open} from all K185E constructs was used for the data analysis. The construct with all four subunits disrupted showed very low ATP sensitivity (K_A > 20mM, τ_A < 0.05 and IC_{50} > 20mM) (Fig. I-III-3E). When the first wt subunit was introduced, the wt-3K185E channel gained ATP sensitivity drastically, with the IC_{50} reduced to submillimolar range (530μM, h 0.9). The increase in ATP sensitivity was due to a great leap in the ATP binding affinity (K_A 650μM) although the efficacy was still low (τ_A = 0.08; Fig. I-III-3A,E; Table I-III-1). Another significant leap in ATP sensitivity was seen with addition of the second wt subunit at the *trans* position (IC_{50} = 240 μM and h = 1.1), which was contributed by both K_A (230 μM) and τ_A (0.14). The ATP binding affinity and efficacy were further increased (K_A = 180 μM, τ_A = 0.15) in the *cis* 2wt-2K185E, and the IC_{50} was reduced to 180 μM suggesting that ATP prefers two subunits at adjacent positions. Interestingly, introduction of the third wt subunit produced almost no change in the ATP sensitivity (IC_{50} = 180 μM, h = 1.1) with nearly the same K_A (180 μM) and τ_A (0.16) levels as the *cis* 2wt-2K185E. The IC_{50} was lowered to 150 μM with the fourth wt subunit, due to the improved ATP binding affinity (K_A = 130 μM) and efficacy (τ_A = 0.19).

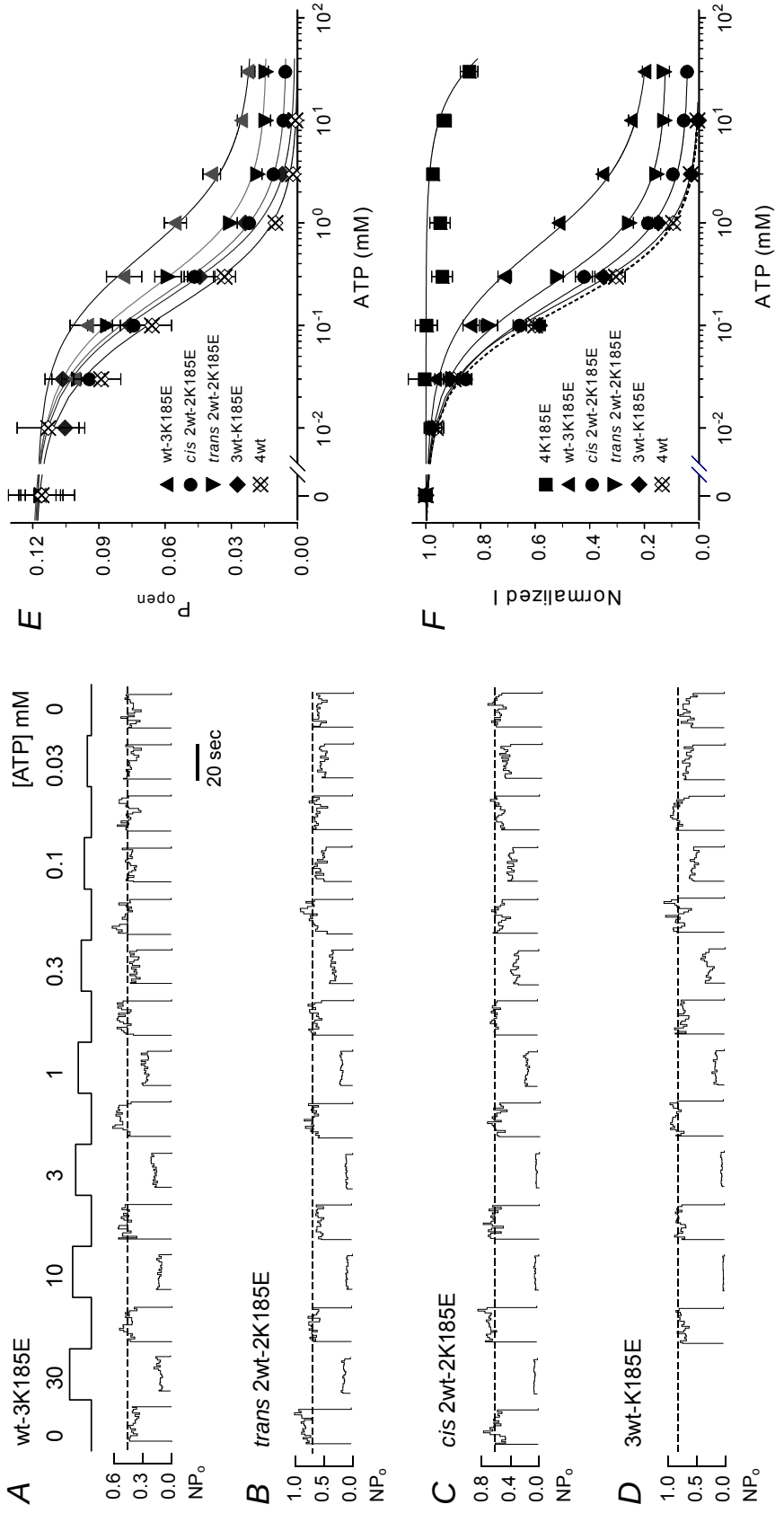
A
wt-3K185E
[ATP] mM
0
30
10
3
1
0.3
0.1
0.03
0
20 sec
NPo
B
trans 2wt-2K185E
C
cis 2wt-2K185E
D
3wt-K185E
E
Popen
ATP (mM)
wt-3K185E
cis 2wt-2K185E
trans 2wt-2K185E
3wt-K185E
4wt
F
Normalized I
4K185E
wt-3K185E
cis 2wt-2K185E
trans 2wt-2K185E
3wt-K185E
4wt
ATP (mM)

Fig. I-III-3. Effects of intracellular ATP on the channel activity of tetrameric K185E constructs. ***A.*** Single channel activity was recorded in the same condition as in Fig. I-III-1 with the membrane potential held at -80 mV. The P_{open} was obtained with each ATP concentration. Fast and reversible inhibition in the single channel activity was seen in the wt-3K185E. The inhibition reached the maximum level with 10 mM ATP, and no further inhibition was found with higher concentrations. ***B.*** The inhibitory effect of ATP was stronger in the *tans* 2wt-2K185E, and the maximum inhibition was reached with 10 mM. ***C.*** The ATP sensitivity further increased in the *cis* 2wt-2K185E, and 3 mM ATP produced maximum effect. Note that the residue channel activity was reduced with increasing numbers of wt subunits. ***D.*** The 3wt-K185E was fully inhibited with 10 mM ATP. ***E.*** The single-channel activity is expressed as a function of the intracellular ATP concentration using equation 2 based on the operational model (see method). The baseline P_{open} averaged 0.116. The ATP sensitivity and the maximum inhibitory effect increases with more wt subunits. ATP has larger inhibitory effect on the *cis* 2wt-2K185E than on the *tans* 2wt-2K185E. Incomplete inhibition was seen in channels carrying 2 or more disrupted subunits. ***F.*** The ATP-current relationship curves were also fitted with Hill equation after normalizing the baseline activity to 1.0. The IC_{50} levels obtained are comparable to those calculated with operational model (Table I-III-1).

For comparison, we also fitted the data with the Hill equation. The IC_{50} and h values obtained were rather comparable to those predicted with the operational model (Fig. I-III-3F,E; Table I-III-1). The maximum inhibition of the constructs increased with addition of wt subunits, and the increase was less when there were more wt subunits (Table I-III-1).

I-III-2-d. Subunit stoichiometry for channel gating

To understand the subunit stoichiometry for channel gating, tandem-tetrameric channels were constructed with C166S-disrupted subunits. Described with the Hill equation, the ATP sensitivity of the homomeric 4C166S (IC_{50} = 7.0 mM) was comparable with the corresponding monomeric and dimeric channels (Fig. I-III-5A_2; Table I-III-1), indicating that the tandem linkage of four pore-forming subunits does not disrupt the ATP-dependent gating of the channel.

A prominent effect of the C166S-subunit disruptions was a graded increase in baseline channel activity. The baseline P_{open} rose from 0.116 in the wt channel to 0.723 in the 4C166S, while other constructs showed intermediate levels of baseline P_{open} (Table I-III-1). This observation as well as previous mutational analysis of homomeric channels showing that the Cyc166 mutation disrupted the long closures (Trapp et. al., 1998a) suggests that this site may be involved in setting a working range of the conformational change that results from ATP binding and is necessary for channel gating. The greater the working range, the greater the IC_{50} would be for fulfilling channel gating. Consistent with this idea, our results showed that the ATP sensitivity decreased gradually with introducing more C166S subunits (Fig. I-III-5A_2). Since both the ATP sensitivity and the

magnitude of channel activity changed in the C166S constructs, we decided to continue using the operational model to describe the ATP-current relationship, instead of using the Hill equation by normalizing all baseline channel activity to the same level. Based on the baseline P_{open} and ATP sensitivity, the K_C and τ_C were calculated according to equation 5 in Methods, where K_C is the affinity constant determined by K_A and τ_A, and τ_C is the allosteric constant that sets the working range of the second step of conformational change for channel gating. Our results showed that the τ_C increased from 0.19 to 2.50, and K_C changed from 0.15 mM to 21.00 mM with stepwise C166S-subunit disruptions. These led to a change in IC_{50} levels similar to those described with the Hill equation (Fig. I-III-5A_1,A_2). It is remarkable that the disruption of channel gating did not change the efficacy of ATP-induced channel inhibition or the maximum inhibition (Fig. I-III-4D,I-III-5A_1), which was in clear contrast with the K185E-disruption of ATP binding.

A similar trend of the changes in baseline P_{open} and IC_{50} was also seen in tetramers carrying T71Y mutation. With the addition of T71Y disrupted subunits, the baseline P_{open} increased from 0.116 to 0.738, and the τ_C rose from 0.19 to 2.50. The predicted IC_{50} values (0.15 to >20 mM) were also similar to those measured with the Hill equation in these mutations (Fig. I-III-5B_1,B_2; Table I-III-1). Also similar to the C166S constructs was the unchanged maximum inhibition with graded subunit disruptions (I-III-4E, and I-III-5B_1).

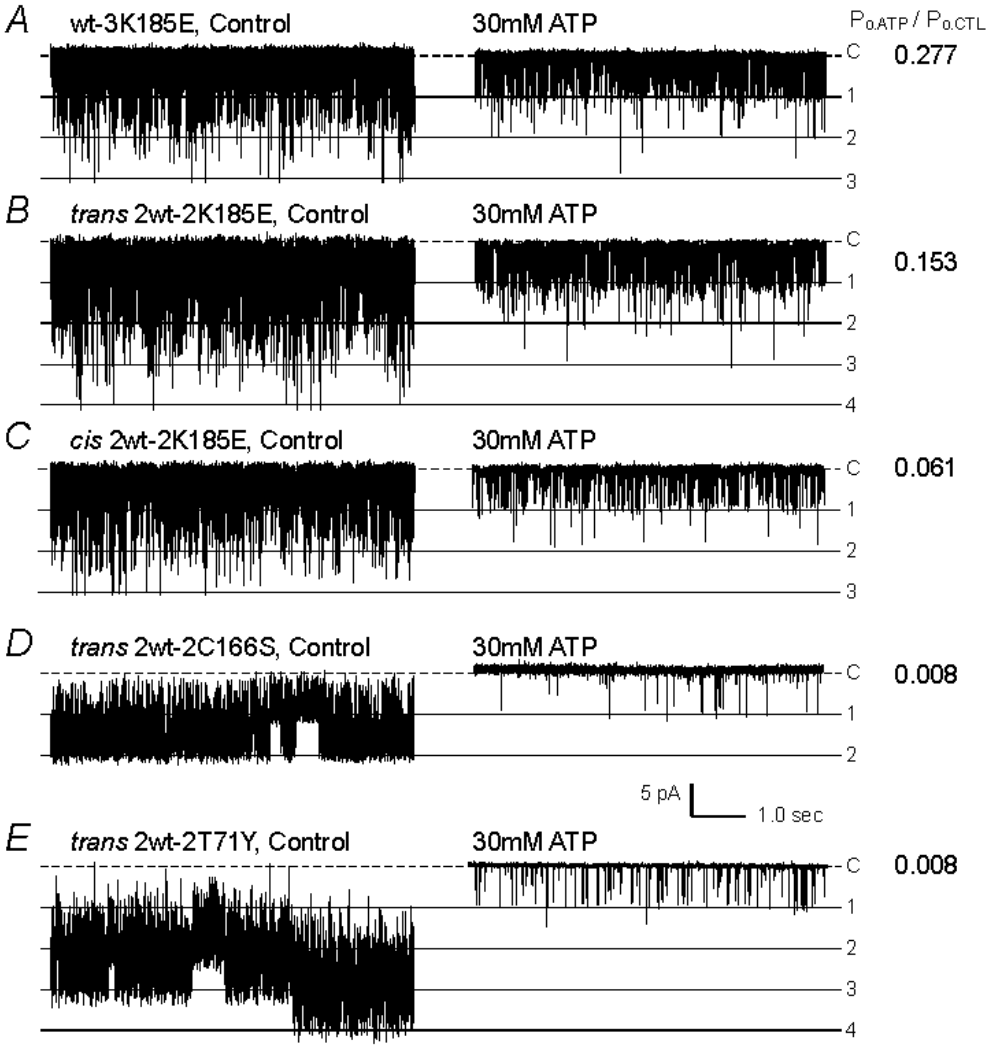

Fig. I-III-4. Single-channel activity of tetrameric channels recorded with and without ATP. Although all channels were inhibited by 30mM ATP, substantial uninhibited currents were seen in constructs containing K185E mutations. The ratio of the uninhibited channel activity was calculated based on the P_{open} with ATP ($P_{o.ATP}$) divided by that without ($P_{o.CTL}$), which was 27.7% for the 3wt-K185E (***A***), 15.3% for the *trans* 2wt-2K185E channel (***B***) and 6.1% for the *cis* 2wt-2K185E channel (***C***). In contrast, the *trans* 2wt-2C166S (***D***) and *trans* 2wt-2T71Y channels (***E***) were almost completely inhibited by 30 mM ATP with residue channel activity less than 1%.

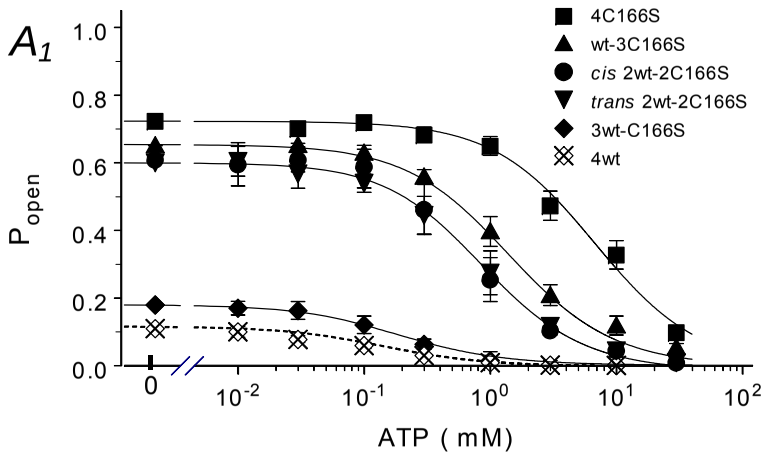
A1
P open
ATP (mM)
4C166S
wt-3C166S
cis 2wt-2C166S
trans 2wt-2C166S
3wt-C166S
4wt

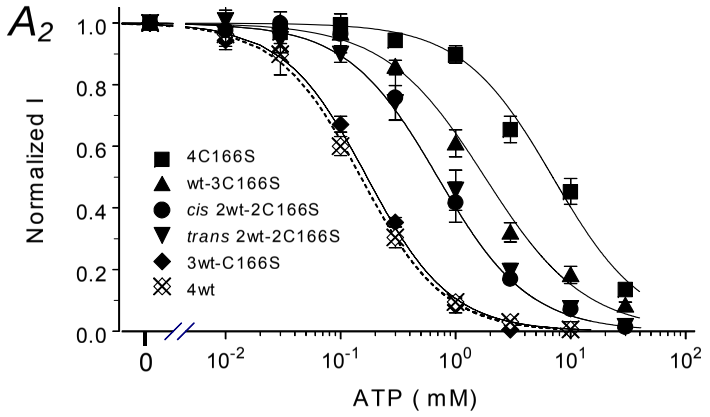
A2
Normalized I
ATP (mM)
4C166S
wt-3C166S
cis 2wt-2C166S
trans 2wt-2C166S
3wt-C166S
4wt

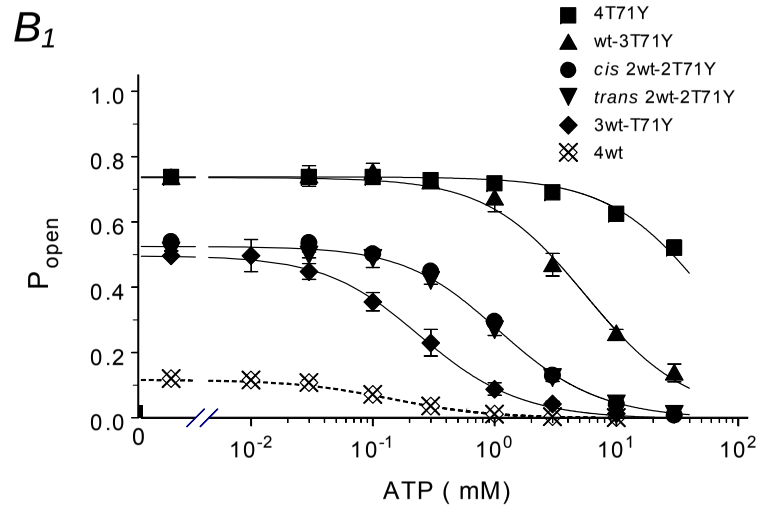
B1
P open
ATP (mM)
4T71Y
wt-3T71Y
cis 2wt-2T71Y
trans 2wt-2T71Y
3wt-T71Y
4wt

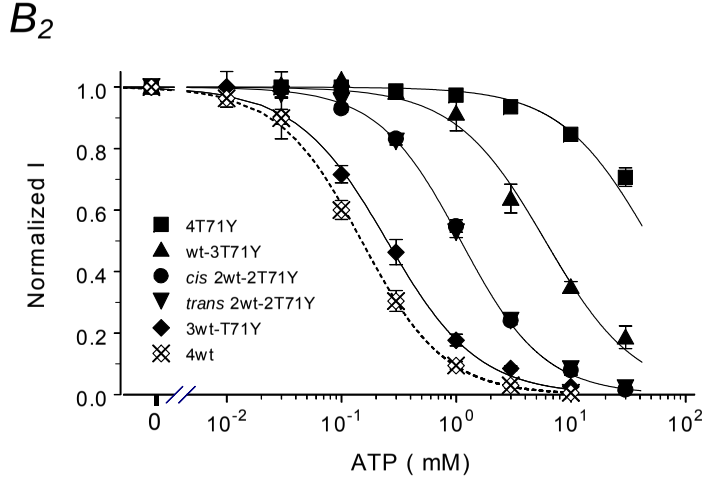
B2
Normalized I
ATP (mM)
4T71Y
wt-3T71Y
cis 2wt-2T71Y
trans 2wt-2T71Y
3wt-T71Y
4wt

Fig. I-III-5. The ATP sensitivity of tetramers with disruptions of channel gating. ***A_1-A_2.*** The ATP-current relationship of the C166S tetramers. ***A_1.*** The dose-response relationship of these tetramers is fitted with equation 3 according to baseline P_{open} of each C166S tetramer. The maximum inhibition reached zero in these tetramers. Their baseline P_{open} and IC_{50} decreased with addition of wt subunits. With three wt subunits, the ATP sensitivity of the 3wt-C166S was almost the same as the 4wt channel. The *cis* and *tans* 2wt-2C166S behaved just the same. ***A_2.*** The data were also fitted with Hill equation, and almost the same IC_{50} levels were obtained (Table I-III-1). ***B_1-B_2.*** Similar results were obtained in tetrameric T71Y constructs with the same data analysis.

I-III-2-e. Subunit cooperativity and coordination

To elucidate the subunit cooperativity and coordination, we plotted the IC_{50} values against the number of wt subunits, and compared our results to two classes of models with and without cooperativity. The HH model describes channel gating process produced by independent action of individual subunits (Hodgkin and Huxley, 1952), whereas the MWC model describes positive cooperativity, in which four subunits undergo a single concerted transition between channel opening and closure (Monod *et al.,* 1965). We found that our data could not be described with the HH model (Fig. I-III-6A-C), suggesting that four subunits do not act independently in either ATP binding or channel gating. The IC_{50} plot of K185E constructs was far from the MWC predication and even went below the HH predication (Fig. I-III-6A), suggesting the existence of negative cooperativity between subunits in ATP binding. In contrast, the IC_{50} plots of the C166S and T71Y tetramers were located in between of those predicted by the MWC and HH models (Fig. I-III-6B,C), suggesting moderate positive cooperativity. Further supporting the presence of positive cooperativity in channel gating were the baseline P_{open} plots against the number of wt subunits, as the baseline P_{open} plots were superimposed or even above the predicted values by the MWC model (Fig. I-III-6E,F).

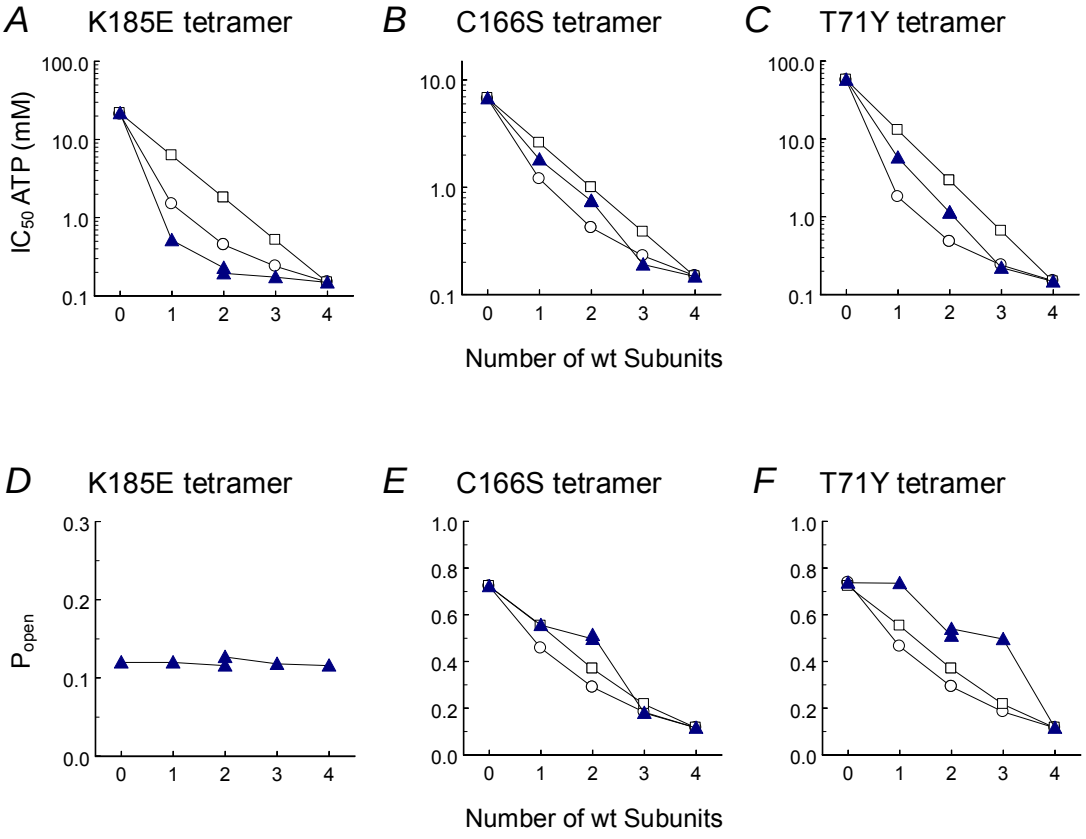

Fig. I-III-6. Subunit cooperativity and coordination of the Kir6.2 channel. ***A-C.*** IC_{50} plots versus number of wt subunits. Open square, data predictions based on the MWC model; open circle, data predictions based on the HH model. ***A.*** The IC_{50} plot of tetrameric K185E constructs (solid triangles) is far from the MWC prediction and even runs below the HH prediction. ***B,C.*** Unlike the K185E constructs, the plots of the C166S and T71Y tetramers are in between the predictions by the MWC and HH models. ***D-F.*** Changes of baseline P_{open} with number of wt subunits. ***D.*** The baseline P_{open} levels remain unchanged in all K185E mutations. ***E-F.*** The P_{open} plots of C166S and T71Y tetramers are both higher than the MWC prediction. Although each wt subunits decreases the baseline P_{open}, the greatest changes come with the first and third wt subunits in C166S tetramers and the second and fourth ones in T71Y tetramers.

These plots also suggested special forms of subunit coordination for ligand binding and channel gating (Fig. I-III-6E,F). Interruption of the ATP binding did not alter the baseline P_{open} of the K185E-disrupted channels (Fig. I-III-6D). Changes in baseline P_{open} were only seen when the binding-gating coupling was disrupted with C166S or T71Y mutations. In tetramers with the C166S mutation, the working range of P_{open} was greatly reduced by introducing the first wt subunits, while the second one gave rise to a smaller effect. The pattern of baseline P_{open} changes was nicely repeated when the third and fourth subunits were introduced (Fig. I-III-6E), indicating the existence of functional dimers between subunits, as previous shown in other ion channels (Liu et al., 1998). Such a subunit coordination was also found in the T71Y tetramers. The pattern of baseline P_{open} changes repeated when every other wt subunit was introduced although the major contribution came from the introduction of the second and fourth wt subunits (Fig. I-III-6F). It is possible that the functional dimers occurred in T71Y tetramers only between two wt subunits, whereas they may be formed between one wt and one mutant subunit in the C166S constructs.

I-III-2-f. Inter-subunit signal coupling

To gain insight into the coupling mechanisms of ATP-binding to channel gating in the Kir6.2 channel, concatenated dimers were constructed with the disruption of ATP binding or gating in the same or alternative subunit. We reasoned that if the coupling only existed within the same subunit, i.e., *cis*-coupling, it would be completely blocked in the K185E-T71Y and K185E-C166S concatenated dimers; if the coupling were only mediated by two adjacent subunits, i.e. *trans*-coupling, it would be disabled in the wt-

K185E/T71Y and wt-K185E/C166S constructs. The ATP sensitivity of these constructs was studied, and data were fitted with operational model since their baseline P_{open} and maximum inhibition were both different from the wt channel.

All these constructs showed similar baseline P_{open} (range from 0.538 to 0.581, $P>0.05$). With additional disruption of the coupling mechanism in alternative subunits, the working range of P_{open} ($\tau = 0.42$) was expanded in the K185E-C166S and K185E-T71Y, and the maximum inhibitory effect (48.2~49.4%) was reduced in comparison to the *trans* 2wt-2K185E channels (Fig. I-III-7A,D; Table I-III-1). Their ATP sensitivity was well retained (both were fitted with the equation with IC_{50} = 1.20mM, h = 1.0), suggesting the existence of the *trans* coupling.

The wt-K185E/T71Y responded to ATP exactly the same as the K185E-T71Y and K185E-C166S (Fig. I-III-7B,D; Table I-III-1). Higher ATP sensitivity was observed in the wt-K185E/C166S channel. Although the baseline P_{open} was not much different from that of the wt-K185E/T71Y, the maximum inhibition (72.2%) was much greater (Fig. I-III-7C,D; Table I-III-1). Its ligand binding affinity was similar to all other dimers (K_A = 1.4~1.7), and its IC_{50} (0.85mM) shifted to the left without evident change in the h value. These results suggest that *cis* coupling also exists, and the *cis* coupling in the C terminus appears to contribute more to the channel gating than the *trans* coupling.

To see whether the *cis* coupling in a single functional subunit is sufficient for the ATP-dependent gating, we constructed a tetramer by blocking all *cis* and *trans* couplings in three of the subunits using the wt-3C166S/K185E. Our test showed that there was no significant inhibition of this construct by intracellular ATP up to 30mM (Fig. I-III-7D).

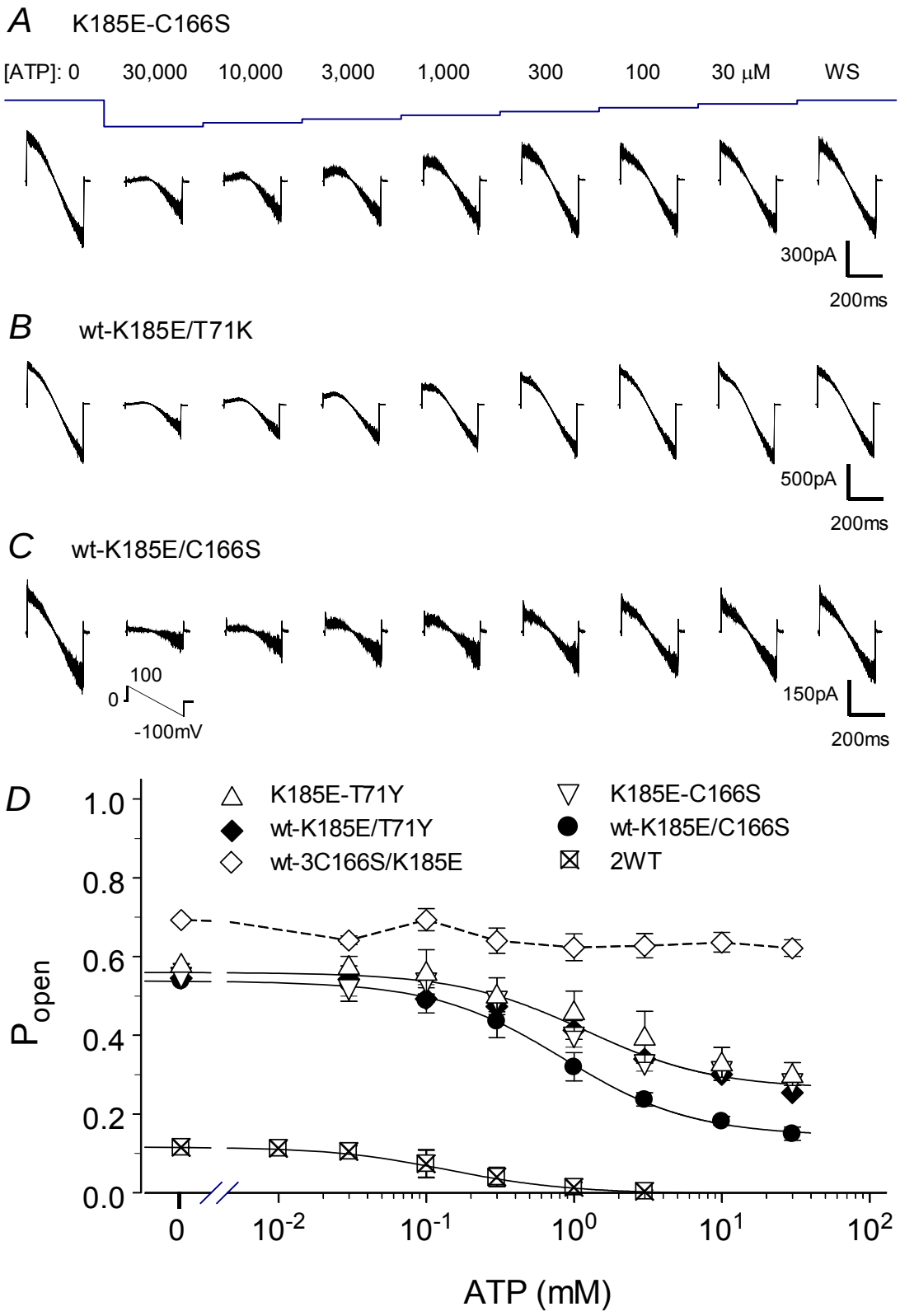
A
K185E-C166S
[ATP]: 0
30,000
10,000
3,000
1,000
300
100
30 μM
WS
300pA
200ms
B
wt-K185E/T71K
500pA
200ms
C
wt-K185E/C166S
100
0
-100mV
150pA
200ms
D
K185E-T71Y
wt-K185E/T71Y
wt-3C166S/K185E
K185E-C166S
wt-K185E/C166S
2WT
P open
1.0
0.8
0.6
0.4
0.2
0.0
0
10-2
10-1
100
101
102
ATP (mM)

Fig. I-III-7. The ATP sensitivity of dimers with disruptions of both ATP binding and channel gating. ***A.*** With the *cis* coupling mechanism being blocked in K185E-C166S channel, the currents were still sensitive to ATP, but the maximum inhibitory effect was only 50.6% with 30mM ATP. ***B.*** The response was the same in the wt-K185E/T71Y dimer that only allow the *cis* coupling in alternative subunits. ***C.*** The similar *cis* coupling in the dimeric wt-K185E/C166S channels gave rise to a higher ATP sensitivity, and 72.2% maximum inhibition was reached. ***D.*** The ATP-current relationship curves of these dimers are fitted with operational model. All dimers have higher baseline channel activity than the 2wt channel. The dimeric K185E-C166S, K185E-T71Y and wt-K185E/T71Y showed the same P_{open}, ATP sensitivity and maximum inhibitory effect, so that their ATP-current relationships were fitted with a single equation. Greater ATP sensitivity and maximum inhibition were seen in the wt-K185E/C166S dimer. With only one functional subunit, the wt-3CK channel lost almost totally its ATP sensitivity.

I-III-3. Discussion

By selective disruption of functional subunits for ATP-binding or channel gating, we have studied the subunit stoichiometry of the Kir6.2 channel in the ATP-dependent channel gating. These stoichiometric studies as well as the data analysis based on the operational model have led to several novel findings in the K_{ATP} channels.

I-III-3-a. Subunit stoichiometry in other ion channels.

Subunit stoichiometric studies provide important information about ligand-dependent channel gating. Disruption of ligand binding in CNG and hyperpolarization and cyclic nucleotide-gated (HCN) channels leads to reduction in potency and efficacy of ligand gating (Tibbs et al., 1997; Liu et al., 1998; Paoletti et al., 1999; Young et al., 2001; Ulens and Siegelbaum, 2003; Young et al., 2004). Prevention of certain subunits from binding to cyclic nucleotide reduces efficacy of ligand gating in CNG and HCN channels (Liu et al., 1998; Ulens and Siegelbaum, 2003). Mutation of the polyamine binding site in the Kir2.1 or the ATP binding pocket on Kir6.2 has a similar effect (Yang et al., 1995; Markworth et al., 2000). On the other hand, mutations of certain residues that are unlikely related to ligand binding produce a parallel shift of the dose-response curves (Schönherr et al., 1999). Also, increase in β subunit numbers that contribute to the inactivation of the BK channel shifts the G-V curves without changing the maximum activation (Wang et al., 2002). It is known that the opening of the CNG and HCN channels requires binding to one cyclic nucleotide, and nucleotide bindings to additional subunits give rise to further channel activation (Liu et al., 1998; Ulens and Siegelbaum, 2003). A similar effect is also seen in AMPA glutamate receptors (Rosenmund et al., 1998).

In Kir channels, our previous studies have revealed that one functional subunit is sufficient to activate the pH-dependent channel gating, although all four subunits are required for the complete pH sensitivity of the Kir1.1 channel (Wang et al., 2005b). Similarly, the Kir2.1 channel largely retains its sensitivity to intracellular Mg^{2+} and polyamines when there is only one functional subunit (Yang et al., 1995). Activation of the GIRK channels by $G_{\beta\gamma}$ has graded effects, with three $G_{\beta\gamma}$ subunits being required for the full channel activation (Sadja et al., 2002). In K_{ATP} channels, the binding of ATP to one of the four sites of the channel protein is sufficient to close the channel (Markworth et al., 2000). However, the inhibitory gate of the K_{ATP} channels needs the participation of all four subunits, and the contribution of each subunit to the gating transition is exponentially related to the number of functional subunits (Drain et al., 2004).

Stoichiometric studies have shown specific subunit cooperativity and coordination. Activation of BK channel by intracellular Ca^{2+} is highly positively cooperative (Niu and Magleby, 2002). Similar positive cooperativity has also been revealed in the gating transition of the K_{ATP} channel (Drain et al., 2004). The four subunits in the CNG, HCN and Kir1.1 channels are suggested to be associated as two independent dimers in the ligand-dependent channel gating (Liu et al., 1998; Ulens and Siegelbaum, 2003; Wang et al., 2005b).

I-III-3-b. ATP binding versus channel gating

The gating of a ligand-gated channel starts with ligand binding to the channel protein, which initiates a cascade of conformational changes leading to the opening or closure of the ion permeable pathway. The conformational changes produced by ligand binding may in turn affect the ligand binding affinity (Colquhoun, 1998). Therefore the effect of ligand binding and channel gating are often entangled together making the differentiation of binding from gating rather difficult. This problem is not limited to functional studies, since the conformational changes are known to affect results of binding assays as well (Colquhoun, 1998). Differentiation of binding from gating sites may be possible if 1) the protein structure is resolved in presence of the ligand, 2) the binding affinity is constant and unaffected by subsequent conformational changes following ligand binding, or 3) there are special residues and protein domains that affect channel gating by a specific ligand but not another. The K_{ATP} channel appears to satisfy the latter criterion. Intense studies of the channel over the past decade have revealed several sites critical for ATP binding and channel gating. Mutation of Lys185 abolished the ATP-dependent channel gating but not the proton- or sulfonylurea-dependent gating (Reimann et al., 1999; Trapp et al., 2003; Wu et al., 2002b; Ribalet et al., 2003). This Lys185 has been shown to interact with the ATP molecule directly (Drain et al. 1998; Tucker et al. 1998; Reimann et al., 1999; Tanabe et al., 1999; Trapp et al., 2003; Dong et al., 2005). In contrast, the Cys166 and Thr71 are likely to be involved in gating since mutations of these residues affect channel gating by multiple regulators (Trapp et al., 1998a; Piao et al., 2001; Wang et al., 2005a). Such a characterization of these sites makes

it possible to understand subunit stoichiometry for ligand binding and channel gating in the K_{ATP} channel.

The K185E tandem tetramers are special among all our constructs. In addition to the graded loss of the ATP sensitivity with more disrupted subunits, we saw substantial residue channel activity that was not inhibited by 30mM ATP. The reduction in efficacy of ligand gating in the K185E constructs thus is consistent with that found previously in the CNG and HCN channels indicating that ligand binding is disrupted (Tibbs et al., 1997; Liu et al., 1998; Paoletti et al., 1999; Young et al., 2001; Ulens and Siegelbaum, 2003; Young et al., 2004). The similarity of the effect to partial receptor antagonism has led us to adopt the operational model for description of the ATP-channel interaction by considering both potency and efficacy. The ATP-current relationship, indeed, is very well expressed with the operational model. The predicated IC_{50} values for all K185E constructs are almost identical to those measured with the Hill equation. Therefore, the model provides another level of understanding of the change in ATP sensitivity with respect to potential and efficacy. Furthermore, our results strongly suggest that Lys185 contributes to ATP binding with special subunit coordination and cooperativity (see below).

Unlike the K185E constructs, the C166S and T71Y tandem tetramers were fully inhibited by high concentrations of ATP. Although their ATP-current relationship can be described with the Hill equation, subunit disruptions with the C166S and T71Y mutations increase not only the IC_{50} but also the baseline P_{open}, both of which have been previously observed in monomeric C166S and T71Y and explained to be a result of the disruption of

the channel closure in the gating mechanism (Trapp et al., 1998a; Cui et al., 2003). In the present study, we have attempted to explain these phenomena by fitting our data using the operational model. We assumed that Cys166 and Thr71 may set a range of conformational changes for probability of channel opening and closure in the wt channel. Such a working range, perhaps determined by the flexibility of these local regions, increases with the disruption of these residues, leading to the augmentation of baseline P_{open}. The P_{open} change can be nicely described with τ_C in the operational model. Then, why does the K_C as well as IC_{50} value also increase with the disruption of the sites that are apparently not involved in ATP binding? The simplest explanation is that subunit disruption with the C166S or T71Y mutations expands the working range for channel gating process, and consequently higher concentrations of ATP are needed to inhibit the channel activity. The operational model may help to further understand its molecular basis. According to the operational model, multiple steps of conformational changes occur following ligand binding, including the formation of ligand-channel complex, the consequent conformational change of ligand binding domain, signal transduction or coupling, and channel gating movement (Trzeciakowski, 1999a, 1999b). These steps are arranged in series with the conformational change of a given step depending not only on its previous step but also to certain degree on its successor. It is likely that the subunit disruption with the C166S or T71Y impairs the necessary conformational change in a gating or coupling step. Without the necessary conformational change in the step, its prior events including the ATP binding affinity are thus affected. Therefore, K_C is

determined by the conformational change of its predecessor, i.e., K_A and τ_A, and its change produced by C166S or T71Y subunit disruptions also affects the IC_{50} of ATP.

I-III-3-c. Subunit coordination and cooperativity

Our subunit stoichiometry studies have also revealed interesting subunit cooperativity, coordination and minimum number of functional subunits required for ATP binding and channel gating. Subunit disruption with the K185E mutation greatly reduces the ATP binding affinity and efficacy. The IC_{50} value of ATP decreases with addition of wt subunits. The greatest change occurs with the introduction of the first wt subunit in the 3wt-K185E, while smaller effects are seen with additional ones. The relationship of IC_{50} with number of wt subunits suggests strong negative cooperativity, when it is compared with the HH and MWC models. Similar analysis of the C166S and T71Y constructs reveals positive cooperativity for channel gating, which was supported by both IC_{50} and P_{open} plots against number of wt subunits. The presence of both negative cooperativity for ATP binding and positive cooperativity for channel gating may explain several previous observations showing the lack of cooperativity, as the K_{ATP} channels have rather low h values that remain unchanged with mutations of several critical residues for the ATP-dependent channel gating (Trapp et al., 1998a; Reimann et al., 1999; Markworth et al., 2000).

Channel gating does not show preference for *cis* or *trans* configurations. However, the channel with two wt subunits in the *cis* positions has a better ATP binding affinity and greater inhibitory efficacy than the *trans* configuration, suggesting that the

ATP binding site is likely to be made of intracellular domains from multiple subunits, which is consistent with modeling studies based on the KirBac 1 and KcsA channels (Antcliff et al., 2005). Our results suggest that such an ATP binding site may consist of at least two different subunits with two adjacent subunits surpassing two diagonal ones. The coordination between two subunits also suggests functional dimers that may be formed in the ATP-dependent channel gating. Supporting this idea are also the baseline P_{open} plots. The baseline P_{open} changes repeat when every other functional subunit is introduced. These are consistent with previous demonstrations of dimer of dimers in CNG, HCN and Kir1.1 channels (Liu et al., 1998; Ulens and Siegelbaum, 2003; Wang et al., 2005b). Both the ATP binding and inter-subunit interaction between cytosolic termini of the channel protein are likely to contribute to the functional dimers (Lin et al., 2003). With the subunit coordination and cooperativity, two functional subunits seem adequate to achieve over 90% of the ATP sensitivity, while the ATP-dependent channel gating cannot be fulfilled by a single wt subunit (wt-3C166S/K185E) with intact ATP-binding and channel-gating mechanisms. Action of four subunits as dimer of dimers may facilitate the ligand binding domain to form a four-fold symmetric gating ring as seen in the crystal structure of the KirBac1.1 and CNG channels (Kuo et al., 2003; Zagotta et al., 2003).

I-III-3-d. Potential coupling mechanisms

Another finding from the present study is that the effect of ligand-binding can be coupled to channel gating not only within the same subunit (*cis* coupling) but also between two adjacent subunits (*trans* coupling). Our results show that by blocking the *cis* coupling, the K185E-T71Y and K185E-C166S channels still respond to intracellular ATP

suggesting that the binding-gating coupling is mediated by inter-subunit interaction or *trans* coupling. The *trans* coupling through either N or C termini appears to have the same effect, as both K185E-T71Y and K185E-C166S retained about a half of the maximum effect with the same IC_{50} level. However, the functional *cis* coupling in the C terminus (wt-K185E/C166S) appears to have greater effects on maximum inhibition (72.2%) and IC_{50} than the *cis* coupling in the N terminus (wt-K185E/T71Y), suggesting that a stronger amplification exists via the backbone structure than that via interaction between protein domains of the same and alternate subunits.

In conclusion, our results show that the ATP binding can be differentiated from channel gating, as disruption of the ATP binding in a given number of subunits impairs the maximum channel inhibition produced by ATP, while disruption of the gating mechanism augments the magnitude of channel gating movement. A strong negative cooperativity is found for the ATP binding, and positive cooperativity is seen for channel gating. The ATP-dependent channel gating requires at least two functional subunits as a functional dimer. Although the subunit coordination has no preference in the channel gating, a coordination of two functional subunits in the *cis* configuration is more effective for ATP binding. ATP-binding is coupled to gating not only within the same subunit, but also between two different subunits. These phenomena are well described with the operational model.

I-III-4. Summary and Conclusions

ATP-sensitive K^+ channels are gated by intracellular ATP allowing them to couple intermediary metabolites to cellular excitability, whereas the gating mechanism remains unclear. To understand subunit stoichiometry for the ATP-dependent channel gating, we constructed tandem-multimeric channels with selective disruptions of the binding or gating mechanism in certain Kir6.2 subunits. Disruption of channel gating caused graded losses in ATP sensitivity and increases in baseline P_{open} with no effect on maximum inhibition. Prevention of ATP-binding affected both potency and efficacy. Two adjacent subunits are more favorable for ATP-binding than two diagonal ones. Subunits showed negative cooperativity in ATP binding and positive cooperativity in channel gating. Joint disruptions of the binding and gating mechanisms in the same or alternate subunits of a concatemer revealed that the binding-gating coupling preferred the *cis* to *trans* configuration within the C terminus. No such preference was found between the C and N termini. These phenomena are well described with the operational model used widely for ligand-receptor interactions.

I-IV. Determinant Role of Membrane Helices in K_{ATP} Channel Gating

Results from this study have been published:

Wang, R., Rojas, A., Wu, J., Piao, H., Adams C. Y., Xu, H., Shi, Y. and Jiang, C. (2005). Determinant role of membrane helices in K_{ATP} channel gating. *J. Membr. Biol.* 204:1-10.

Acknowledgement: This study was designed by myself with some input from Dr. Haoxing Xu, Mr. Asheebo Rojas and Dr. Jiang I performed 90-95% molecular constructions and drafted the manuscript. Mr. Asheebo Rojas did most (90-95%) of the whole-cell voltage clamp. Dr. Jianping Wu performed all patch-clamp recording. Mr. Yun Shi contributed to the whole-cell recording (5-10%). Dr. Hailan Piao taught me the molecular techniques, and Ms. Carmen Y. Adams provided me with technical supports on the mini and midi preparation. I assume that they contributed 5-10% to the cDNA constructions. I sincerely thank them for their helps.

I-IV-1. Introduction

The inward rectifier K^+ channels are controlled by second messengers or metabolites and couple chemical signals to cellular excitability (Nichols and Lopatin, 1997). Given intracellular ligand produces stereotypical response in a channel species, i.e., stimulation or inhibition, indicating that such a response is an inherent property of the channel protein. In contrast to the channel response, a ligand molecule often has diverse effects on distinct channel species. For instance, ATP is an antagonist of the K_{ATP} channels, whereas it augments the Kir1.1 channel activity (Noma et al., 1983; Ho et al., 1993). Although the Kir6.1 and Kir6.2 channels are stimulated by intracellular proton (Davies et al., 1990; 1992; Xu et al., 2001a), the Kir1.1, Kir2.3, Kir4.1 and Kir4.1-Kir5.1 channels are strongly inhibited (Coulter et al., 1995; Tsai et al., 1995; Fakler et al., 1996; Zhu et al., 1999; Yang et al., 1999; Yang et al., 2000). How these opposite responses are produced is unknown. The current understanding is that ligand binding produces a specific conformation of the ligand-binding domain which is commensurate with the channel activity, suggesting that the channel response is determined by the ligand-binding domains. According to their conformation with or without ligand binding, the opening or closure of a channel takes place.

Another possibility is that the channel response to a ligand molecule may depend on not only the conformation of the ligand-binding domains but also the gating assembly that is likely to consist of the transmembrane helices and their adjacent regions of the N and C termini (Yellen et al., 2002). As the body of the gating assembly, the TM2 helices are assembled as an inverted teepee lining the inner ion-conductive pore (Doyle et al.,

1998). Experimental evidence suggests that the narrowest part of the TM2 helices is widened when the channels are open allowing certain ions and organic molecules to access the inner cavity (Armstrong et al., 1966; Liu et al., 1997; del Camino et al., 2000; Enkvetchakul et al., 2001; Flynn et al., 2001; Shin et al., 2001; Jin et al., 2002; Phillips et al., 2003). Such a movement could be produced solely by the ligand binding. If so, the gating assembly would be a simple follower of the ligand-binding domains which are located in the intracellular termini. However, some studies suggest that the membrane helices may play a more active role in channel gating, as mutations of certain helical residues reduce or even eliminate the channel responses induced by ligand binding (Trapp et al., 1998a; Minor et al., 1999; Piao et al., 2001; Cui et al., 2003; Wu et al., 2004). It is unclear how the membrane helices act in channel gating. If the membrane helices are not a simple follower, they should be able to influence the consequence of ligand binding. An ultimate demonstration would be that channel activity is determined by their conformations, no matter the ligand is excitatory or inhibitory naturally to the channel.

The Kir6.2 channel is inhibited by ATP and stimulated by proton (Davies et al., 1990; 1992; Xu et al. 2001a; Inagaki et al., 1995). The Kir6.2 gating by ATP and proton requires specific membrane domains in Kir6.2, which cannot be substituted with those in Kir1.1, another member of the Kir family (Piao et al., 2001; Wu et al., 2004). Several residues in these membrane helices are important for the channel gating (Trapp et al., 1998a; Enkvetchakul et al., 2001; Piao et al., 2001; Cui et al., 2003; Wu et al., 2004). Among them are Thr71 and Cys166. When the Cys166 in the TM2 is mutated, the Kir6.2

gating by both ATP and proton is disrupted (Trapp et al., 1998a; Piao et al., 2001). The Thr71 is located at the boundary of the TM1 and N terminus. Full ATP and pH sensitivities require a residue with flexible side-group at this site, while a bulky residue eliminates the ATP- and pH-dependent channel gating (Cui et al., 2003). According to the KirBac1.1 model (Fig. I-IV-1) (Kuo et al., 2003), Thr71 in the Kir6.2 channel is located in the immediate vicinity of Cys166, which is remarkable as their close locations at the interface of the TM1 and TM2 may allow an interaction between these two membrane helices. Thus, the gating mechanism may be accessible for intervention by manipulating their interaction. Therefore, we studied the effect of TM1-TM2 interaction on Kir6.2 gating by placing opposite or identical charges at these two sites. Surprisingly, we found that the gating process of the Kir6.2 channel was completely reversed with opposite charges at these sites, making ATP an activator and proton an inhibitor to the channel.

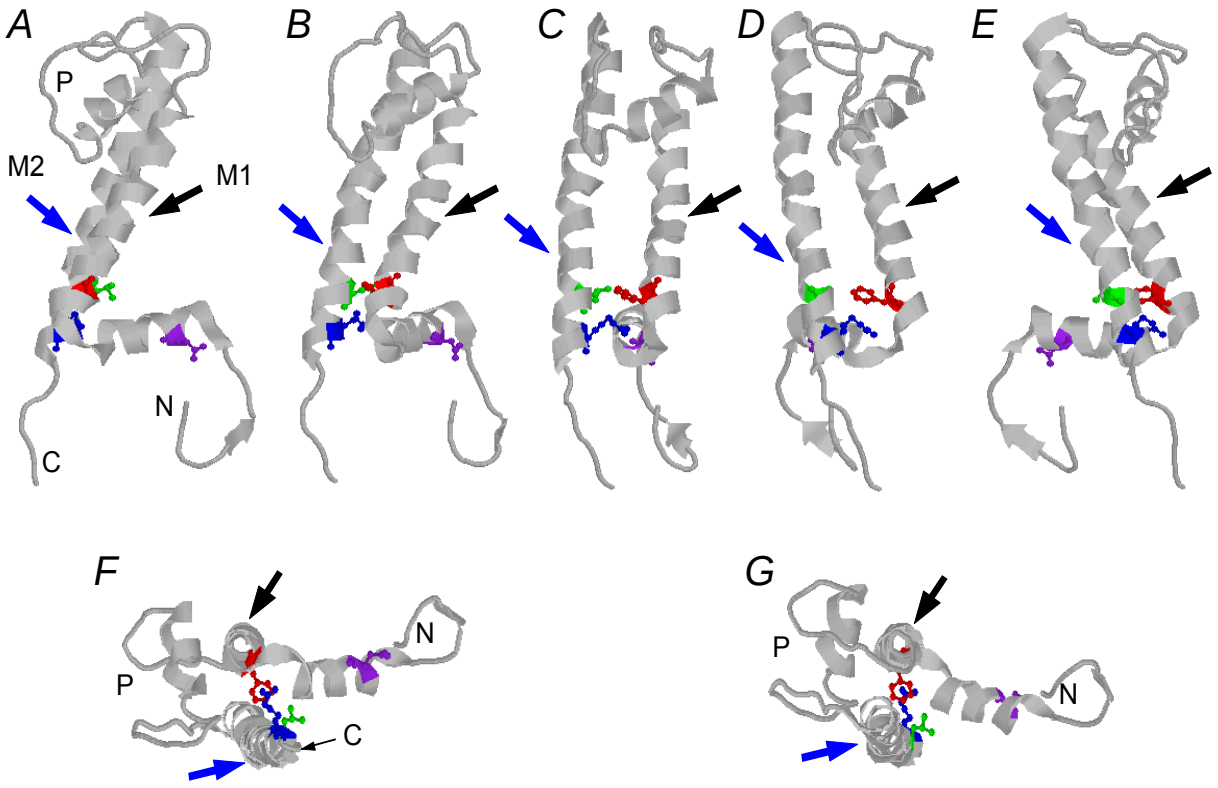

Fig. I-IV-1. Relative locations of Thr71, Cys166 and Lys170. Amino acid sequence of Kir6.2 was aligned with that of KirBac1.1 and a subunit with the first (M1, black arrow) and second (M2, blue arrow) membrane helices displayed based on the crystal structure of the KirBac1.1 (Kuo et al., 2003). Thr71 (red), Cys166 (green) and Lys170 (blue) in the Kir6.2 are shown in the locations of Phe63, Leu144 and Arg148 in the KirBac1.1, respectively. The distance measured using the RasMol (Version 2.6) is 4.7Å between Thr71 and Cys166, and 5.2Å between Thr71 and Lys170. Also shown is Asp50 (purple) that was suggested to interact with Arg148 with a distance of 17.1 Å (Kuo et al., 2003). ***A-E.*** Side view of the TM1 and TM2 helices from one subunit with a 40˚ counter-clockwise rotation as seen extracellularly in each panel. Two lower panels are intra- (***F***) and extracellular (***G***) views of the subunit. Other abbreviations: C, C-terminus; N, N-terminus; P, pore loop,

I-IV-2. Results

I-IV-2-a. Baseline properties

Experiments were performed on the Kir6.2 with 36 AAs truncated in the C terminus, i.e., Kir6.2ΔC36 and its mutant channels. We chose to use the Kir6.2ΔC36 for two reasons: 1) The Kir6.2ΔC36 can be expressed without the SUR subunit that is known to be involved in the channel gating (Tucker et al., 1997), and 2) like the wt channel, the Kir6.2ΔC36 is gated by ATP and pH (Wu et al., 2002b). A bath solution (KD90) containing 90mM K^+ was used to record whole-cell K^+ currents in two-electrode voltage clamp. These currents showed clear inward rectification with an amplitude of 2.1 ± 0.3μA (n = 14 measured at –160mV). They were inhibited by Ba^{++} and activated by azide (Piao et al., 2001; Wu et al., 2002b). In contrast, oocytes that received an injection of the expression vector alone did not express such inward rectifying currents. The small currents recorded (0.1-0.4μA) were insensitive to Ba^{++} and azide.

The ATP sensitivity was studied in inside-out patches after the expression of inward rectifying currents was identified in each cell. These patches were exposed to symmetric concentrations of K^+ (145mM) on both sides of the plasma membranes with command potentials from -100mV to 100mV (-150mV to 150mV in some cells) applied through the recording pipette. Under such a condition, the inward rectifying currents showed a single channel conductance of ~75pS and were inhibited by ATP (K^+ Salt) in a concentration-dependent fashion. The IC_{50} was ~100μM.

Table I-VI-1. List of all wild-type and mutant channels studied and their ATP and pH sensitivities

Name	IC_{50} ATP (μM)	pK_a	pH_i effect (%)	BL Current (μA)
Kir6.2ΔC36	109±10 (9)	–	128.6±11.4 (16)	2.0±0.5 (16)
Kir6.2 + SUR1	6±1 (5)	–	131.4±25.2 (5)	2.2±3.1 (5)
Kir2.1	–	4.96±0.01 (6)	2.8±1.1 (6)	16.3±5.0 (6)
Kir6.2 mutant				
T71E	740±73 (5)	–	44.0±11.1 (11)	20.4 ± 4.7 (11)
T71K	600±47 (5)	–	–13.9 ± 4.2 (12)	2.4 ± 0.3 (12)
C166E	2,500±188 (4)	–	17.1±6.7 (8)	18.1±1.5 (8)
C166K	NF	NF	NF	NF
C166S	>10,000	–	–0.5±1.8 (6)	18.7±5.0 (6)
T71K/C166E	EC_{50} 829±125 (9)	–	–78.9±5.2 (7)	13.4±2.8 (7)
T71R/C166E	EC_{50} 6,500±1,323 (5)	–	–79.9±5.7 (4)	10.4±2.8 (4)
T71E/C166K	NF	NF	NF	NF
T71D/C166K	NF	NF	NF	NF
T71E/C166R	NF	NF	NF	NF
T71E/C166K/K170T	NF	NF	NF	NF
T71D/C166S	361±18 (5)	–	–61.0±3.6 (6)	7.0±1.1 (6)
T71E/C166E	1,059±298(6)	–	765.2±93.4 (6)	3.5±0.5 (6)
T71D/C166E	NF	–	NF	NF
T71K/C166K	EC_{50} 2,080±462 (7)	–	–41.5±5.0 (11)	8.4±0.3 (11)
T71K/C166K/K170T	>8,000 (5)	–	–17.3±4.1 (8)	14.8±2.5 (8)
T71E/C166E/K170T	NF	NF	NF	NF
Kir2.1 mutant				
M84K	–	6.84±0.02 (4)	–50.0±4.3 (14)	5.5±1.3 (14)
M84E	–	–	–4.9±5.5 (10)	18.2±3.9 (10)
A178E	–	–	23.1±15.9 (7)	3.7±1.0 (7)
M84E/A178E	–	7.14±0.05 (5)	263.3±36.7 (6)	1.8±0.2 (6)
M84K/A178E	NF	NF	NF	NF
M84D/A178S	NF	NF	NF	NF
M84E/A178S	–	6.44±0.05 (4)	-14.0±2.4 (6)	10.7±2.3(6)
M84E/A178S/K182N	NF	NF	NF	NF
M84K/A178D	NF	NF	NF	NF

The ATP sensitivity was studied in excised patches and is expressed by fitting the data using the Hill equation as shown in Fig. J-IV-2B. Hill coefficients are 0.9-1.2 (not shown) with n shown in the parenthesis. The pH sensitivity was studied in whole-cell recording using 15% CO_2 (pH_i 6.6) and is expressed as % change in the current amplitude. All Kir6.2 mutants were created with the Kir6.2ΔC36. Abbreviations: BL, whole-cell baseline, NF, nonfunctional. All the IC_{50}, EC_{50} and pKa values were obtained by Dr. Jianping Wu. Most pHi effects and baseline currents were obtained by Mr. Asheebo Rojas. Mr. Yun Shi did the whole cell recording for T71R/C166E.

The Kir6.2ΔC36 channel was strongly activated during an exposure to 15% CO_2, and this level of CO_2 causes intra- and extracellular acidifications (pH_i 6.6, pH_o 6.2) (Zhu et al., 2000; Xu et al., 2000b), and augments the Kir6.2ΔC36 currents by ~130% (Xu et al., 2001a; Piao et al., 2001). We have previously shown that pH_o has no effect on the Kir6.2 channel, and the current augmentation is solely produced by intracellular acidification (Xu et al., 2001a). To avoid the channel rundown which is constantly seen at acidic pH levels in excised patches (Xu et al., 2001a; Wu et al., 2002b), all pH experiments on the Kir6.2ΔC36 and its mutant channels were performed in whole-cell recordings using 15% CO_2.

I-IV-2-b. Double mutations have drastic effects on both ATP and pH sensitivity.

Previous study shows that Cys166 is not susceptible to thiol-reactive agent (Trapp et al., 1998b). We also failed when we attempt to test the interaction by mutating the Thr71 to Cysteine and see whether it can form disulfide bond with Cys166. Subsequently, the interaction between these residues was studied by introducing charged AAs to replace Thr71 and Cys166.

Joint mutations of Thr71 to lysine and Cys166 to glutamate produced functional currents that showed clear inward rectification in the absence of exogenous polyamines with the single channel conductance of 74.4±1.3pS (n=8). The open state probability (P_o=0.099±0.023, n=6) was ~4 folds higher than the Kir6.2ΔC36. Surprisingly, we found that the T71K/C166E currents were no longer inhibited by ATP. Instead, the currents were strongly augmented by intracellular ATP (Fig. I-IV-2A). The channel activity increased by 181.0±9.2% (n=9) in the presence of 3mM ATP.

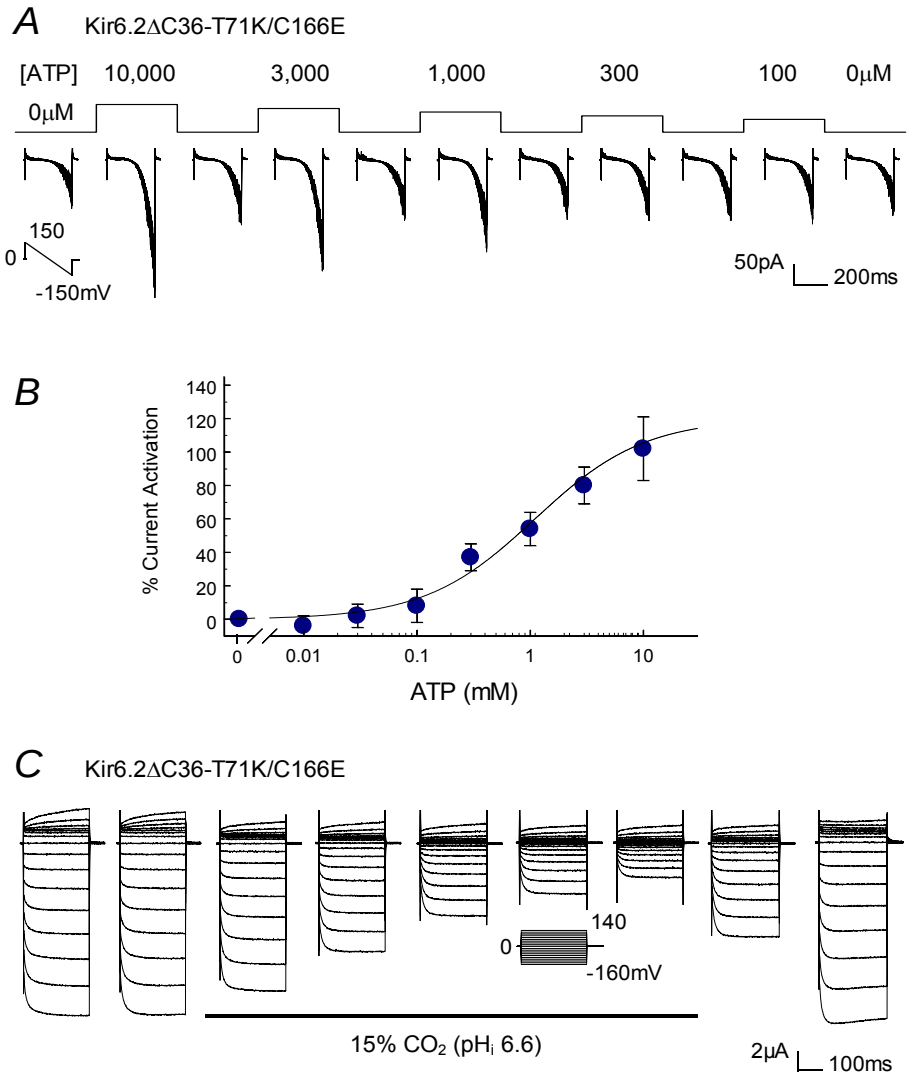

Fig. I-IV-2. Effects of ATP and pH on Kir6.2ΔC36 with T71K/C166E mutations. ***A.*** Microscopic currents were recorded from a giant inside-out patch with 145mM K^+ on both sides of the patch membrane. Perfusates with different concentrations of ATP were applied to the intracellular membrane for 1 minute. Ramp potentials from -150mV to 150mV are given at a holding potential of 0mV. In contrast to the Kir6.2ΔC36 (Xu et al., 2001b), the T71K/C166E currents were inhibited by intracellular ATP in a concentration-dependent fashion. Note that eight superimposed traces are shown in each panel. ***B.*** The dose-response curve is fitted with Hill equation modified from Equation 3 ($y=Im/(1+(EC_{50}/[ATP])^h$), where [ATP] = ATP concentration; EC_{50} (1.1mM) = is the ATP concentration for 50% current stimulation; h (0.9) = Hill coefficient; and Im = maximal current activation***. C.*** Whole-cell currents were studied in voltage clamp in an oocyte. The T71K/C166E currents were strongly inhibited by intracellular acidification produced with an exposure to 15% CO_2 (pH_i 6.6) for 6 min. The ATP responses in panel *A.* and *B.* were obtained by Dr. Jianping Wu. The CO_2 sensitivity of the channel was tested by Mr. Asheebo Rojas.

The dose-response relationship showed the EC_{50} concentration of ATP to be ~800μM (Fig. I-IV-2B). This channel activation is not produced by protein phosphorylation as the non-hydrolysable ATP analog 5'-adenylyl β,γ-imidodiphosphate (AMP-PNP, 3mM) had a similar effect (202.5±12.9%, n=4; P>0.05). Thus, these mutations make ATP an activator of the Kir6.2ΔC36 channel.

Consistent with ATP, the pH effect on whole-cell T71K/C166E currents was also completely reversed. The baseline T71K/C166E currents were much larger (13.4±2.8μA, n=7) than the Kir6.2ΔC36 (2.0±0.5μA, n=16). These currents were strongly inhibited when the cells were exposed to 15% CO_2 (Fig. I-IV-2C). The inhibition took place within 1min, reached a plateau in 3-4 min, and was fully reversible with washout (Fig. I-IV-2C). Repetitive exposures to CO_2 had the same effect. Similar reversal of the ATP and pH sensitivities was observed in the T71R/C166E mutant (Fig. I-IV-3A,C,D; Table I-IV-1), suggesting that the effects are likely to be produced by the electrostatic interaction between these two sites.

When these residues were mutated to alternative sets of opposite charged AAs (T71E/C166K, T71D/C166K, and T71E/C166R), none of the mutant channels expressed detectable currents. However, the T71D/C166S mutant produced inward rectifying currents, in which a reversal of the pH but not ATP sensitivity was observed (Fig. I-IV-3E,F). Since such a reversal of ATP and pH sensitivities was not seen in individual mutation of either Thr71 or Cys166 (Table I-IV-1), these results suggest that the manipulation of these two residues may have restructured the gating mechanism.

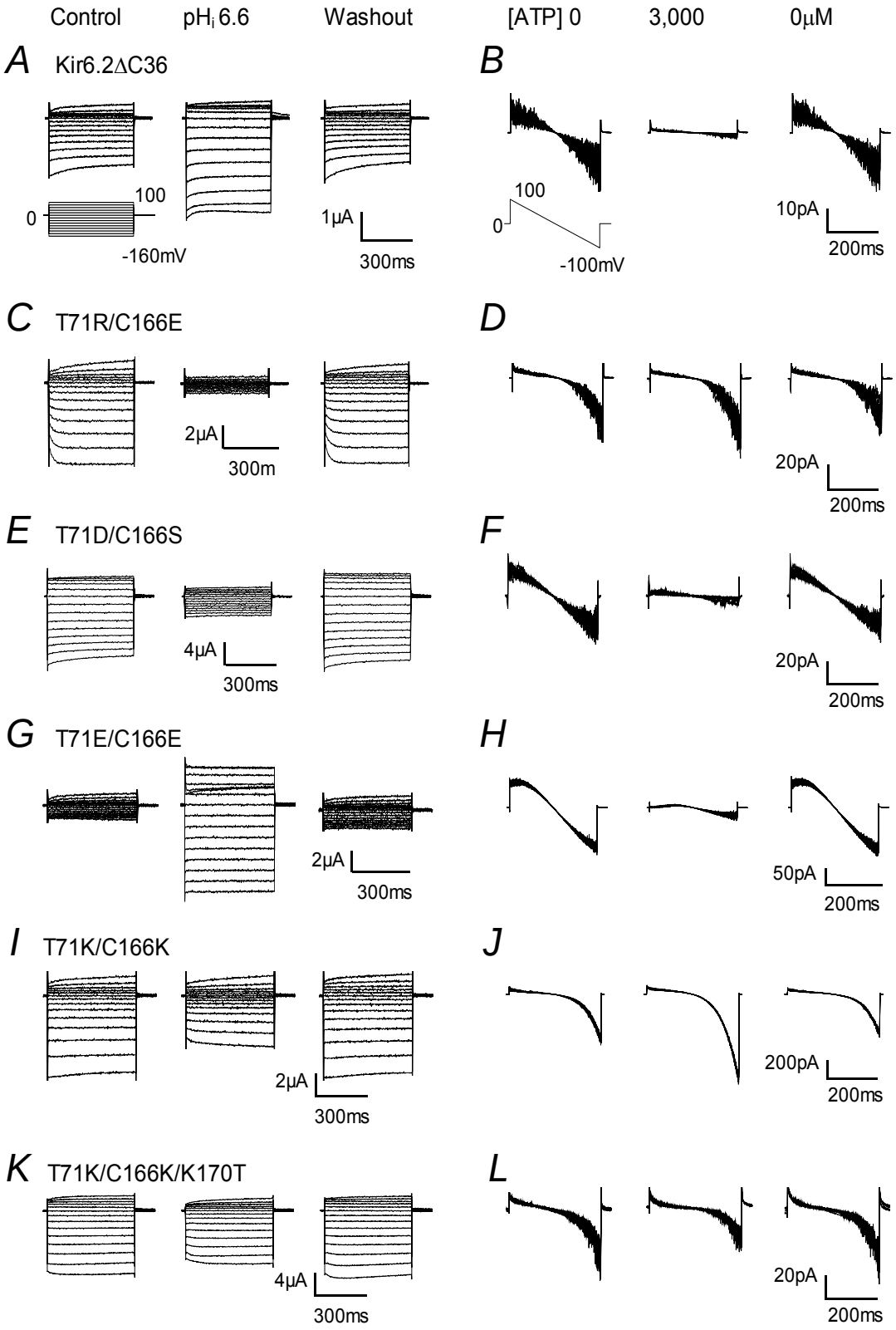
Control
pH$_i$ 6.6
Washout
[ATP] 0
3,000
0μM
A
Kir6.2ΔC36
100
0
-160mV
1μA
300ms
B
100
0
-100mV
10pA
200ms
C
T71R/C166E
2μA
300m
D
20pA
200ms
E
T71D/C166S
4μA
300ms
F
20pA
200ms
G
T71E/C166E
2μA
300ms
H
50pA
200ms
I
T71K/C166K
2μA
300ms
J
200pA
200ms
K
T71K/C166K/K170T
4μA
300ms
L
20pA
200ms

Fig. I-IV-3. Responses of several Kir6.2ΔC36 mutants to ATP and acidic pH. Channel responses to pH and ATP were studied as in Fig. I-IV-2A,C. ***A, B.*** The Kir6.2ΔC36 channel was stimulated by hypercapnic acidosis and inhibited by 3mM ATP. ***C, D.*** The T71R/C166E was inhibited by acid pH, and modestly stimulated by 3mM ATP. ***E, F***. The pH but not ATP sensitivity was reversed in the T71D/C166S mutant. ***G, H.*** The T71E/C166E currents were strongly augmented by low pH, and inhibited by ATP. ***I, J***. The pH and ATP sensitivities were both reversed in the T71K/C166K. ***K, L.*** By adding a third mutation, the T71K/C166K/K170T was inhibited by both ATP and acidic pH. Note that all records for the ATP sensitivity are shown with eight superimposed traces. The CO_2 sensitivity of these channels was tested by Mr. Asheebo Rojas, and the ATP sensitivity of these channels was tested by Dr. Jianping Wu. Mr. Yun Shi did the whole cell recording for T71R/C166E.

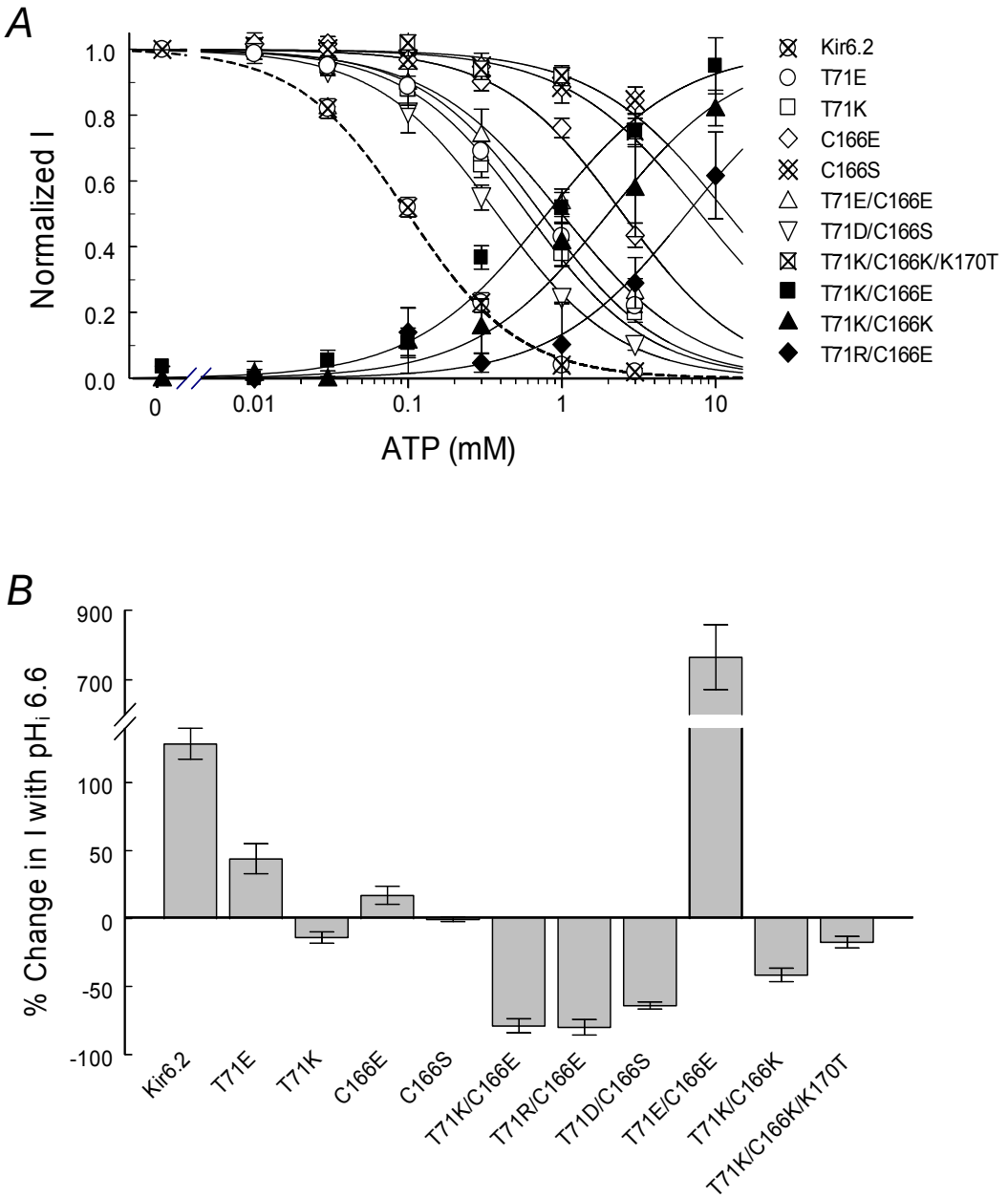

Fig. I-IV-4. ATP and pH sensitivities of Kir6.2ΔC36 mutants. ***A.*** Dose-response relationship of Kir6.2ΔC36 mutants was studied using the equation 3 (see method). Whereas most mutant channels remained to be inhibited by intracellular ATP, T71K/C166E, T71R/C166E and T71K/C166K were augmented. See Table I-IV-1 for the IC_{50} and EC_{50}. The h = 0.9 – 1.2; n (number of patches) = 4 – 9. ***B.*** The pH sensitivity was studied using 15% CO_2 as shown in Fig. I-IV-2C. The T71K/C166E, T71R/C166E T71D/C166S and T71K/C166K were markedly inhibited at pH_i 6.6. In contrast, the T71E/C166E was strongly stimulated at this pH level. The CO_2 sensitivity of these channels was tested by Mr. Asheebo Rojas, and the ATP sensitivity of these channels was tested by Dr. Jianping Wu.

To create a repulsive force between these two sites, both Thr71 and Cys166 were mutated to identically charged residues. The T71E/C166E mutant expressed inward rectifying currents. This mutant was inhibited by ATP and stimulated by hypercapnic acidosis (Fig. I-IV-3G,H). Although its ATP sensitivity was lower than the wt channel, the stimulatory effect of pH was much greater (Table I-IV-1; Fig. I-IV-4B). With two positive charges at these locations, the T71K/C166K was inhibited by proton and stimulated by ATP, a phenotype that is more like the T71K/C166E than the T71E/C166E (Figs. I-IV-3I,J; I-IV-4A,B). According to the KirBac1.1 model (Fig. I-IV-1) (Kuo et al., 2003), there is an basic residue (Lys170) at the surrounding area of Thr71 and Cys166. Since the Lys170 is situated at just one helical turn below Cys166 and also faces Thr71, it is possible that the Lys170 is also involved in the newly created electrostatic interactions between the TM1 and TM2 residues. Thus, we additionally mutated the Lys170 to a neutral threonine. The inhibitory effect of pH on the T71K/C166K/K170T was significantly smaller (–17.3±4.1%, n=8) than the T71K/C166K (–41.5±5.0%, n=11; $P<0.01$) (Fig. I-IV-3K,L). More importantly, the T71K/C166K/K170T was inhibited, but not stimulated, by ATP (Fig. I-IV-4A; Table I-IV-1), further suggesting that the opening and closure of the Kir6.2 channel can be predetermined by strengthening or weakening the interaction of the TM1 with TM2 helices. In this study, mutant channels were identified by their conductance in excised patches.

I-IV-2-c. Similar effects were also observed in the Kir2.1 channel.

To elucidate whether the electrostatic interactions at these two locations affect the gating process of other Kir channels, we performed similar studies on the Kir2.1 channel known

to be insensitive to pH (Fakler et al., 1996; Zhu et al., 1999; Qu et al., 2000) (Fig. I-IV-5A). With identical charges at sites corresponding to Thr71 and Cys166 in Kir6.2, the M84E/A178E was strongly stimulated by acidic pH (Fig. I-IV-5B), consistent with the T71E/C166E mutant in Kir6.2. Although the M84K/A178E and M84E/A178K mutations did not yield functional channels, the M84E/A178S expressed inward rectifying currents. Exposure to hypercapnic acidosis caused inhibition of the M84E/A178S mutant (Fig. I-IV-5C). The pH-current relationship was studied using inside-out patches. The dose-response curves of these two mutants were exactly opposite to each other (Fig. I-IV-6). Thus, the gating mechanism in the Kir2.1 channel can also be rearranged by the electrostatic interactions at these two sites.

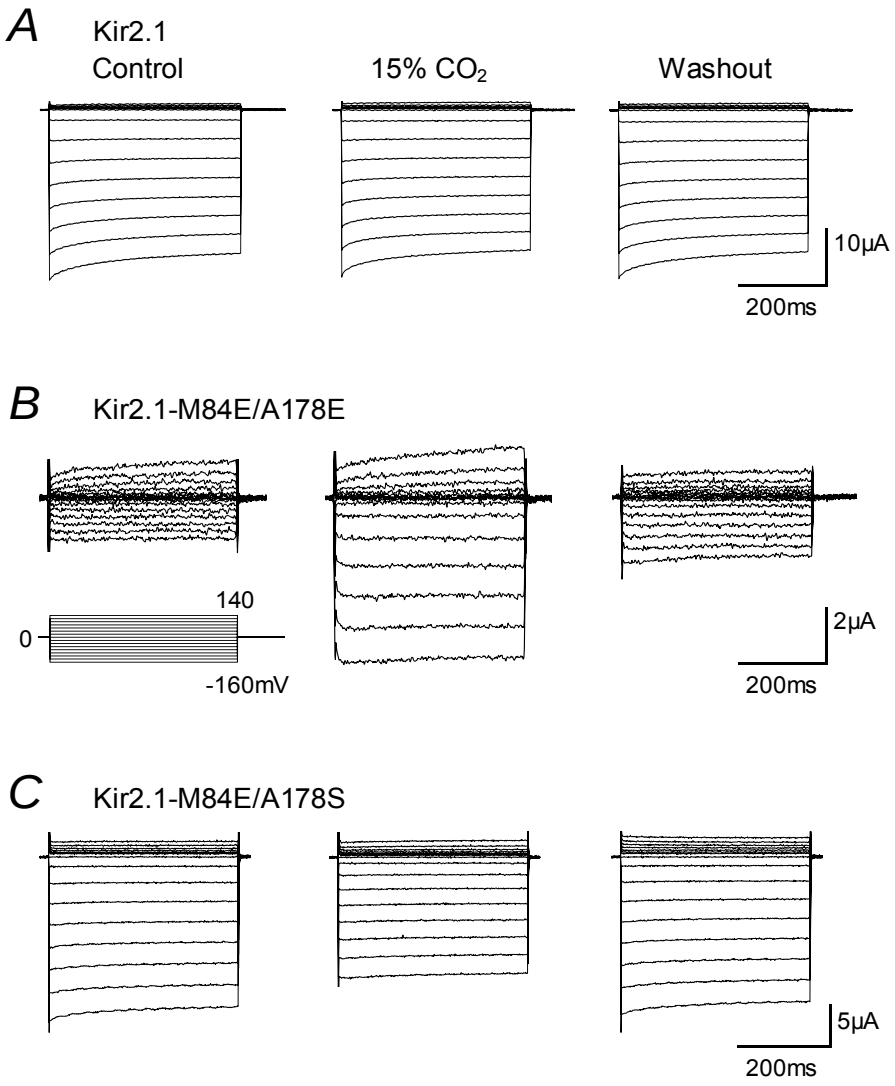

Fig. I-IV-5. The effect of acidic pH on Kir2.1 mutants. Intracellular acidification was produced using 15% CO_2 and channel response was studied as in Fig. I-IV-2C. ***A.*** The wt Kir2.1 channel was unaffected by 15% CO_2. ***B.*** The M84E/A178E mutant had small baseline currents. This channel was strongly augmented by 15% CO_2. ***C.*** In contrast, the M84E/A178S mutant was inhibited. The whole cell recordings were performed by Mr. Asheebo Rojas.

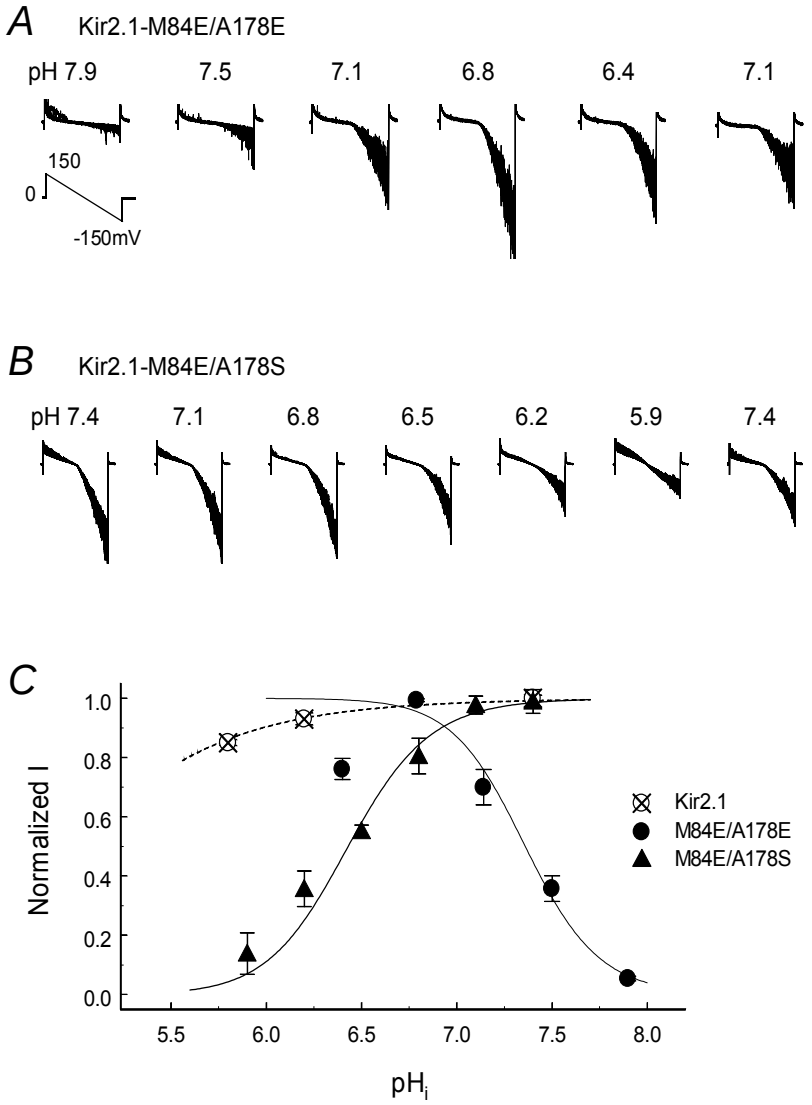

Fig. I-IV-6. The pH sensitivity of Kir2.1 mutants studied in inside-out patches. ***A.*** the Kir2.1-M84E/A178E currents were rather small at pH 7.9. Reduction of pH levels in the internal solution produced graded augmentation of the Kir2.1-M84E/A178E currents. The maximal channel activation is reached at pH 6.8. The currents started being inhibited at pH 6.4. ***B.*** The Kir2.1-M84E/A178S mutant showed rather large currents at baseline (pH 7.4), and was inhibited with graded reductions in pH. ***C.*** The dose-response relationship of these two mutants was expressed using the Hill equation. The Kir2.1-M84E/A178E currents were half activated at pH 7.14 (n=5), and the Kir2.1-M84E/A178S was half inhibited at pH 6.40 (n=4). Dr. Jianping Wu conducted the patch-clamp recordings.

I-IV-3. Discussion

Recent studies suggest that membrane helices may play a more active role in the channel gating. The opening and closure of the two-pore chloride channel, gap junction channels, and the influenza virus TM2 proton channel are determined by the side-chain movement of a few pore-lining residues (Bennett et al., 1991; Tang et al., 2002; Dutzler et al., 2003). The gating of the MscL channel involves concerted movements of membrane helices and the side-group of two phenylalanine residues in the S1 domain (Sukharev et al., 2001). It is known that the membrane helices of the ligand-gated and also may be the voltage-gated channels change their conformations during gating (Kuo et al., 2003; Yellen et al., 2002). TM1 and TM2 helices undergo a counter-clock wise rotation after ligand binding. The narrowest part of the TM2 is widened. The opening of the channels allows certain ions and organic molecules to access the inner cavity (Armstrong et al., 1966; Liu et al., 1997; del Camino et al., 2000; Enkvetchakul et al., 2001; Flynn et al., 2001; Shin et al., 2001; Jin et al., 2002; Phillips et al., 2003; Perozo et al., 1999). Our current studies present another novel finding that the gating mechanism is not fixed in Kir channels but can indeed be reset by manipulating electrostatic interaction between the TM1 and TM2.

Based on the KirBac1.1 model (Kuo et al., 2003), the TM1 crosses the TM2 at the inner pore region, where Thr71 and Cys166 are found in the Kir6.2 channel. Our results clearly show that electrostatic forces introduced between these two sites dramatically affect the channel gating, suggesting that the TM1 and TM2 helices in Kir6.2 channels do not act independently. In contrast they appear to interact with each other, determining the

consequence of ligand binding. It is likely that the electrostatic interaction causes a change in the relative distance of the TMs and perhaps their membrane position as well. Such a change may assign a new conformation to the gating assembly affecting its operation by ligand binding. We believe that the Kir6.2 channel gating by ATP and proton depends on specific movements of the TM2 and TM1, including rotation, anti-parallel sliding and lateral movement (del Camino et al., 2000; Jin et al., 2002; Dutzler et al., 2003; Perozo et al., 1999; Johnson et al., 2001; Schulte et al., 2001; Jiang et al., 2002b). Such conformational changes are interfered or disrupted with the additional electrostatic forces between the membrane helices. The T71K/C166E and T71R/C166E mutations switch the movement to the opposite direction and reverse the gating process. With the T71E/C166E mutation, the helical movements are slightly altered, so that the mutant still responds to ATP and pH similarly to the wt channel. This phenomenon is not only limited to the Kir6.2 channel, as we have observed channel activation and inhibition by acidic pH in the Kir2.1 channel by similar manipulations of corresponding residues. It is noting that the close location of Thr71 to Cys166 is predicted with the KcsA and KirBac1.1 models. Their relative locations may be different in the open stat since both these channels were crystallized in their closed state.

It is possible that Kir channel gating involves multiple interactions between TM1 and TM2 residues, as there is evidence showing that specific protein domains and AA residues in the membrane helices are required for channel gating. Not only one AA mutations can produce effects from modest reduction to complete loss of the gating as shown in the channel sensitivity to intracellular ligand molecules (Enkvetchakul et al.,

2001; Trapp et al., 1998a; Piao et al., 2001; Cui et al., 2003; Wu et al., 2004). Since both TM1 and TM2 undergo rotation during channel gating (Perozo et al., 1999), one residue may face and interact with different AAs on the other TM domain. In our study, the Lys170 close to the Cys166 at just one helical turn below is also involved in the electrostatic interaction, as the T71K/C166K/K170T is gated differently from the T71K/C166K. With three positive charges, the T71K/C166K mutant behaves more like the T71K/C166E. How this occurs is unclear. The interaction may involve residues beyond these three AAs, which we can not answer concerning difficulties to explore all potential interactions. We believe that the Thr71 plays a key role in the multiple interactions because most mutants with a lysine at this position respond to ATP and pH similarly. However, the dominant effect of Thr71 should not compromise the contribution of Cys166 to the channel gating, as the gating of T71K mutant is not totally reversed. The channel inhibition by acidic pH is unlikely to be produced by titration of the newly created lysine residue, because the T71K/C166E and T71D/C166S are gated similarly by pH, and because the ATP sensitivity is also reversed. Although there are still unexplained phenomena, our studies have shown for the first time that the TM1 and TM2 helices can interact with each other, and the Kir channel gating can be intervened with their interaction at the inner pore region.

Beyond the consistency with previous findings that both membrane helices participate in channel gating, our results strongly suggest that the membrane helices are not simply followers of the intracellular ligand-binding domains whose conformation ultimately governs the position and movement of the membrane helices as shown in the

bacterial MthK channel (Jiang et al. 2002b). These helices in the mammalian Kir6.2 channel seem to be sufficient to determine the channel opening or closure following binding to the same ligand, depending on how they interact with each other in their local environment.

In conclusions, the Kir6.2 gating involves Thr71 in the TM1 and Cys166 in TM2. Creation of electrostatic attraction at these sites completely reverses the channel gating by ATP and proton. Similar results were observed in the pH-dependent gating of the Kir2.1 channel. Thus, the membrane helices do not seem to act as followers of the C terminus in these mammalian K^+ channels, and they instead may determine whether these channels are open or closed following ligand binding to the channel protein.

I-IV-4. Summary and Conclusions

The K_{ATP} channels couple chemical signals to cellular activity, in which controlling channel opening and closure (i.e., channel gating) is crucial. Transmembrane helices play an important role in channel gating. Here we report that the gating of Kir6.2, the core subunit of pancreatic and cardiac K_{ATP} channels, can be switched by manipulating the interaction between two residues at the TM1 and TM2 helices. The Kir6.2 channel is gated by ATP and proton which inhibits and activates the channel, respectively. The channel gating involves two residues, i.e., Thr71 and Cys166 located at the interface of the TM1 and TM2. Creation of electrostatic attraction between these sites reverses the channel gating, which makes the ATP an activator and proton an inhibitor of the channel. Electrostatic repulsion with two acidic residues retains or even enhances the wild-type channel gating. A similar switch of the pH-dependent channel gating was observed in the Kir2.1 channel which is normally pH-insensitive. Thus, how the TM1 and TM2 helices interact appears to determine whether the channels are open or closed following ligand binding.

J. GENERAL DISCUSSION

The present study was focused on one of the central mechanisms for the control of ion channel activity, i.e., channel gating. Several novel findings have been made. Using asymmetric Kir channel constructs, I were able to gain insight into how individual subunits work in highly organized gating movements. These special constructs allow me to separate ligand binding from channel gating, dissect pathways for coupling ligand binding to the gating, and reveal actions of each subunit in ligand binding and channel gating. Evidence for subunit coordination and cooperativity was shown. By manipulating the interaction of two gating sites located at the interface of the two transmembrane domains of Kir6.2 channel, I found that the opening and closure of Kir6.2 channels can be determined by the transmembrane helixes following binding to the same ligand molecules.

J-I. Ligand binding versus channel gating

Although ligand binding is conceptually distinct from channel gating, their effects are always intertwined. This problem is not limited to functional studies but also seen in protein chemistry. On one hand, a conformational change caused by ligand binding has to be coupled to the corresponding conformational change in channel gating to produce biological effects. On the other hand, the conformational change in channel gating may in turn affect the binding affinity for the ligand. Therefore, information obtained from mutational studies in terms of ligand sensitivity can only tell whether the site studied is necessary for the multi-event signal transduction and amplification. Any further

interpretations regarding binding, gating and coupling require great caution. The most effective way to differentiate ligand binding from gating, at present, is to test channel sensitivities to multiple ligands. A site is likely to be involved in gating if its disruption affects multiple ligand sensitivities. Otherwise, it probably takes part in ligand binding if it is required for a specific ligand. However, such an approach is not always feasible since the ligand binding sites are not always independent. Allosteric effects among different ligand binding sites may make interpretation more complicated. Thus these sites are only demonstrated in a few ion channels. In my dissertation study, I have tackled the binding vs. gating problem with an alternative approach based on ideas from studies of ligand-receptor interactions combined with the well defined ligand binding and channel gating sites.

It is known that the most characteristic difference between full and a partial agonists is their binding specificity. The partial agonist has less binding specificity because the efficacy and potency in the dose-response curves are both compromised (Pliska, 1999). Similarly, disruption of ligand binding in a receptor tends to impair both efficacy and potency. Using several asymmetric constructs, we have found that disruptions in ATP binding indeed affect efficacy and potency, whereas disruptions of gating sites affect the baseline activities but not the maximum channel inhibition by ATP. The difference between ligand binding and channel gating is likely to be general, and may exist in other ion channels. Therefore, such characteristic changes can be used to identify unknown channel structures based on their effects on ligand binding or channel gating. These characteristics identified in the current study may also benefit the discovery

of new medicines targeting at ion channels. An approach to specifically target ligand binding or channel gating mechanisms based on a better understanding of drug-channel interaction and their effect patterns on potency and efficacy should significantly advance the drug discovery and design.

J-II. Coupling between ligand binding and channel gating

Channel activity is controlled by intermediate coupling mechanisms in addition to ligand binding and channel gating. Binding-gating coupling may rely on a series of conformational changes that convey ligand binding to the gating movement. Also ligand binding should be able to propagate to the gate not only in the same subunit but also in neighboring subunits. This is evidenced by the gating of asymmetric nicotinic Ach receptors in which ligand binding to two subunits leads to synergetic movements of all five subunits for channel gating. Similarly, the intersubunit (*trans*) binding-gating coupling is shown in these studies, as the homomeric Kir1.1 channel with two functional subunits is well gated by intracellular protons. Our single channel analysis on this channel suggests that all four subunits are involved in pH-dependent gating. More direct evidence is shown in the study of Kir6.2 channel gating by intracellular ATP. With selective blockage of the intra- (*cis*) or intersubunit (*trans*) coupling, our results indicate that functional gating can be produced with either *trans* or *cis* coupling alone, although *cis* coupling is more efficient. *Trans* coupling is necessary since channel with only a single *cis* coupling is not gated by ATP. In contrast, a single ligand binding site can fulfill the channel gating mechanism. Therefore, the gating movement of one subunit is inadequate for gating the whole channel. With both *trans* or *cis* couplings, the channel

can recruit other subunits for the gating movement after one subunit is activated by ligand binding. Such a mechanism may be related to subunit coordination and cooperativity and is important for the detection of low levels of ligands.

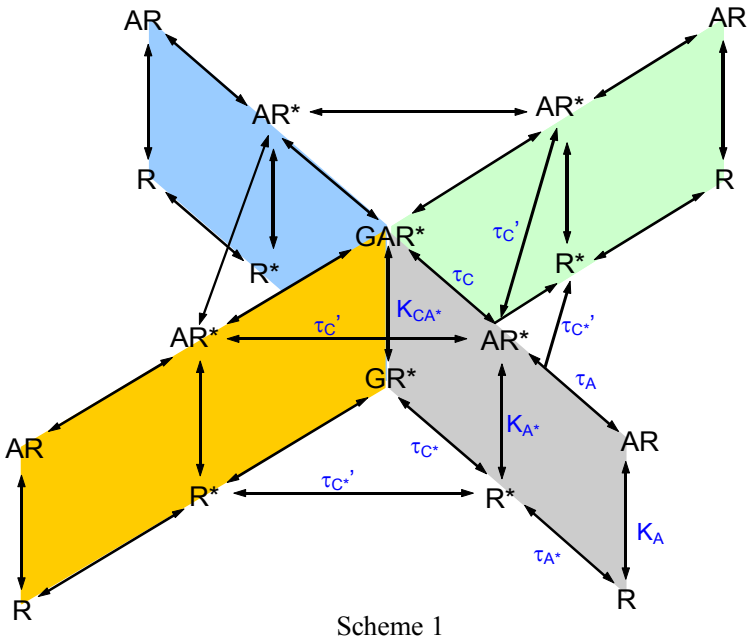

Scheme 1

Based on the extended ternary operational model for ligand receptor interaction, I have developed a model to describe our results (Scheme 1). The model has four arms with each representing one functional subunit. In each subunit, the ATP-dependent channel gating is initiated with ATP (A) binding to its binding site (R), and the binding affinity is determined by K_A. With ligand binding, the channel forms a ligand-receptor complex (AR) that triggers the first step of conformational change with signal amplification (AR*). The amplification rate is determined by τ_A. The conformational change needs to be coupled to the physical gate in the same subunit in which another conformational change (GAR*) controlled by τ_C occurs, and eventually causes channel closure (*cis* coupling). Since the binding-coupling-gating is carried out by a series of conformational changes, disruption of an intermediate step in the coupling pathways, such as C166S and T71Y mutations, can compromise the magnitude of the conformational change, leading to the change in the working range of

the channel activity. The correct conformational change of the intermediate step is necessary for the successive step of conformational change, and can in turn affect the conformation produced in the previous step. Thus τ_C controls the working range and determines the efficiency of coupling. The conformational change in one subunit can also be coupled to an adjacent subunit through inter-subunit interaction (*trans* coupling), and this coupling pathway controlled by τ_C' also contributes to the coupling efficiency. Since K_C is a function of K_A and $\tau_A$with a undefined relationship, the IC_{50} value of a construct therefore is determined by K_A, τ_A and τ_C. With an intact coupling mechanism (assuming the coupling efficiency is 100%), the IC_{50} of K185E tetramers is determined by the K_A and τ_A. With disruption of coupling pathways, τ_C and K_C become larger leading to an increase in the IC_{50}. The bottom level of the model refers to the spontaneous channel activation.

J-III. Subunit coordination

One evolutionary advantage of the multimeric design is that channel activity can be controlled by a subtle movement of each individual subunit (Doyle, 2004). Such a design would also represent a challenge to the control of channel activity if all subunits were allowed to act independently. Ligand binding is a dynamic process with a fast transition between association and dissociation states. It is almost impossible to achieve binding or dissociation of every subunit at the same time. If the action of every subunit in an ion channel were entirely independent, the channel pore would always stay at sub-conduction levels with certain subunits out of position most the time. This would dramatically reduce

ligand sensitivity, slow down the response time to ligand binding, and compromise working efficiency. Fortunately, independent activity is rare in normal conditions, and there are mechanisms for synchronizing the movement of individual subunits to full opening or closure. Supporting the existence of such a subunit coordination mechanism are previous stoichiometry studies on HCN and CNG channels showing that two subunits in a tetrameric channel are coordinated as a functional dimer (Liu et al., 1998; Ulens and Siegelbaum, 2003). Structural evidence for subunit dimerization has also been found in protein chemistry studies in which proteins purified in the presence or absence of ligands have different sizes (Clayton et al., 2004). The present study provides additional evidence for subunit coordination as functional dimers, regarding substates of conductance of Kir1.1 channel and the repetitive patterns of IC_{50} changes with the recruitment of functional subunits in the Kir6.2 channel. Subunit coordination seems to be able to improve greatly the gating efficiency of Kir channels by stabilizing the channels at full open and closed states.

Since channel gating is a dynamic process with a fast transition between different opening and closure states, it is reasonable to think that dimers between two single subunits are also dynamic rather than fixed. The homomeric channels such as the Kir1.1 and Kir6.2 channels have four exactly identical subunits with each of them possessing a set of gating machinery. We have found that the chances for coordination of functional dimers appear to be the same among four subunits, and the *cis* and *trans* configurations of Kir1.1 channels have the same pH and CO_2 sensitivity, single channel kinetic, long time closure and substates of conductance. This phenomenon can only be explained by

assuming that four subunits act as two dynamic dimers. Otherwise two wt subunits at *cis* and *trans* positions would not produce these same effects no of matter the dimers were fixed between two adjacent or diagonal subunits.

Based on the Kir1.1 studies, we propose a model of dynamic functional dimers (DFD) to explain how the Kir1.1 subunits may be coordinated in channel gating (Scheme 2). In this model, we assume that subunit interaction is not fixed but takes place as a short-lasting and dynamic event. DFDs are assumed to form between a wt subunit (open circle) and another subunit (wt or K80M-mutant, solid circle) in either *cis* or *trans* conformation as shown with gray boxes. In the 4wt (bottom), there are six potential ways for the subunits to interact (N = 6), a number that is equal to the total combinations of dimers (M) in a tetramer, i.e., 4 ! / (2 ! × (4 - 2) !) = 6. Thus, the possibility of subunit pairing (η) in the 4wt is 1 (6/6), yielding two DFDs at any time. There is no DFD in the 4K80M because of the lack of wt subunit (top). In the wt-3K80M (2nd row from top), the total possible number of dimeric interactions is 3. Since

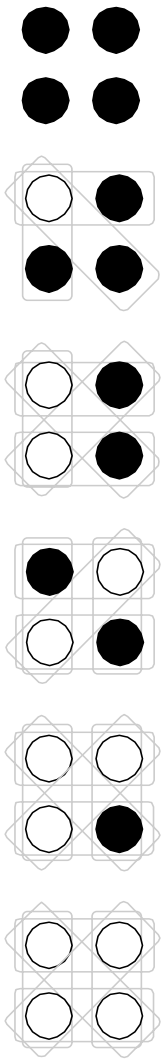

N	η	DFD
0	0	0
3	3/6	1
5	5/6	1.67
5	5/6	1.67
6	6/6	2
6	6/6	2

Scheme 2

the maximal likelihood for dimer formation is 6 in a tetramer, the possibility of subunit pairing (η) is 3/6 or 0.5 in the wt-3K80M, leading to one DFD at any given time. In the *trans* and *cis* 2wt-2K80Ms, there are 5 potential dimeric interactions, resulting in η = 0.833 (i.e., 5/6) or 1 ⅔ DFDs. When there are 3 or 4 wt subunits in a tetrameric channel (3wt-K80M, 4wt), two DFDs can be seen at any time, i.e. η = 1. Generally, η values and the number of DFDs are calculated for all tandem tetramers. Column #1, tandem tetramers; Column 2, number (N) of all potential dimeric interactions in a tetramer. Column 3, η = N / M; Column 4, dynamic functional dimer DFD = η • 2.

Most of findings from our Kir1.1 studies are consistent with those predicted by the model of DFDs. Moreover, the model can also explain some phenomena found in wt Kir1.1 channels such as the substate conductance. 1) The wt channel openings and closures seen during acidosis may require two functional dimers, and are also found in the 3wt-K80M, *trans* 2wt-2K80M and *cis* 2wt-2K80M that all have two DFDs most the time. 2) It is likely that occasional desynchronization of the dimers in the wt channel rather than the freedom of individual subunits leads to the single substate conductance with amplitude of ~40% full conductance. The same substate conductance is also seen in the 3wt-K80M, *trans* 2wt-2K80M and *cis* 2wt-2K80M because they all have two DFDs. 3) There is no dimer formation and all subunits act independently in the 4K80M, leading to smaller and identical substate conductances, while one of the sublevels of conductances is eliminated following the formation of one DFD in the wt-3K80M. 4) The IC_{50} of H^+ concentrations increases by 0.86 μM with recruitment of the first wt subunit, which is half of total 1.66 μM changes in IC_{50} produced by four wt subunits, consistent

with the changes in η and DFD in these tetramers (Scheme 2). 5) Because of their identical η (0.833) and DFDs (1.67), both *trans* and *cis* 2wt-2K80Ms are identical in terms of the pH sensitivity and single-channel properties. 6) Although both 3wt-K80M and 4wt have the same η value, all DFDs in the 4wt consist of wt subunits and have slightly more effect than those in the 3wt-K80M, suggesting that the wt dimer is more effective than the wt-mutant. Interestingly, the model predicts identical effect of the *cis* and *trans* 2wt-2K80M, which is consistent with our experimental data and makes a clear contrast to the functional dimers proposed for the CNG and HCN channels (Liu et al., 1998; Ulens and Siegelbaum, 2003). With the dynamic functional dimers, subunits tend to be recruited in pairs to achieve better coordination and greater effect on channel gating than when activated individually. More importantly, wild types of channel closure, substates of conductance and pH sensitivity may be largely maintained when one or two of the subunits are disrupted.

J-IV. Subunit cooperativity

Subunit cooperativity serves as another mechanism to improve the working efficiency of ion channels with ligand binding. The presence of specific ligands is detected by the binding sites when ligand-channel complex is formed. Information about the quantity of ligands is encoded by the number of subunits with ligand binding and the number of channels being activated. The signal of ligand binding is augmented during propagation along the coupling pathways. Since the channels are composed of multiple subunits, the gating transition depends on the time of not only individual but also all subunits as a whole to be switched to and maintained in one state. One mechanism to

affect the speed of the gating transition and the state maintenance is the cooperativity among subunits. It is known that binding of ligands to one subunit can affect the binding affinity of another subunit to the same ligand. Positive cooperativity occurs when the binding affinity of the second subunit is augmented, while negative cooperativity exists occurs when binding affinity of the second subunit is reduced. As a result, the whole channel tends to stay in one special state rather than another.

Cooperativity has been well studied in receptors and enzymes with three theories developed (Hodgkin and Huxley, 1952; Monod et al., 1965; Koshland et al., 1966). These theories have been applied to the studies of ion channels to describe the ligand channel interaction. In the present study, we have used the theories to describe the gating transitions after ligand binding (Liu et al., 1998; Ulens and Siegelbaum, 2003). Activation of one subunit after ligand binding may alter the free energy required for the gating transition of the second subunit and make its gating transition faster and earlier, consistent with positive coorperativity. Accordingly, we have found positive cooperativity in the pH- and ATP-dependent channel gating of Kir6.2 channel. The results from pH-dependent channel gating indicate a double amplification in both proton binding and channel gating. These are consistent with the high h values found in the Kir channel titration curves. In contrast, ATP-dependent gating shows negative cooperativity in ligand binding and positive cooperativity in channel gating. Although this phenomenon has not been reported in any other channel, the total effect appears to be no cooperativity as revealed by the low Hill coefficient previously observed in K_{ATP} channels. Is it possible that such contradictory effects lead to a waste of energy and represents no

evolutionary advantage? We do not believe so. Since ATP is a major regulator of the K_{ATP} channel, and since the channel is crucial in regulating insulin secretion, cardiac and skeleton muscle contraction and vascular tone, detection of intracellular ATP levels in a wide range may be important for cell survival. The negative cooperativity in ligand binding and positive cooperativity in channel gating may extend the range of its responses to ATP according to the shallow slope of the dose-response curve. This mechanism may allow the cell to respond to the changes in ATP levels even if the level becomes too high or low under extreme conditions.

The subunit cooperativity of the same channel can vary greatly in response to different ligands. In the Kir6.2 channel, positive cooperativity is revealed for proton binding, while negative cooperativity occurs for ATP binding. No cooperativity is suggested for PIP_2 binding to the Kir6.2 channel (MacGregor et al., 2002). With different cooperativity for each specific ligand, the slope of the dose-response curves for the ligands differs, allowing channels to respond to the ligands differently. Therefore, whether a response is needed to cover a wide range of concentrations or to detect certain concentrations of the ligands with high sensitivity can be determined.

J-V. Minimum number of functional subunits required for ligand binding and channel gating

Subunit coordination and intersubunit binding-gating coupling allow recruitment of multiple subunits in channel gating when one subunit is activated by ligand. Therefore not all subunits need to bind to a ligand to activate the channel. Then what is the minimum requirement of such subunits in Kir channel gating? The present study has

provided several pieces of evidence to answer this question. First, ligand-dependent gating of these channels can be initiated with one ligand binding. Second, the Kir1.1 and Kir6.2 channels with one subunit carrying proton binding site retain their pH sensitivity to a significant degree. Third, most of the ATP sensitivity is retained by the Kir6.2 channel when the channel has only one ATP binding sites. Finally, single channel properties of the Kir1.1 channel show that multiple subunits are recruited by the binding of a single ligand. Since a subunit may produce only limited conformational changes for channel gating, an amplification mechanism seems to exist to spread the information of ligand binding to other subunits. The subunit coordination and intersubunit binding-gating coupling may be parts of the amplification system. Due to the amplification system a single subunit is sufficient for ligand gating, however, all four subunits are still needed for maximal pH-dependent gating of the Kir6.2 and Kir1.1 channel as shown in the present study. For ATP-dependent Kir6.2 channel gating, three intact subunits can provide the full ATP sensitivity, which may be due to negative cooperativity in ATP binding. The requirement for some but not all subunits to elicit the channel gating may allow the channels to perform their functions when mutations or other functional disruptions occur in some subunits.

The ability of channel gating to tolerate mutations in some subunits makes the TM2 helix bundle of crossing or inner gate clearly distinct from the selectivity filter. The selectivity filter is such a delicate device for ion selectivity that a single mutation of one of the K^+ signature residues will completely distort ion cages formed by pore-lining residues and disable the channel. In the inner helix, defective sites may be tolerated,

allowing some degree of gating transitions between open and closed states. The tolerance of defective residues in subunit activation is most likely to due to subunit coordination and intersubunit binding-gating coupling, which are carried out by more than one pair of interactions as shown in previous reports (Tsuboi et al., 2004). These interactions are critical for recruiting the neighboring subunits with defects, and sometimes may even determine the gating movement after ligand binding.

J-VI. Determinants of channel gating after specific ligand binding

The present study suggests that interactions between transmembrane helices are more important than just an executer of the gating movement following ligand binding. It is known that different channel species respond to a ligand differently, which has been explained to be a result of the ligand binding domain and coupling mechanism but not the transmembrane helical gating mechanism. As described above, the inner part of the transmembrane helices in the Kir channels plays an important role in channel gating. A few residues critical for channel gating have been identified in this region, a single mutation of which causes complete elimination of the channel gating, such as Thr71, Cys166, Thr171, etc. in the Kir6.2 channel (Cui et al., 2003; Trapp et al., 1998a; Drain et al., 2004). This as well as the close location of some of them leads us to believe that the gating mechanism is accessible by manipulating their relative distance or positions. Thus we performed studies to test this hypothesis. Our results clearly show that the Kir6.2 channel gating can be set and reset depending on how the inner transmembrane helices interact with each other. By setting the switch to a special position, the response of a channel to the same ligand can be different from another channel. Therefore, the inner

helix bundle of crossing appears not only to serve as a gate but also determine the consequence of ligand binding. The results are not only a surprise but also have major implications for understanding ion channel gating. Since the helix bundle of crossing is evolutionarily conserved among a number of ion channels, such a mechanism may also exist in other channels.

K. CONCLUSIONS

In this dissertation, I have systematically studied several critical events occurring in ligand-dependent Kir channel gating. Several novel findings have been made. Some of the results constitute strong evidence for several decade-long open questions such as what is the measurable difference of the ligand binding from channel gating; how ligand binding is coupled to channel gating; and whether the inner helices have a more instrumental role in channel gating than an executer of ligand binding. Technically, these studies have demonstrated the feasibility of understanding ion channels using certain asymmetric preparations and preparations that allow an access to multiple protein domains based on all known crystallographic information. The information obtained should also have impact on the understanding of mis- or dysregulation of ion channels in certain channelopathies and the design of more specific medicines in targeting ligand binding, channel gating or their coupling.

L. REFERENCE

Akabas, M. H., Stauffer, D. A., Xu, M., & Karlin, A. (1992). Acetylcholine receptor channel structure probed in cysteine-substitution mutants. *Science* **258**, 307-310.

Alekseev, A. E., Brady, P. A., & Terzic, A. (1998). Ligand-insensitive state of cardiac ATP-sensitive K^+ channels. Basis for channel opening. *J. Gen.Physiol.* **111**, 381-394.

Antcliff, J. F., Haider, S., Proks, P., Sansom, M. S., & Ashcroft, F. M. (2005). Functional analysis of a structural model of the ATP-binding site of the K_{ATP} channel Kir6.2 subunit. *EMBO J.* **24**, 229-239.

Armstrong, C. M. (1966). Time course of TEA^+-induced anomalous rectification in squid giant axons. *J.Gen.Physiol.* **273**, F516-F529.

Ashcroft, F. M., Harrison, D. E., & Ashcroft, S. J. (1984). Glucose induces closure of single potassium channels in isolated rat pancreatic beta-cells. *Nature* **312**, 446-448.

Ashcroft, F. M. & Gribble, F. M. (1998). Correlating structure and function in ATP-sensitive K^+ channels. *Trends Neurosci.* **1**, 288-294.

Ashcroft, F. M. (2000). Ion channels and disease. Acdemic press, London, UK. pp. 125-160.

Baukrowitz, T., Schulte, U., Oliver, D., Herlitze, S., Krauter, T., Tucker, S. J., Ruppersberg, J. P., & Fakler, B. (1998). PIP_2 and PIP as determinants for ATP inhibition of K_{ATP} channels. *Science* **282**, 1141-1144.

Behrens, M. I., Jalil, P., Serani, A., Vergara, F., & Alvarez, O. (1994). Possible role of apamin-sensitive K^+ channels in myotonic dystrophy. *Muscle Nerve* **17**, 1264-1270.

Bennett, M. V., Barrio, L. C., Bargiello, T. A., Spray, D. C., Hertzberg, E., & Saez, J. C. (1991). Gap junctions: new tools, new answers, new questions. *Neuron* **6**, 305-320.

Berridge, M. J. (1993). Inositol trisphosphate and calcium signalling. *Nature* **361**, 315-325.

Betanzos, M., Chiang, C. S., Guy, H. R., & Sukharev, S. (2002). A large iris-like expansion of a mechanosensitive channel protein induced by membrane tension. *Nat.Struct.Biol.* **9**, 704-710.

Bezanilla, F., Perozo, E., & Stefani, E. (1994). Gating of Shaker K^+ channels: II. The components of gating currents and a model of channel activation. *Biophys.J* **66**, 1011-1021.

Bichet, D., Haass, F. A., & Jan, L. Y. (2003). Merging functional studies with structures of inward-rectifier K^+ channels. *Nat.Rev.Neurosci.* **4**, 957-967.

Black, J. W. & Leff, P. (1983). Operational models of pharmacological agonism. *Proc.R.Soc.Lond. B Biol.Sci.* **220**, 141-162.

Black, J. W., Leff, P., Shankley, N. P., & Wood, J. (1985). An operational model of pharmacological agonism: the effect of E/[A] curve shape on agonist dissociation constant estimation. *Br.J. Pharmacol.* **84**, 561-571.

Bohr C. 1905. Blutgase and respiratoresche Gaswechsel. In *Handbueke der physiologie des menschen.* ed. W Nagel. 1:54

Brunet, L. J., Gold, G. H., & Ngai, J. (1996). General anosmia caused by a targeted disruption of the mouse olfactory cyclic nucleotide-gated cation channel. *Neuron* **17**, 681-693.

Chanchevalap, S., Yang, Z., Cui, N., Qu, Z., Zhu, G., Liu, C., Giwa, L. R., Abdulkadir, L., & Jiang, C. (2000). Involvement of histidine residues in proton sensing of ROMK1 channel. *J.Biol.Chem.* **275**, 7811-7817.

Chang, G., Spencer, R. H., Lee, A. T., Barclay, M. T., & Rees, D. C. (1998). Structure of the MscL homolog from *Mycobacterium tuberculosis*: a gated mechanosensitive ion channel. *Science* **282**, 2220-2226.

Choe, H., Zhou, H., Palmer, L. G., & Sackin, H. (1997). A conserved cytoplasmic region of ROMK modulates pH sensitivity, conductance, and gating. *Am.J.Physiol.* **273**, F516-F529.

Clayton, G. M., Silverman, W. R., Heginbotham, L., & Morais-Cabral, J. H. (2004). Structural basis of ligand activation in a cyclic nucleotide regulated potassium channel. *Cell* **119**, 615-627.

Curtis, H.J. & Cole, K. S. (1940) Membrane action potentials from the squid giant axon. *J. Cell. & Comp. Physiol.* **15**: 147-157

Colquhoun, D. (1998). Binding, gating, affinity and efficacy: the interpretation of structure-activity relationships for agonists and of the effects of mutating receptors. *Br.J. Pharmacol.* **125**, 924-947.

Connolly, C. N. & Wafford, K. A. (2004). The Cys-loop superfamily of ligand-gated ion channels: the impact of receptor structure on function. *Biochem.Soc.Trans.* **32**, 529-534.

Cook, D. L. & Hales, C. N. (1984). Intracellular ATP directly blocks K^+ channels in pancreatic B-cells. *Nature* **311**, 271-273.

Coulter, K. L., Perier, F., Radeke, C. M., & Vandenberg, C. A. (1995). Identification and molecular localization of a pH-sensing domain for the inward rectifier potassium channel HIR. *Neuron* **15**, 1157-1168.

Cruickshank, C. C., Minchin, R. F., Le Dain, A. C., & Martinac, B. (1997). Estimation of the pore size of the large-conductance mechanosensitive ion channel of *Escherichia* coli. *Biophys.J.* **73**, 1925-1931.

Cui, N., Wu, J., Xu, H., Wang, R., Rojas, A., Piao, H., Mao, J., Abdulkadir, L., Li, L., & Jiang, C. (2003). A threonine residue (Thr71) at the intracellular end of the m1 helix plays a critical role in the gating of kir6.2 channels by intracellular ATP and protons. *J.Membr.Biol.* **192**, 111-122.

Davies, N. W. (1990). Modulation of ATP-sensitive K^+ channels in skeletal muscle by intracellular protons. *Nature* **343**, 375-377.

Davies, N. W., Pettit, A. I., Agarwal, R., & Standen, N. B. (1991). The flickery block of ATP-dependent potassium channels of skeletal muscle by internal 4-aminopyridine. *Pflugers Arch.* **419**, 25-31.

Davies, N. W., Standen, N. B., & Stanfield, P. R. (1992). The effect of intracellular pH on ATP-dependent potassium channels of frog skeletal muscle. *J.Physiol.* **445**, 549-568.

Deane, C. M. & Lummis, S. C. (2001). The role and predicted propensity of conserved proline residues in the 5-HT_3 receptor. *J Biol.Chem.* **276**, 37962-37966.

del Camino, D., Holmgren, M., Liu, Y., & Yellen, G. (2000). Blocker protection in the pore of a voltage-gated K^+ channel and its structural implications. *Nature* **403**, 321-325.

Dong, K., Tang, L. Q., MacGregor, G. G., Leng, Q., & Hebert, S. C. (2005). Novel nucleotide-binding sites in ATP-sensitive potassium channels formed at gating interfaces. *EMBO .J* **24**, 1318-1329.

Dorschner, H., Brekardin, E., Uhde, I., Schwanstecher, C., & Schwanstecher, M. (1999). Stoichiometry of sulfonylurea-induced ATP-sensitive potassium channel closure. *Mol.Pharmacol.* **55**, 1060-1066.

Doyle, D. A., Morais, C. J., Pfuetzner, R. A., Kuo, A., Gulbis, J. M., Cohen, S. L., Chait, B. T., & MacKinnon, R. (1998). The structure of the potassium channel: molecular basis of K^+ conduction and selectivity. *Science* **280**, 69-77.

Doyle, D. A. (2004). Structural changes during ion channel gating. *Trends Neurosci.* **27**, 298-302.

Drain, P., Li, L., & Wang, J. (1998). K_{ATP} channel inhibition by ATP requires distinct functional domains of the cytoplasmic C terminus of the pore-forming subunit. *Proc.Natl.Acad.Sci.U.S.A.*. **95**, 13953-13958.

Drain, P., Geng, X., & Li, L. (2004). Concerted gating mechanism underlying K_{ATP} channel inhibition by ATP. *Biophys.J.* **86**, 2101-2112.

Du, X., Zhang, H., Lopes, C., Mirshahi, T., Rohacs, T., & Logothetis, D. E. (2004). Characteristic interactions with phosphatidylinositol 4,5-bisphosphate determine regulation of kir channels by diverse modulators. *J Biol.Chem.* **279**, 37271-37281.

Dutzler, R., Campbell, E. B., & MacKinnon, R. (2003). Gating the selectivity filter in ClC chloride channels. *Science* **300**, 108-112.

Enkvetchakul, D., Loussouarn, G., Makhina, E., & Nichols, C. G. (2001). ATP interaction with the open state of the K_{ATP} channel. *Biophys.J.* **80**, 719-728.

Fakler, B., Schultz, J. H., Yang, J., Schulte, U., Brandle, U., Zenner, H. P., Jan, L. Y., & Ruppersberg, J. P. (1996). Identification of a titratable lysine residue that determines sensitivity of kidney potassium channels (ROMK) to intracellular pH. *EMBO J.* **15**, 4093-4099.

Flagg, T. P., Tate, M., Merot, J., & Welling, P. A. (1999). A mutation linked with Bartter's syndrome locks Kir 1.1a (ROMK1) channels in a closed state. *J.Gen.Physiol.* **114**, 685-700.

Flagg, T. P., Yoo, D., Sciortino, C. M., Tate, M., Romero, M. F., & Welling, P. A. (2002). Molecular mechanism of a COOH-terminal gating determinant in the ROMK channel revealed by a Bartter's disease mutation. *J.Physiol.* **544**, 351-362.

Flynn, G. E. & Zagotta, W. N. (2001). Conformational changes in S_6 coupled to the opening of cyclic nucleotide-gated channels. *Neuron* **30**, 689-698.

Galvani, L. (1791). De viribus electricitatis in motu musculari commentarius, *Bonon. Sci. Art. Inst. Acad. Comment.* 7:363-418.

Gentet, L. J. & Clements, J. D. (2002). Binding site stoichiometry and the effects of phosphorylation on human alpha1 homomeric glycine receptors. *J.Physiol.* **544**, 97-106.

Gunderson, K. L. & Kopito, R. R. (1994). Effects of pyrophosphate and nucleotide analogs suggest a role for ATP hydrolysis in cystic fibrosis transmembrane regulator channel gating. *J.Biol.Chem.* **269**, 19349-19353.

Hamill, O. P., Marty, A., Neher, E., Sakmann, B., & Sigworth, F. J. (1981). Improved patch-clamp techniques for high-resolution current recording. *Pflugers Arch. Eur. J. Physiol.* **391,** 85–100.

Harman, J. G. (2001). Allosteric regulation of the cAMP receptor protein. *Biochim.Biophys.Acta* **1547**, 1-17.

Hebert, S. C. (2003). Bartter syndrome. *Curr.Opin.Nephrol.Hypertens.* **12**, 527-532.

Henry, P., Pearson, W. L., & Nichols, C. G. (1996). Protein kinase C inhibition of cloned inward rectifier (HRK1/KIR2.3) K^+ channels expressed in Xenopus oocytes. *J. Physiol.* **495,** 681-688.

Hilgemann, D. W., Feng, S., & Nasuhoglu, C. (2001). The complex and intriguing lives of PIP_2 with ion channels and transporters. *Sci.STKE.* **2001**, RE19.

Ho, K., Nichols, C. G., Lederer, W. J., Lytton, J., Vassilev, P. M., Kanazirska, M. V., & Hebert, S. C. (1993). Cloning and expression of an inwardly rectifying ATP-regulated potassium channel. *Nature* **362**, 31-38.

Hodgkin, A. L. & Huxley, A. F. (1952). A quantitative description of membrane current and its application to conduction and excitation in nerve. *J.Physiol.* **117**, 500-544.

Huang, C. L. (2001). Regulation of ROMK trafficking and channel activity. *Curr.Opin.Nephrol.Hypertens.* **10**, 693-698.

Hughes, B. A., Kumar, G., Yuan, Y., Swaminathan, A., Yan, D., Sharma, A., Plumley, L., Yang-Feng, T. L., & Swaroop, A. (2000). Cloning and functional expression of human retinal kir2.4, a pH-sensitive inwardly rectifying K^+ channel. *Am.J.Physiol. Cell Physiol.* **279**, C771-C784.

Inagaki, N., Gonoi, T., Clement, J. P., Namba, N., Inazawa, J., Gonzalez, G., Aguilar-Bryan, L., Seino, S., & Bryan, J. (1995). Reconstitution of IK_{ATP}: an inward rectifier subunit plus the sulfonylurea receptor. *Science* **270**, 1166-1170.

Jan, L. Y. & Jan, Y. N. (1997). Receptor-regulated ion channels. *Curr.Opin.Cell Biol.* **9**, 155-160.

Jiang, C., Qu, Z., & Xu, H. (2002a). Gating of inward rectifier K^+ channels by proton-mediated interactions of intracellular protein domains. *Trends Cardiovasc.Med.*. **12**, 5-13.

Jiang, Y., Lee, A., Chen, J., Cadene, M., Chait, B. T., & MacKinnon, R. (2002b). Crystal structure and mechanism of a calcium-gated potassium channel. *Nature* **417**, 515-522.

Jin, P., Walther, D., Zhang, J., Rowe-Teeter, C., & Fu, G. K. (2004). Serine 171, a conserved residue in the gamma-aminobutyric acid type A ($GABA_A$) receptor gamma2 subunit, mediates subunit interaction and cell surface localization. *J Biol.Chem.* **279**, 14179-14183.

Jin, T., Peng, L., Mirshahi, T., Rohacs, T., Chan, K. W., Sanchez, R., & Logothetis, D. E. (2002). The beta-gamma subunits of G proteins gate a K^+ channel by pivoted bending of a transmembrane segment. *Mol.Cell* **10**, 469-481.

Johnson, J. P., Jr. & Zagotta, W. N. (2001). Rotational movement during cyclic nucleotide-gated channel opening. *Nature* **412**, 917-921.

Kahle, K. T., Wilson, F. H., Leng, Q., Lalioti, M. D., O'Connell, A. D., Dong, K., Rapson, A. K., MacGregor, G. G., Giebisch, G., Hebert, S. C., & Lifton, R. P. (2003). WNK4 regulates the balance between renal NaCl reabsorption and K^+ secretion. *Nat.Genet.* **35**, 372-376.

Kenakin, T. (2004). Principles: receptor theory in pharmacology. *Trends Pharmacol.Sci.* **25**, 186-192.

Kohler, M., Hirschberg, B., Bond, C. T., Kinzie, J. M., Marrion, N. V., Maylie, J., & Adelman, J. P. (1996). Small-conductance, calcium-activated potassium channels from mammalian brain. *Science* **273**, 1709-1714.

Koshland, D. E., Jr., Nemethy, G., & Filmer, D. (1966). Comparison of experimental binding data and theoretical models in proteins containing subunits. *Biochemistry* **5**, 365-385.

Koshland, D. E., Jr. & Hamadani, K. (2002). Proteomics and models for enzyme cooperativity. *J Biol.Chem.* **277**, 46841-46844.

Krapivinsky, G., Gordon, E. A., Wickman, K., Velimirovic, B., Krapivinsky, L., & Clapham, D. E. (1995). The G-protein-gated atrial K^+ channel IK_{ACh} is a heteromultimer of two inwardly rectifying K^+-channel proteins. *Nature* **374**, 135-141.

Kubo, Y., Baldwin, T. J., Jan, Y. N., & Jan, L. Y. (1993). Primary structure and functional expression of a mouse inward rectifier potassium channel. *Nature* **362**, 127-133.

Kunzelmann, K., Hubner, M., Vollmer, M., Ruf, R., Hildebrandt, F., Greger, R., & Schreiber, R. (2000). A Bartter's syndrome mutation of ROMK1 exerts dominant negative effects on K^+ conductance. *Cell Physiol. Biochem.* **10**, 117-124.

Kuo, A., Gulbis, J. M., Antcliff, J. F., Rahman, T., Lowe, E. D., Zimmer, J., Cuthbertson, J., Ashcroft, F. M., Ezaki, T., & Doyle, D. A. (2003). Crystal structure of the potassium channel KirBac1.1 in the closed state. *Science* **300**, 1922-1926.

Kuzhikandathil, E. V. & Oxford, G. S. (2000). Dominant-negative mutants identify a role for GIRK channels in D3 dopamine receptor-mediated regulation of spontaneous secretory activity. *J.Gen.Physiol.* **115**, 697-706.

Labarca, C., Nowak, M. W., Zhang, H., Tang, L., Deshpande, P., & Lester, H. A. (1995). Channel gating governed symmetrically by conserved leucine residues in the M2 domain of nicotinic receptors. *Nature* **376**, 514-516.

Labro, A. J., Raes, A. L., & Snyders, D. J. (2005). Coupling of voltage sensing to channel opening reflects intrasubunit interactions in kv channels. *J. Gen.Physiol.* **125**, 71-80.

Lederer, W. J. & Nichols, C. G. (1989). Nucleotide modulation of the activity of rat heart ATP-sensitive K^+ channels in isolated membrane patches. *J. Physiol.* **419**, 193-211.

Lei, Q., Jones, M. B., Talley, E. M., Garrison, J. C., & Bayliss, D. A. (2003). Molecular mechanisms mediating inhibition of G protein-coupled inwardly-rectifying K^+ channels. *Mol..Cells* **15**, 1-9.

Leipziger, J., MacGregor, G. G., Cooper, G. J., Xu, J., Hebert, S. C., & Giebisch, G. (2000). PKA site mutations of ROMK2 channels shift the pH dependence to more alkaline values. *Am.J.Physiol. Renal Physiol.* **279**, F919-F926.

Lester, H. A., Dibas, M. I., Dahan, D. S., Leite, J. F., & Dougherty, D. A. (2004). Cys-loop receptors: new twists and turns. *Trends Neurosci.* **27**, 329-336.

Leung, Y. M., Zeng, W. Z., Liou, H. H., Solaro, C. R., & Huang, C. L. (2000). Phosphatidylinositol 4,5-bisphosphate and intracellular pH regulate the ROMK1 potassium channel via separate but interrelated mechanisms. *J.Biol.Chem.* **275**, 10182-10189.

Liao, Y. J., Jan, Y. N., & Jan, L. Y. (1996). Heteromultimerization of G-protein-gated inwardly rectifying K^+ channel proteins GIRK1 and GIRK2 and their altered expression in weaver brain. *J. Neurosci.* **16**, 7137-7150.

Light, P. E., Bladen, C., Winkfein, R. J., Walsh, M. P., & French, R. J. (2000). Molecular basis of protein kinase C-induced activation of ATP-sensitive potassium channels. *Proc.Natl.Acad.Sci.U.S.A.* **97**, 9058-9063.

Lin, D., Sterling, H., Lerea, K. M., Giebisch, G., & Wang, W. H. (2002). Protein kinase C (PKC)-induced phosphorylation of ROMK1 is essential for the surface expression of ROMK1 channels. *J.Biol.Chem.* **277**, 44278-44284.

Lin, Y. W., Jia, T., Weinsoft, A. M., & Shyng, S. L. (2003). Stabilization of the activity of ATP-sensitive potassium channels by ion pairs formed between adjacent Kir6.2 subunits. *J. Gen.Physiol.* **122**, 225-237.

Liu, D. T., Tibbs, G. R., Paoletti, P., & Siegelbaum, S. A. (1998). Constraining ligand-binding site stoichiometry suggests that a cyclic nucleotide-gated channel is composed of two functional dimers. *Neuron* **21**, 235-248.

Liu, J, Siegelbaum, S. A. (2000). Change of pore helix conformational state upon opening of cyclic nucleotide-gated channels. *Neuron* 28:899-909.

Liu, Y., Holmgren, M., Jurman, M. E., & Yellen, G. (1997). Gated access to the pore of a voltage-dependent K^+ channel. *Neuron* **19**, 175-184.

Logothetis, D. E., Kurachi, Y., Galper, J., Neer, E. J., & Clapham, D. E. (1987). The beta gamma subunits of GTP-binding proteins activate the muscarinic K^+ channel in heart. *Nature* **325**, 321-326.

Lopez-Barneo, J., Hoshi, T., Heinemann, S. H., & Aldrich, R. W. (1993). Effects of external cations and mutations in the pore region on C-type inactivation of Shaker potassium channels. *Receptors.Channels* **1**, 61-71.

Loussouarn, G., Makhina, E. N., Rose, T., & Nichols, C. G. (2000). Structure and dynamics of the pore of inwardly rectifying K_{ATP} channels. *J. Biol.Chem.* **275**, 1137-1144.

MacGregor, G. G., Dong, K., Vanoye, C. G., Tang, L., Giebisch, G., & Hebert, S. C. (2002). Nucleotides and phospholipids compete for binding to the C terminus of K_{ATP} channels. *Proc.Natl.Acad.Sci.U.S.A.* **99**, 2726-2731.

MacKinnon, R. (2004). Nobel Lecture. Potassium channels and the atomic basis of selective ion conduction. *Biosci.Rep.* **24**, 75-100.

Manning Fox, J. E., Nichols, C. G., & Light, P. E. (2004). Activation of adenosine triphosphate-sensitive potassium channels by acyl coenzyme A esters involves multiple phosphatidylinositol 4,5-bisphosphate-interacting residues. *Mol.Endocrinol.* **18**, 679-686.

Mao, J., Li, L., McManus, M., Wu, J., Cui, N., & Jiang, C. (2002). Molecular determinants for activation of G-protein-coupled inward rectifier K^+ (GIRK) channels by extracellular acidosis. *J. Biol.Chem.* **277**, 46166-46171.

Markworth, E., Schwanstecher, C., & Schwanstecher, M. (2000). ATP_{4-} mediates closure of pancreatic beta-cell ATP-sensitive potassium channels by interaction with 1 of 4 identical sites. *Diabetes* **49**, 1413-1418.

McLerie, M. & Lopatin, A. (2003). Dominant-negative suppression of $I(K_1)$ in the mouse heart leads to altered cardiac excitability. *J.Mol.Cell Cardiol.* **35**, 367-378.

McNicholas, C. M., Wang, W., Ho, K., Hebert, S. C., & Giebisch, G. (1994). Regulation of ROMK1 K^+ channel activity involves phosphorylation processes. *Proc.Natl.Acad.Sci.U.S.A.* **91** , 8077-8081.

McNicholas, C. M., MacGregor, G. G., Islas, L. D., Yang, Y., Hebert, S. C., & Giebisch, G. (1998). pH-dependent modulation of the cloned renal K^+ channel, ROMK. *Am.J.Physiol.* **275**, F972-F981.

Meera, P., Wallner, M., Song, M., & Toro, L. (1997). Large conductance voltage- and calcium-dependent K^+ channel, a distinct member of voltage-dependent ion channels with seven N-terminal transmembrane segments (S_0-S_6), an extracellular N terminus, and an intracellular (S_9-S_{10}) C terminus. *Proc.Natl.Acad.Sci.U.S.A.* **94**, 14066-14071.

Mikami, A., Imoto, K., Tanabe, T., Niidome, T., Mori, Y., Takeshima, H., Narumiya, S., & Numa, S. (1989). Primary structure and functional expression of the cardiac dihydropyridine-sensitive calcium channel. *Nature* **340**, 230-233.

Minor, D. L., Lin, Y. F., Mobley, B. C., Avelar, A., Jan, Y. N., Jan, L. Y., & Berger, J. M. (2000). The polar T1 interface is linked to conformational changes that open the voltage-gated potassium channel. *Cell* **102**, 657-670.

Minor, D. L., Jr., Masseling, S. J., Jan, Y. N., & Jan, L. Y. (1999). Transmembrane structure of an inwardly rectifying potassium channel. *Cell* **96**, 879-891.

Miyazawa, A., Fujiyoshi, Y., Stowell, M., & Unwin, N. (1999). Nicotinic acetylcholine receptor at 4.6 Å resolution: transverse tunnels in the channel wall. *J. Mol.Biol.* **288**, 765-786.

Miyazawa, A., Fujiyoshi, Y., & Unwin, N. (2003). Structure and gating mechanism of the acetylcholine receptor pore. *Nature* **423**, 949-955.

Monod, J., Wyman, J., & Changeux, J. P. (1965). On the nature of allosteric transitions: a plausible model. *J.Mol.Biol.* **12**, 88-118.

Nakamura, T. & Gold, G. H. (1987). A cyclic nucleotide-gated conductance in olfactory receptor cilia. *Nature* **325**, 442-444.

Neylon, C. B., Lang, R. J., Fu, Y., Bobik, A., & Reinhart, P. H. (1999). Molecular cloning and characterization of the intermediate-conductance Ca^{2+}-activated K^+ channel in vascular smooth muscle: relationship between K_{Ca} channel diversity and smooth muscle cell function. *Circ.Res.* **85**, e33-e43.

Nichols, C. G. & Lopatin, A. N. (1997). Inward rectifier potassium channels. *Annu.Rev.Physiol.* **59**, 171-191.

Nishida, M. & MacKinnon, R. (2002). Structural basis of inward rectification: cytoplasmic pore of the G protein-gated inward rectifier GIRK1 at 1.8 Å resolution. *Cell* **111**, 957-965.

Niu, X. & Magleby, K. L. (2002). Stepwise contribution of each subunit to the cooperative activation of BK channels by Ca^{2+}. *Proc.Natl.Acad.Sci.U.S.A.* **99**, 11441-11446.

Noda, M., Takahashi, H., Tanabe, T., Toyosato, M., Furutani, Y., Hirose, T., Asai, M., Inayama, S., Miyata, T., & Numa, S. (1982). Primary structure of alpha-subunit precursor of Torpedo californica acetylcholine receptor deduced from cDNA sequence. *Nature* **299**, 793-797.

Noda, M., Shimizu, S., Tanabe, T., Takai, T., Kayano, T., Ikeda, T., Takahashi, H., Nakayama, H., Kanaoka, Y., Minamino, N., & . (1984). Primary structure of Electrophorus electricus sodium channel deduced from cDNA sequence. *Nature* **312**, 121-127.

Noma, A. (1983). ATP-regulated K^+ channels in cardiac muscle. *Nature* **305**, 147-148.

Paoletti, P., Young, E. C., & Siegelbaum, S. A. (1999). C-Linker of cyclic nucleotide-gated channels controls coupling of ligand binding to channel gating. *J. Gen.Physiol.* **113**, 17-34.

Papazian, D. M., Schwarz, T. L., Tempel, B. L., Jan, Y. N., & Jan, L. Y. (1987). Cloning of genomic and complementary DNA from Shaker, a putative potassium channel gene from Drosophila. *Science* **237**, 749-753.

Perozo, E., Cortes, D. M., & Cuello, L. G. (1999). Structural rearrangements underlying K^+-channel activation gating. *Science* **285**, 73-78.

Perozo, E., Kloda, A., Cortes, D. M., & Martinac, B. (2001). Site-directed spin-labeling analysis of reconstituted Mscl in the closed state. *J. Gen.Physiol.* **118**, 193-206.

Perozo, E., Cortes, D. M., Sompornpisut, P., Kloda, A., & Martinac, B. (2002). Open channel structure of MscL and the gating mechanism of mechanosensitive channels. *Nature* **418**, 942-948.

Pessia, M., Tucker, S. J., Lee, K., Bond, C. T., & Adelman, J. P. (1996). Subunit positional effects revealed by novel heteromeric inwardly rectifying K^+ channels. *EMBO J.* **15**, 2980-2987.

Pessia, M., Imbrici, P., D'Adamo, M. C., Salvatore, L., & Tucker, S. J. (2001). Differential pH sensitivity of Kir4.1 and Kir4.2 potassium channels and their modulation by heteropolymerisation with Kir5.1. *J.Physiol.* **532**, 359-367.

Phillips, L. R., Enkvetchakul, D., & Nichols, C. G. (2003). Gating dependence of inner pore access in inward rectifier K^+ channels. *Neuron* **37**, 953-962.

Piao, H., Cui, N., Xu, H., Mao, J., Rojas, A., Wang, R., Abdulkadir, L., Li, L., Wu, J., & Jiang, C. (2001). Requirement of multiple protein domains and residues for gating K_{ATP} channels by intracellular pH. *J.Biol.Chem.* **276**, 36673-36680.

Pliska, V. (1999). Partial agonism: mechanisms based on ligand-receptor interactions and on stimulus-response coupling. *J. Recept.Signal.Transduct.Res.* **19**, 597-629.

Proks, P., Antcliff, J. F., & Ashcroft, F. M. (2003). The ligand-sensitive gate of a potassium channel lies close to the selectivity filter. *EMBO Rep.* **4**, 70-75.

Pugh, E. N., Jr. (1996). Cooperativity in cyclic nucleotide-gated ion channels. *J. Gen.Physiol.* **107**, 165-167.

Qu, Z., Yang, Z., Cui, N., Zhu, G., Liu, C., Xu, H., Chanchevalap, S., Shen, W., Wu, J., Li, Y., & Jiang, C. (2000). Gating of inward rectifier K^+ channels by proton-mediated interactions of N- and C-terminal domains. *J.Biol.Chem.* **275**, 31573-31580.

Rojas, A., Wu, J., Wang, R., & Jiang, C. (2005) Gating of the ATP-sensitive K^+ channel by a pore-lining phenylalanine residue. *Am.J.Physiol.* in submission.

Reeves, D. C., Goren, E. N., Akabas, M. H., & Lummis, S. C. (2001). Structural and electrostatic properties of the 5-HT3 receptor pore revealed by substituted cysteine accessibility mutagenesis. *J. Biol.Chem.* **276**, 42035-42042.

Reimann, F., Ryder, T. J., Tucker, S. J., & Ashcroft, F. M. (1999). The role of lysine 185 in the kir6.2 subunit of the ATP-sensitive channel in channel inhibition by ATP. *J. Physiol.* **520 Pt 3**, 661-669.

Renaud, J. F., Desnuelle, C., Schmid-Antomarchi, H., Hugues, M., Serratrice, G., & Lazdunski, M. (1986). Expression of apamin receptor in muscles of patients with myotonic muscular dystrophy. *Nature* **319**, 678-680.

Ribalet, B., John, S. A., & Weiss, J. N. (2003). Molecular basis for Kir6.2 channel inhibition by adenine nucleotides. *Biophys.J.* **84**, 266-276.

Rosenmund, C., Stern-Bach, Y., & Stevens, C. F. (1998). The tetrameric structure of a glutamate receptor channel. *Science* **280**, 1596-1599.

Roux, B. & MacKinnon, R. (1999). The cavity and pore helices in the KcsA K^+ channel: electrostatic stabilization of monovalent cations. *Science* **285**, 100-102.

Ruiz, M. L. & Karpen, J. W. (1997). Single cyclic nucleotide-gated channels locked in different ligand-bound states. *Nature* **389**, 389-392.

Sadja, R., Alagem, N., & Reuveny, E. (2002). Graded contribution of the Gbeta gamma binding domains to GIRK channel activation. *Proc.Natl.Acad.Sci.U.S.A.* **99**, 10783-10788.

Santa, N., Kitazono, T., Ago, T., Ooboshi, H., Kamouchi, M., Wakisaka, M., Ibayashi, S., & Iida, M. (2003). ATP-sensitive potassium channels mediate dilatation of basilar artery in response to intracellular acidification in vivo. *Stroke* **34**, 1276-1280.

Schonherr, R., Hehl, S., Terlau, H., Baumann, A., & Heinemann, S. H. (1999). Individual subunits contribute independently to slow gating of bovine EAG potassium channels. *J.Biol.Chem.* **274**, 5362-5369.

Schulte, U., Hahn, H., Konrad, M., Jeck, N., Derst, C., Wild, K., Weidemann, S., Ruppersberg, J. P., Fakler, B., & Ludwig, J. (1999). pH gating of ROMK (K(ir)1.1) channels: control by an Arg-Lys-Arg triad disrupted in antenatal Bartter syndrome. *Proc.Natl.Acad.Sci.U.S.A.* **96**, 15298-15303.

Schulte, U., Weidemann, S., Ludwig, J., Ruppersberg, J., & Fakler, B. (2001). K^+-dependent gating of Kir1.1 channels is linked to pH gating through a conformational change in the pore. *J.Physiol.* **534**, 49-58.

Seino, S. (1999). ATP-sensitive potassium channels: a model of heteromultimeric potassium channel/receptor assemblies. *Annu.Rev.Physiol.* **61**, 337-362.

Shin, K. S., Rothberg, B. S., & Yellen, G. (2001). Blocker state dependence and trapping in hyperpolarization-activated cation channels: evidence for an intracellular activation gate. *J.Gen.Physiol.* **117**, 91-101.

Shuck, M. E., Piser, T. M., Bock, J. H., Slightom, J. L., Lee, K. S., & Bienkowski, M. J. (1997). Cloning and characterization of two K^+ inward rectifier Kir1.1 potassium channel homologs from human kidney (Kir1.2 and Kir1.3). *J.Biol.Chem.* **272**, 586-593.

Shyng, S. L. & Nichols, C. G. (1998). Membrane phospholipid control of nucleotide sensitivity of K_{ATP} channels. *Science* **282**, 1138-1141.

Sixma, T. K. & Smit, A. B. (2003). Acetylcholine binding protein (AChBP): a secreted glial protein that provides a high-resolution model for the extracellular domain of pentameric ligand-gated ion channels. *Annu..Rev. Biophys.Biomol.Struct.* **32**, 311-334.

Srivastava, M., Eidelman, O., & Pollard, H. B. (1999). Pharmacogenomics of the cystic fibrosis transmembrane conductance regulator (CFTR) and the cystic fibrosis drug CPX using genome microarray analysis. *Mol.Med.* **5**, 753-767.

Sukharev, S., Betanzos, M., Chiang, C. S., & Guy, H. R. (2001). The gating mechanism of the large mechanosensitive channel MscL. *Nature* **409**, 720-724.

Sun, Z. P., Akabas, M. H., Goulding, E. H., Karlin, A., & Siegelbaum, S. A. (1996). Exposure of residues in the cyclic nucleotide-gated channel pore: P region structure and function in gating. *Neuron* **16**, 141-149.

Tanabe, K., Tucker, S. J., Matsuo, M., Proks, P., Ashcroft, F. M., Seino, S., Amachi, T., & Ueda, K. (1999). Direct photoaffinity labeling of the Kir6.2 subunit of the ATP-sensitive K^+ channel by 8-azido-ATP. *J. Biol..Chem.* **274**, 3931-3933.

Tang, Y., Zaitseva, F., Lamb, R. A., & Pinto, L. H. (2002). The gate of the influenza virus M2 proton channel is formed by a single tryptophan residue. *J.Biol..Chem.* **277**, 39880-39886.

Tibbs, G. R., Goulding, E. H., & Siegelbaum, S. A. (1997). Allosteric activation and tuning of ligand efficacy in cyclic-nucleotide-gated channels. *Nature* **386**, 612-615.

Trapp, S., Proks, P., Tucker, S. J., & Ashcroft, F. M. (1998a). Molecular analysis of ATP-sensitive K channel gating and implications for channel inhibition by ATP. *J.Gen..Physiol.* **112**, 333-349.

Trapp, S., Tucker, S. J., & Ashcroft, F. M. (1998b). Mechanism of ATP-sensitive K channel inhibition by sulfhydryl modification. *J.Gen.Physiol.* **112**, 325-332.

Trapp, S., Haider, S., Jones, P., Sansom, M. S., & Ashcroft, F. M. (2003). Identification of residues contributing to the ATP binding site of Kir6.2. *EMBO J.* **22**, 2903-2912.

Trzeciakowski, J. P. (1999a). Stimulus amplification, efficacy, and the operational model. Part I--binary complex occupancy mechanisms. *J. Theor.Biol.* **198**, 329-346.

Trzeciakowski, J. P. (1999b). Stimulus amplification, efficacy, and the operational model. Part II--ternary complex occupancy mechanisms. *J. Theor.Biol.* **198**, 347-374.

Tsai, T. D., Shuck, M. E., Thompson, D. P., Bienkowski, M. J., & Lee, K. S. (1995). Intracellular H^+ inhibits a cloned rat kidney outer medulla K^+ channel expressed in Xenopus oocytes. *Am.J.Physiol.* **268**, C1173-C1178.

Tsuboi, T., Lippiat, J. D., Ashcroft, F. M., & Rutter, G. A. (2004). ATP-dependent interaction of the cytosolic domains of the inwardly rectifying K^+ channel Kir6.2 revealed by fluorescence resonance energy transfer. *Proc.Natl.Acad.Sci.U.S..A* **101**, 76-81.

Tucker, S. J., Gribble, F. M., Zhao, C., Trapp, S., & Ashcroft, F. M. (1997). Truncation of Kir6.2 produces ATP-sensitive K^+ channels in the absence of the sulphonylurea receptor. *Nature* **387**, 179-183.

Tucker, S. J., Gribble, F. M., Proks, P., Trapp, S., Ryder, T. J., Haug, T., Reimann, F., & Ashcroft, F. M. (1998). Molecular determinants of K_{ATP} channel inhibition by ATP. *EMBO J.* **17**, 3290-3296.

Tucker, S. J. & Ashcroft, F. M. (1999). Mapping of the physical interaction between the intracellular domains of an inwardly rectifying potassium channel, Kir6.2. *J.Biol.Chem.* **274**, 33393-33397.

Ulens, C. & Siegelbaum, S. A. (2003). Regulation of hyperpolarization-activated HCN channels by cAMP through a gating switch in binding domain symmetry. *Neuron* **40**, 959-970.

Unwin, N. (1995). Acetylcholine receptor channel imaged in the open state. *Nature* **373**, 37-43.

Unwin, N. (2003). Structure and action of the nicotinic acetylcholine receptor explored by electron microscopy. *FEBS Lett.* **555**, 91-95.

Varnum, M. D. & Zagotta, W. N. (1997). Interdomain interactions underlying activation of cyclic nucleotide-gated channels. *Science* **278**, 110-113.

Wang, R., Rojas, A., Wu, J., Piao, H., Adams, C. Y., Xu, H., Shi, Y., Wang, Y., & Jiang, C. (2005a). Determinant role of membrane helices in K ATP channel gating. *J. Membr.Biol.* **204**, 1-10.

Wang, R., Su, J., Wang, X., Piao, H., Zhang, X., Adams, C. Y., Cui, N., & Jiang, C. (2005b). Subunit stoichiometry of the Kir1.1 channel in proton-dependent gating. *J.Biol.Chem.* **280**, 13433-13441.

Wang, W. (1999). Regulation of the ROMK channel: interaction of the ROMK with associate proteins. *Am.J.Physiol.* **277**, F826-F831.

Wang, X., Wu, J., Li, L., Chen, F., Wang, R., & Jiang, C. (2003). Hypercapnic acidosis activates K_{ATP} channels in vascular smooth muscles. *Circ.Res.* **92**, 1225-1232.

Wang, Y. W., Ding, J. P., Xia, X. M., & Lingle, C. J. (2002). Consequences of the stoichiometry of Slo_1 alpha and auxiliary beta subunits on functional properties of large-conductance Ca^{2+}-activated K^+ channels. *J. Neurosci.* **22**, 1550-1561.

Wilson, G. & Karlin, A. (2001). Acetylcholine receptor channel structure in the resting, open, and desensitized states probed with the substituted-cysteine-accessibility method. *Proc.Natl.Acad.Sci.U.S.A.* **98**, 1241-1248.

Wu, J., Xu, H., Yang, Z., Wang, Y., Mao, J., & Jiang, C. (2002a). Protons activate homomeric Kir6.2 channels by selective suppression of the long and intermediate closures. *J.Membr.Biol.* **190**, 105-116.

Wu, J., Cui, N., Piao, H., Wang, Y., Xu, H., Mao, J., & Jiang, C. (2002b). Allosteric modulation of the mouse Kir6.2 channel by intracellular H^+ and ATP. *J.Physiol.* **543**, 495-504.

Wu, J., Piao, H., Rojas, A., Wang, R., Wang, Y., Cui, N., Shi, Y., Chen, F., & Jiang, C. (2004). Critical protein domains and amino acid residues for gating the KIR6.2 channel by intracellular ATP. *J.Cell Physiol.* **198**, 73-82.

Xu, H., Yang, Z., Cui, N., Giwa, L. R., Abdulkadir, L., Patel, M., Sharma, P., Shan, G., Shen, W., & Jiang, C. (2000a). Molecular determinants for the distinct pH sensitivity of Kir1.1 and Kir4.1 channels. *Am.J.Physiol Cell Physiol.* **279**, C1464-C1471.

Xu, H., Cui, N., Yang, Z., Qu, Z., & Jiang, C. (2000b). Modulation of kir4.1 and kir5.1 by hypercapnia and intracellular acidosis. *J.Physiol.* **524 Pt 3**, 725-735.

Xu, H., Yang, Z., Cui, N., Chanchevalap, S., Valesky, W. W., & Jiang, C. (2000c). A single residue contributes to the difference between Kir4.1 and Kir1.1 channels in pH sensitivity, rectification and single channel conductance. *J.Physiol.* **528 Pt 2**, 267-277.

Xu, H., Cui, N., Yang, Z., Wu, J., Giwa, L. R., Abdulkadir, L., Sharma, P., & Jiang, C. (2001a). Direct activation of cloned K_{ATP} channels by intracellular acidosis. *J.Biol.Chem.* **276**, 12898-12902.

Xu, H., Wu, J., Cui, N., Abdulkadir, L., Wang, R., Mao, J., Giwa, L. R., Chanchevalap, S., & Jiang, C. (2001b). Distinct histidine residues control the acid-induced activation and inhibition of the cloned K_{ATP} channel. *J.Biol.Chem.* **276**, 38690-38696.

Yang, J., Jan, Y. N., & Jan, L. Y. (1995). Determination of the subunit stoichiometry of an inwardly rectifying potassium channel. *Neuron* **15**, 1441-1447.

Yang, Z. & Jiang, C. (1999). Opposite effects of pH on open-state probability and single channel conductance of kir4.1 channels. *J.Physiol.* **520 Pt 3**, 921-927.

Yang, Z., Xu, H., Cui, N., Qu, Z., Chanchevalap, S., Shen, W., & Jiang, C. (2000). Biophysical and molecular mechanisms underlying the modulation of heteromeric Kir4.1-Kir5.1 channels by CO_2 and pH. *J Gen.Physiol.* **116**, 33-45.

Yellen, G. (2002). The voltage-gated potassium channels and their relatives. *Nature* **419**, 35-42.

Yoo, D., Kim, B. Y., Campo, C., Nance, L., King, A., Maouyo, D., & Welling, P. A. (2003). Cell surface expression of the ROMK (Kir1.1) channel is regulated by the aldosterone-induced kinase, SGK-1, and protein kinase A. *J.Biol..Chem.* **278**, 23066-23075.

Young, E. C., Sciubba, D. M., & Siegelbaum, S. A. (2001). Efficient coupling of ligand binding to channel opening by the binding domain of a modulatory (beta) subunit of the olfactory cyclic nucleotide-gated channel. *J. Gen.Physiol.* **118**, 523-546.

Young, E. C. & Krougliak, N. (2004). Distinct structural determinants of efficacy and sensitivity in the ligand-binding domain of cyclic nucleotide-gated channels. *J. Biol.Chem.* **279**, 3553-3562.

Zagotta, W. N., Olivier, N. B., Black, K. D., Young, E. C., Olson, R., & Gouaux, E. (2003). Structural basis for modulation and agonist specificity of HCN pacemaker channels. *Nature* **425**, 200-205.

Zhu, G., Chanchevalap, S., Cui, N., & Jiang, C. (1999). Effects of intra- and extracellular acidifications on single channel Kir2.3 currents. *J.Physiol.* **516 (Pt 3)**, 699-710.

Zhu, G., Liu, C., Qu, Z., Chanchevalap, S., Xu, H., & Jiang, C. (2000). CO_2 inhibits specific inward rectifier K^+ channels by decreases in intra- and extracellular pH. *J.Cell Physiol.* **183**, 53-64.

M. LIST OF SUBMITTED AND PUBLISHED PAPERS

1. **Wang, R.**, Su, J., Wang, X., Piao, H., Zhang, X., Adams, C Y., Cui, N., & Jiang, C. (2005). Stoichiometry of the Kir1.1 channel in proton-dependent gating. *J.Biol.Chem.* **280,** 13433-41.
2. **Wang, R.**, Rojas, A., Wu, J., Piao, H., Xu, H., & Jiang, C. (2005). Membrane helical domains determine the opening and closure of mammalian ligand-gated K^+ channels. *J.Membr.Biol.* **204**, 1-10.
3. **Wang, R.**, Su, J., Zhang, X., Piao, H., Wang, X., Shi, Y., Cui, Y., Onyebuchi, V A., & Jiang, C. (2005). Kir6.2 channel gating by intracellular protons: subunit stoichiometry for ligand binding and channel gating. Submitted.
4. **Wang, R.**, Zhang, X., Cui, N., Wu, J., & Jiang, C. (2005). Subunit-stoichiometric evidence for Kir6.2 channel gating, ATP binding and binding-gating coupling. Submitted.
5. Rojas, A., Wu, J., **Wang, R**., & Jiang, C. (2005) Gating of the ATP-sensitive K^+ channel by a pore-lining phenylalanine residue. *Am.J.Physiol.* in submission.
6. Jiang, C., Rojas, A., **Wang, R**., & Wang, X. (2004). CO_2 central chemosensitivity: Why are there so many sensing molecules? *Respir. Physiol. Neurobiol.* 145:115-26.
7. Wu, J., Piao, H., Rojas, A., **Wang, R.,** Wang, Y., Cui, N., Shi, Y., Chen, F., & Jiang, C. (2004). Critical protein domains and amino acid residues for gating the Kir6.2 channel by intracellular ATP. *J.Cell. Physiol.* **198**, 73-81.
8. Mao, J., Wang, X., Chen, F., **Wang, R.,** Rojas, A., Shi, Y., Piao, H., & Jiang, C. (2004). Molecular basis for the inhibition of G protein-coupled inward rectifier K^+ channels by protein kinase C. *Proc.Natl.Acad.Sci.U.S.A.* **101**, 1087-1092.
9. Wang, X., Wu, J., Li, L., Chen, F., **Wang, R.,** & Jiang, C. (2003). Hypercapnic acidosis activates K_{ATP} channels in vascular smooth muscles. *Circ.Res.* **92**, 1225-1232.
10. Cui, N., Wu, J., Xu, H., **Wang, R.,** Rojas, A., Piao, H., Mao, J., Abdulkadir, L., Li, L., & Jiang, C. (2003). A threonine residue (Thr71) at the intracellular end of the M1 helix plays a critical role in the gating of Kir6.2 channels by intracellular ATP and protons. *J.Membr.Biol.* **192**, 111-122.
11. Piao, H., Cui, N., Xu, H., Mao, J., Rojas, A., **Wang, R.,** Abdulkadir, L., Li, L., Wu, J., & Jiang, C. (2001). Requirement of multiple protein domains and residues for gating K_{ATP} channels by intracellular pH. *J.Biol.Chem.* **276**, 36673-36680.
12. Xu, H., Wu, J., Cui, N., Abdulkadir, L., **Wang, R.,** Mao, J., Giwa, L. R., Chanchevalap, S., & Jiang, C. (2001). Distinct histidine residues control the acid-induced activation and inhibition of the cloned K_{ATP} channel. *J.Biol.Chem.* **276**, 38690-38696.

N. LIST OF MEETING PRESENTATIONS

1. **Wang, R.,** Su, J., Zhang, X., Shi, Y., Jiang, C. Kir6.2 channel gating by intracellular protons: subunit stoichiometry for ligand binding and channel gating. *Society for Neuroscience 35th Annual Meeting,* 2005, 609.1.
2. **Wang, R.**, Su, J., Wang, X., & Jiang C. Subunit stoichiometry for Kir6.2 channel gating by intracellular ATP. *49th Biophysical Society Annual Meeting.* 2005, 2326-Pos.
3. **Wang**, **R.**, Su, J., Wang, X., Piao, H., Adams, C.Y., & Jiang, C. Dept. of Biol., Georgia State Univ. 24 Peachtree Center Ave. Atlanta, GA 30303. Subunit stoichiometry of the Kir1.1 channel in proton-dependent gating. *Society for Neuroscience 34th Annual Meeting,* 2004, 851.14.
4. Mao, J., **Wang, R.**, Wang, X., Rojas, A., & Jiang C. Molecular bases for the inhibition of G-protein coupled inward rectifier K^+ channels by protein kinase C. *48th Biophysical Society Annual Meeting*. 2004, 2280-Pos.
5. Wu, J., Rojas, A., **Wang, R**., & Jiang C. Kir6.2 channel gating may involve spatial hindrance effect at the inner ion-conductive pore. *Society for Neuroscience 33th Annual Meeting,* 2003, 368.13.
6. **Wang, R**. Rojas, A. Wu, J., & Jiang, C. Kir6.2 Channel gating may be determined by relative distance between the TM1 and TM2 helices. *Society for Neuroscience 33th Annual Meeting,* 2003, 53.19.
7. Rojas, A., **Wang, R**., Wallace, T., Cui, N., & Jiang, C. Phe168 at the narrowest part of the ion-conductive pore is involved in Kir6.2 channel gating by intracellular protons. *47th Biophysical Society Annual Meeting,* 2003, 394-pos.
8. **Wang, R**., Rojas, A., Cui, N., & Jiang, C. Gating of Kir6.2 channel by interactions of two amino acid residues at the inner mouth of the ion-conductive pore. *Society for Neuroscience 32th Annual Meeting,* 2002, 438.18.